NCDOT

2012-11

Final Report

Performance Evaluation of NCDOT W-beam Guardrails under MASH TL-2 Conditions

Prepared By

Howie Fang
Matthew Gutowski
Ning Li
Matthew DiSogra

The University of North Carolina at Charlotte
Department of Mechanical Engineering & Engineering Science
Charlotte, NC 28223-0001

November 2013

Technical Report Documentation Page

1. Report No. **FHWA/NC/2012-11**	2. Government Accession No.	3. Recipient's Catalog No.	
4. Title and Subtitle **Performance Evaluation of NCDOT W-beam Guardrails under MASH TL-2 Conditions**		5. Report Date **November 2013**	
		6. Performing Organization Code	
7. Author(s) **Howie Fang, Matthew Gutowski, Ning Li, Matthew DiSogra**		8. Performing Organization Report No.	
9. Performing Organization Name and Address **The University of North Carolina at Charlotte** 9201 University City Boulevard Charlotte, NC 28223-0001		10. Work Unit No. (TRAIS)	
		11. Contract or Grant No.	
12. Sponsoring Agency Name and Address North Carolina Department of Transportation Research and Development 1549 MSC Raleigh, North Carolina 27699-1549		13. Type of Report and Period Covered **Final Report** **08/2011 – 08/2013**	
		14. Sponsoring Agency Code **2012-11**	

Supplementary Notes:

16. Abstract

This report summarizes the research efforts of using finite element modeling and simulations to evaluate the performance of W-beam guardrails for different heights under MASH Test Level 2 (TL-2) and Test Level 3 (TL-3) impact conditions. A literature review is included on performance evaluation of W-beam guardrails as well as applications of finite element modeling and simulations in roadside safety research.

The modeling and simulation work was conducted on W-beam guardrails placed at a height of 27, 29 and 31 inches with vehicular impacts of a 1996 Dodge Neon and a 2006 Ford F250. All three W-beam guardrail placement heights were evaluated and compared to MASH TL-2 conditions, i.e., both vehicles were tested at an impact speed of 44 mph (70 km/hour) and a 25° impact angle. The 29- and 31-inch W-beam guardrails were also evaluated under MASH TL-3 conditions, i.e., both vehicles were tested at an impact speed of 62 mph (100 km/hour) and a 25° impact angle.

The simulation results demonstrated the effectiveness of the 27-, 29- and 31-inch guardrails under MASH TL-2 conditions. They also showed the effects of guardrail heights on the vehicles' post-impact responses such as redirection, snagging and large exit angles. The use of finite element simulations was shown to be both effective and efficient because they were nondestructive, repeatable, modifiable, and inexpensive. Furthermore, finite element simulations can be used to study crash scenarios that are difficult and/or extremely expensive to conduct with physical crash testing. Finite element modeling and simulations are recommended for future investigations of other research issues.

17. Key Words *W-beam; Median barrier; Barrier height; 27-inch; 29-inch; 31-inch; Roadside safety; Highway safety; Finite element method*		18. Distribution Statement	
19. Security Classif. (of this report) Unclassified	20. Security Classif. (of this page) Unclassified	21. No. of Pages 78	22. Price

Form DOT F 1700.7 (8-72) **Reproduction of completed page authorized**

DISCLAIMER

The contents of this report reflect the views of the authors and not necessarily the views of the university. The authors are responsible for the facts and the accuracy of the data presented herein. The contents do not necessarily reflect the official views or policies of either the North Carolina Department of Transportation or the Federal Highway Administration. This report does not constitute a standard, specification, or regulation.

ACKNOWLEDGMENTS

This study was supported by the North Carolina Department of Transportation (NCDOT) under Project No. 2012-11. The authors would like to thank NCDOT personnel from the *Roadway Design Unit*, *Transportation Mobility & Safety*, *Highway Division 5*, *Technical Services*, *Work Zone Traffic Control Unit*, *Construction Unit*, *FHWA – NC Division*, and *Research and Development Unit* for the support and cooperation during the grant period.

EXECUTIVE SUMMARY

This report summarizes the research efforts of using finite element modeling and simulations to evaluate the performance of W-beam guardrails for different heights under MASH Test Level 2 (TL-2) and Test Level 3 (TL-3) impact conditions. A literature review is included on performance evaluation of W-beam guardrails as well as applications of finite element modeling and simulations in roadside safety research.

The modeling and simulation work was conducted on W-beam guardrails placed at a height of 27, 29, and 31 inches with vehicular impacts of a 1996 Dodge Neon and a 2006 Ford F250. All three W-beam guardrail placement heights were evaluated and compared to MASH TL-2 conditions, i.e., both vehicles were tested at an impact speed of 44 mph (70 km/hour) and a 25° impact angle. The 29- and 31-inch W-beam guardrails were also evaluated under MASH TL-3 conditions, i.e., both vehicles were tested at an impact speed of 62 mph (100 km/hour) and a 25° impact angle.

The simulation results demonstrated the effectiveness of the 27-, 29- and 31-inch guardrails under MASH TL-2 conditions. They also showed the effects of guardrail heights on the vehicles' post-impact responses such as redirection, snagging and large exit angles. The use of finite element simulations was shown to be both effective and efficient because they were nondestructive, repeatable, modifiable, and inexpensive. Furthermore, finite element simulations can be used to study crash scenarios that are difficult and/or extremely expensive to conduct with physical crash testing. Finite element modeling and simulations are recommended for future investigations of other research issues.

TABLE OF CONTENTS

Title Page i
Technical Report Documentation Page ii
Disclaimer iii
Acknowledgments iv
Executive Summary v
Table of Contents vi
List of Tables vii
List of Figures viii

1. Introduction 1
    1.1 Background 1
    1.2 Research Objectives and Tasks 3
2. Literature Review 7
    2.1 Performance Evaluation of W-beam Guardrails 7
    2.2 Crash Modeling and Simulations 14
3. Finite Element Modeling of Vehicles and W-beam Guardrails 21
    3.1 FE Models of a Passenger Car and Pickup Truck 21
    3.2 FE Model of the W-beam Guardrails 22
    3.3 Simulation Setup 24
4. Simulation Results and Analysis 27
    4.1 The 27-inch W-beam Guardrail 28
    4.2 The 29-inch W-beam Guardrail 34
    4.3 The 31-inch W-beam Guardrail 46
5. Findings and Conclusions 59
6. Recommendations 61
7. Implementation and Technology Transfer Plan 62

References 63

List of Tables

Table 3.1: Categories of simulation work

Table 4.1: The exit box criterion defined in MASH

Table 4.2: Exit box dimensions for the test vehicles of this project

Table 4.3: Simulation results of the 27-inch W-beam guardrail under MASH TL-2 conditions

Table 4.4: Simulation results of the 29-inch W-beam guardrail under MASH TL-2 conditions

Table 4.5: Simulation results of the 29-inch W-beam guardrail under MASH TL-3 conditions

Table 4.6: Simulation results of the 31-inch W-beam guardrail under MASH TL-2 conditions

Table 4.7: Simulation results of the 31-inch W-beam guardrail under MASH TL-3 conditions

Table 4.8: Maximum dynamic deflections of the 27-, 29-, and 31-inch guardrails

List of Figures

Fig. 1.1: A strong-post W-beam guardrail.

Fig. 1.2: A strong post W-beam guardrail with wood block out.

Fig. 1.3: MASH TL-2 conditions under small and large vehicle impacts.

Fig. 1.4: Illustration of the guardrail heights of the three FE guardrail models.

Fig. 1.5: Finite element models of a guardrail and two vehicles.

Fig. 1.6: Vehicle heights in relation to the 27-inch W-beam guardrail.

Fig. 1.7: Vehicle heights in relation to the 29-inch W-beam guardrail.

Fig. 1.8: Vehicle heights in relation to the 31-inch W-beam guardrail.

Fig. 1.9: Definition of vehicle responses.

Fig. 3.1: Finite element models of two vehicles used in crash simulations.

Fig. 3.2: The FE soil models for guardrail posts.

Fig. 3.3: Short-bolts on a guardrail splice.

Fig. 3.4: Simulation model of the 27-inch guardrail impacted by a Dodge Neon.

Fig. 3.5: Simulation model of the 27-inch guardrail impacted by a Ford F250.

Fig. 3.6: A Dodge Neon (left) and Ford F250 (right) impacting a spliced guardrail section.

Fig. 4.1: Exit box criterion in MASH.

Fig. 4.2: A Dodge Neon impacting the 27-inch guardrail at 44 mph and 25°.

Fig. 4.3: Yaw, pitch, and roll angles of Dodge Neon impacting the 27-inch guardrail at 44 mph and 25°.

Fig. 4.4: Permanent deformation of the 27-inch guardrail impacted by a Dodge Neon at 44 mph and 25°.

Fig. 4.5: Four instances of Dodge Neon impacting the 27-inch guardrail at 44 mph and 25°.

Fig. 4.6: Time histories of transverse displacements and velocities of the Dodge Neon impacting the 27-inch guardrail at 44 mph and 25°.

Fig. 4.7: Comparison of dynamic deformation of the 27-inch guardrail under impacts at 44 mph and 25°.

Fig. 4.8: A Ford F250 impacting the 27-inch guardrail at 44 mph and 25°.

Fig. 4.9: Yaw, pitch, and roll angles of Ford F250 impacting the 27-inch guardrail at 44 mph and 25°.

Fig. 4.10: Permanent deformation of the 27-inch guardrail impacted by a Ford F250 at 44 mph and 25°.

Fig. 4.11: Four instances of Ford F250 impacting the 27-inch guardrail at 44 mph and 25°.

Fig. 4.12: Time histories of transverse displacements and velocities of the Ford F250 impacting the 27-inch guardrail at 44 mph and 25°.

Fig. 4.13: A Dodge Neon impacting the 29-inch guardrail at 44 mph and 25°.

Fig. 4.14: Yaw, pitch, and roll angles of Dodge Neon impacting the 29-inch guardrail at 44 mph and 25°.

Fig. 4.15: Permanent deformation of the 29-inch guardrail impacted by a Dodge Neon at 44 mph and 25°.

Fig. 4.16: Four instances of Dodge Neon impacting the 29-inch guardrail at 44 mph and 25°.

Fig. 4.17: Time histories of transverse displacements and velocities of the Dodge Neon impacting the 29-inch guardrail at 44 mph and 25°.

Fig. 4.18: Comparison of dynamic deformation of the 29-inch guardrail under impacts at 44 mph and 25°.

Fig. 4.19: A Ford F250 impacting the 29-inch guardrail at 44 mph and 25°.

Fig. 4.20: Yaw, pitch, and roll angles of Ford F250 impacting the 29-inch guardrail at 44 mph and 25°.

Fig. 4.21: Permanent deformation of the 29-inch guardrail impacted by a Ford F250 at 44 mph and 25°.

Fig. 4.22: Four instances of Ford F250 impacting the 29-inch guardrail at 44 mph and 25°.

Fig. 4.23: Time histories of transverse displacements and velocities of the Ford F250 impacting the 29-inch guardrail at 44 mph and 25°.

Fig. 4.24: A Dodge Neon impacting the 29-inch guardrail at 62 mph and 25°.

Fig. 4.25: Yaw, pitch, and roll angles of Dodge Neon impacting the 29-inch guardrail at 62 mph and 25°.

Fig. 4.26: Permanent deformation of the 29-inch guardrail impacted by a Dodge Neon at 62 mph and 25°.

Fig. 4.27: Four instances of Dodge Neon impacting the 29-inch guardrail at 62 mph and 25°.

Fig. 4.28: Time histories of transverse displacements and velocities of the Dodge Neon impacting the 29-inch guardrail at 62 mph and 25°.

Fig. 4.29: Comparison of dynamic deformation of the 29-inch guardrail under impacts at 62 mph and 25°.

Fig. 4.30: A Ford F250 impacting the 29-inch guardrail at 62 mph and 25°.

Fig. 4.31: Yaw, pitch, and roll angles of Ford F250 impacting the 29-inch guardrail at 62 mph and 25°.

Fig. 4.32: Permanent deformation of the 29-inch guardrail impacted by a Ford F250 at 62 mph and 25°.

Fig. 4.33: Four instances of Ford F250 impacting the 29-inch guardrail at 62 mph and 25°.

Fig. 4.34: Time histories of transverse displacements and velocities of the Ford F250 impacting the 29-inch guardrail at 62 mph and 25°.

Fig. 4.35: A Dodge Neon impacting the 31-inch guardrail at 44 mph and 25°.

Fig. 4.36: Yaw, pitch, and roll angles of Dodge Neon impacting the 31-inch guardrail at 44 mph and 25°.

Fig. 4.37: Permanent deformation of the 31-inch guardrail impacted by a Dodge Neon at 44 mph and 25°.

Fig. 4.38: Four instances of Dodge Neon impacting the 31-inch guardrail at 44 mph and 25°.

Fig. 4.39: Time histories of transverse displacements and velocities of the Dodge Neon impacting the 31-inch guardrail at 44 mph and 25°.

Fig. 4.40: Comparison of dynamic deformation of the 31-inch guardrail under impacts at 44 mph and 25°.

Fig. 4.41: A Ford F250 impacting the 31-inch guardrail at 44 mph and 25°.

Fig. 4.42: Yaw, pitch, and roll angles of Ford F250 impacting the 31-inch guardrail at 44 mph and 25°.

Fig. 4.43: Permanent deformation of the 31-inch guardrail impacted by a Ford F250 at 44 mph and 25°.

Fig. 4.44: Four instances of Ford F250 impacting the 31-inch guardrail at 44 mph and 25°.

Fig. 4.45: Time histories of transverse displacements and velocities of the Ford F250 impacting the 31-inch guardrail at 44 mph and 25°.

Fig. 4.46: A Dodge Neon impacting the 31-inch guardrail at 62 mph and 25°.

Fig. 4.47: Yaw, pitch, and roll angles of Dodge Neon impacting the 31-inch guardrail at 62 mph and 25°.

Fig. 4.48: Permanent deformation of the 31-inch guardrail impacted by a Dodge Neon at 62 mph and 25°.

Fig. 4.49: Four instances of Dodge Neon impacting the 31-inch guardrail at 62 mph and 25°.

Fig. 4.50: Time histories of transverse displacements and velocities of the Dodge Neon impacting the 31-inch guardrail at 62 mph and 25°.

Fig. 4.51: Comparison of dynamic deformation of the 31-inch guardrail under impacts at 62 mph and 25°.

Fig. 4.52: A Ford F250 impacting the 31-inch guardrail at 62 mph and 25°.

Fig. 4.53: Yaw, pitch, and roll angles of Ford F250 impacting the 31-inch guardrail at 62 mph and 25°.

Fig. 4.54: Permanent deformation of the 31-inch guardrail impacted by a Ford F250 at 62 mph and 25°.

Fig. 4.55: Four instances of Ford F250 impacting the 31-inch guardrail at 62 mph and 25°.

Fig. 4.56: Time histories of transverse displacements and velocities of the Ford F250 impacting the 31-inch guardrail at 62 mph and 25°.

1. Introduction

Roadside barrier systems are important devices to ensure transportation safety; they serve the purpose of safely redirecting errant vehicles and preventing them from encroaching into oncoming traffic. Over the years, different types of barriers have been developed and are categorized into rigid, semi-rigid, and flexible systems. Concrete barriers belong to the rigid category and typically have high initial cost and lower maintenance needs. However, the high rigidity may cause more damage to the occupants than other barriers. The W-beam and Thrie-beam guardrails are semi-rigid systems. They are less rigid than concrete barriers and impact energy from the crash is dissipated by the deflection of the barrier with reduced impact force imposed upon the vehicle. Cable barriers are flexible systems that are more forgiving to the vehicle and occupants than concrete and W-beam barriers, but they are typically installed on sites that allow for larger lateral deflections.

W-beam guardrails are widely used safety devices on U.S. highways. Figure 1.1 shows a typical strong-post W-beam guardrail that consists of a steel, W-shaped rail mounted on steel posts. A known issue of the strong-post W-beam guardrail is the wheel snagging problem on the striking vehicle. To solve the problem or reduce its occurrence, a block-out, which is usually made of wood, steel (see Figure 1.2) or rubber composite, is added to create an offset from the rail to the guardrail posts. W-beam guardrails are meant to be sacrificial and thus usually require substantial replacement or repairs after major vehicle crashes. Even low-energy impacts can deform and damage the rails and displace the posts enough such that the barrier might not perform properly in a subsequent crash event. For this reason, the maintenance cost of W-beam guardrails is normally high and reducing the maintenance cost has been a constant challenge to state DOTs.

Fig. 1.1: A strong-post W-beam guardrail.

Fig. 1.2: A strong post W-beam guardrail with wood block-outs.

1.1 Background

All barrier systems used on U.S. highways are designed according to the Roadside Design Guide of the American Association of State Highway and Transportation Officials (AASHTO) (2011). They must be tested to satisfy the safety criteria specified by the AASHTO Manual for Assessing Safety Hardware (MASH) (2009), a replacement of the old standard – Report 350 of the National Cooperative

Highway Research Program (NCHRP) (Ross et al. 1993). The test conditions in MASH are more severe than those in NCHRP Report 350 in terms of the mass of testing vehicles and impact angles. In addition, the language of emphasizing the importance of in-service evaluation is added to MASH. Although existing barrier designs that have been tested to pass the safety criteria of NCHRP Report 350 are not required to be tested to satisfy the corresponding MASH criteria, it is important to evaluate their performance under MASH test conditions for practical safety concerns.

Research on the standard 27-inch G4(1S) W-beam guardrail shows that it does not meet the Test Level 3 (TL-3) criteria of NCHRP Report 350. A revision to the guardrail height is required for new installations of G4(1S) guardrails under TL-3 conditions. According to the USDOT memorandum issued in May 2010 (Nicol 2010), transportation agencies should now ensure a minimum height of 27¾ inches (measured from grade to top of the rail) for newly-installed G4(1S) guardrails . The generic or proprietary designs of 31-inch high guardrails are also recommended to transportation agencies for consideration of adoption as the standard for all new installations instead of the G4(1S) system. The installation height of 31 inches is the nominal height measured from grade to the top of the rail and includes a construction tolerance of plus or minus one inch. These new 31-inch guardrails are shown to have improved crash-test performance under TL-3 conditions of NCHRP Report 350 and increased capacity to safely contain and redirect higher center-of-gravity vehicles such as pickup trucks and SUVs.

Based upon the recommendation that 27-inch G4(1S) guardrails do not meet the TL-3 criteria, it raised a question concerning their performance and usage under MASH Test Level 2 (TL-2) conditions. On one hand, the impact speed of MASH TL-2 conditions is 44 mph (70 km/hour), which is lower than the TL-3 speed of 62 mph (100 km/hour) in NCHRP Report 350. On the other hand, the mass of MASH TL-2 vehicles are larger than the TL-3 vehicles in NCHRP Report 350. In addition, the impact angle for the small vehicle is 25° in MASH TL-2, which is larger than the 20° TL-3 angle of NCHRP Report 350. For G4(1S) guardrails on low speed highways, a practical concern is whether their performance is satisfactory and acceptable under MASH TL-2 conditions. The answer to this question is important to making decisions for new installations and retrofits of W-beam guardrails on such highways. Figure 1.3 illustrates the MASH TL-2 testing configuration and parameters used to evaluate the performance of the various guardrail heights using two test vehicles.

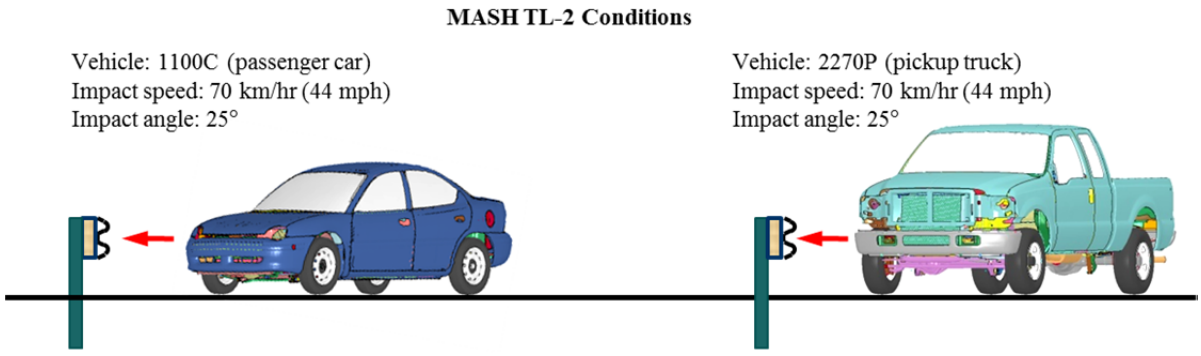

Fig. 1.3: MASH TL-2 conditions under small and large vehicle impacts.

With the rapid development of computer technology and parallel numerical codes, it is now possible to perform full-scale finite element (FE) simulations of vehicle crashes using commercial software such as LS-DYNA (LSTC 2007). Crash simulations using FE analysis are increasingly used to design new roadside safety devices and evaluate the safety performance of current systems under different site and impact conditions. One particular benefit of using simulations is that we can assess the performance limits of roadside devices under conditions full-scale physical crash tests cannot be readily performed.

1.2 Research Objectives and Tasks

The main objective of this research was to evaluate the safety performance of NCDOT 27-inch, 29-inch, and 31-inch W-beam guardrails under MASH TL-2 conditions. Full-scale FE simulations of vehicle-barrier impacts were employed as the major investigation tool to evaluate the guardrail performance under impacts of two types of vehicles. In addition, the NCDOT 29-inch and 31-inch W-beam guardrails were also evaluated under MASH TL-3 conditions to assist decision making on the installation of this newly proposed system. The following gives a summary of the six major tasks for this project.

Task 1: Literature Review and Data Collection

The objective of this task was to review literature on crash testing, modeling, and simulations that are particularly related to W-beam guardrails to assist model validation and crash simulations. The following sources were used in literature search:

- Midwest Roadside Safety Facility (MwRSF)
- National Cooperative Highway Research Program (NCHRP) ongoing projects
- National Crash Analysis Center (NCAC)
- State DOT research reports
- Texas Transportation Institute (TTI)
- Transportation Research Board Roadside Safety Committee website
- Transportation Research Information Services (TRIS)
- Transportation Research Record (TRR) and other technical journals
- Worcester Polytechnic Institute (WPI)

Task 2: Finite Element Model Development and Validation

In this task, the FE models of the 27-inch, 29-inch, and 31-inch W-beam guardrails were developed according to NCDOT specifications from a G4(1S) guardrail model that was originally developed at NCAC. For each of the three W-beam guardrails, an FE model was created to include a 400-ft (122-m) guardrail section whose length of need was determined to be sufficient for MASH TL-2 and TL-3 conditions. The rail heights of the three guardrails were measured from grade to top of the rail, as illustrated in Figure 1.4.

The FE models of a 1996 Dodge Neon and 2006 Ford F250 were also obtained from NCAC and validated to be used in the evaluation of W-beam guardrails. These two vehicles were used in the impact simulations under both MASH TL-2 and TL-3 conditions. The 1996 Dodge Neon was used as the 1100C test vehicle (2,420-lbs or 1,100-kg small passenger car) and the 2006 Ford F250 was used as the 2270P test vehicle (5,000-lbs or 2,270-kg pickup truck). The FE models of the G4(1S) guardrail and the two vehicles are shown in Figure 1.5.

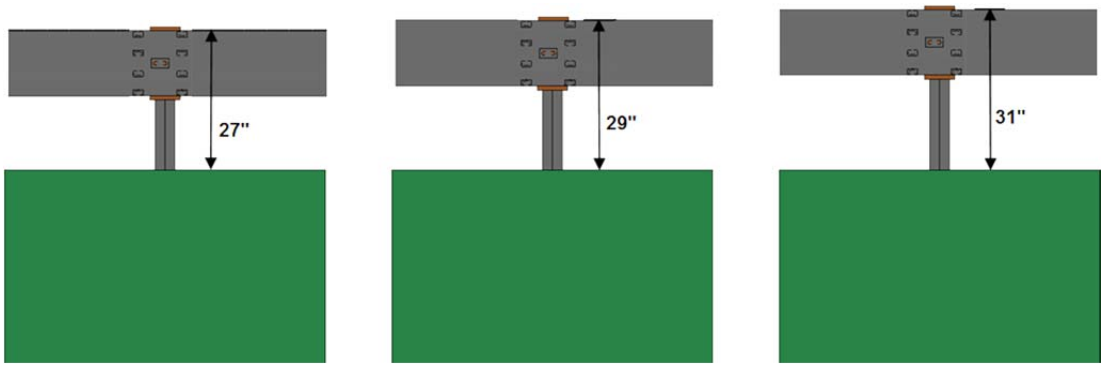

Fig. 1.4: Illustration of the guardrail heights of the three FE guardrail models.

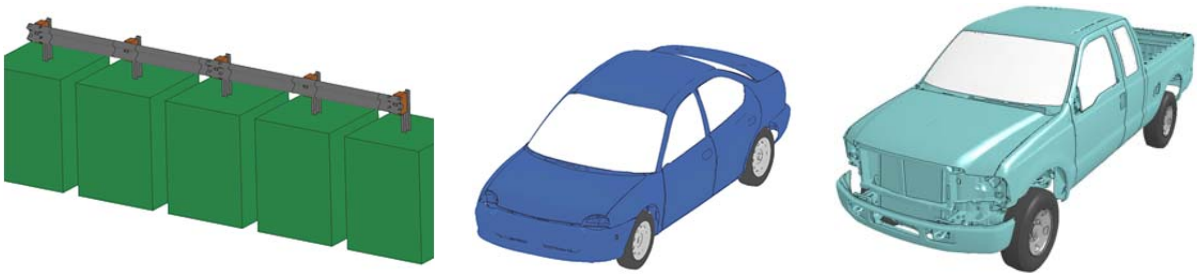

a. G4(1S) W-beam guardrail b. 1996 Dodge Neon c. 2006 Ford F250

Fig. 1.5: Finite element models of a guardrail and two vehicles.

Figures 1.6 to 1.8 show the heights of the 2006 Ford F250 and 1996 Dodge Neon in relation to the 27-, 29- and 31-inch W-beam guardrails, respectively.

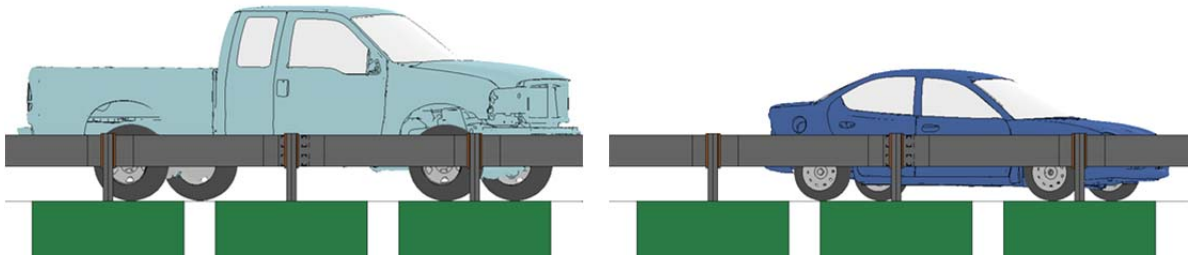

Fig. 1.6: Vehicle heights in relation to the 27-inch W-beam guardrail.

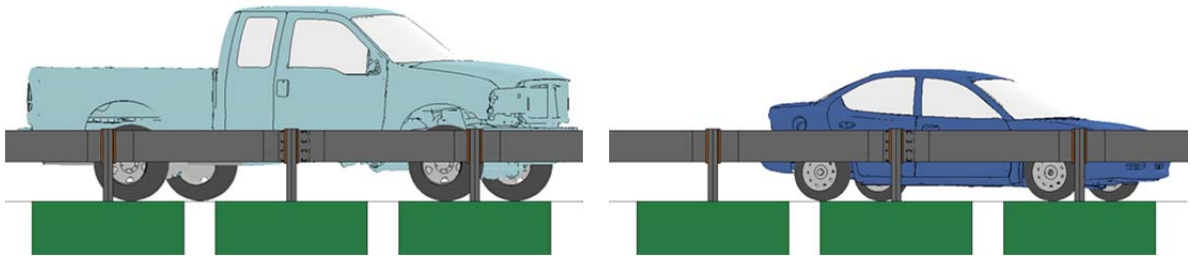

Fig. 1.7: Vehicle heights in relation to the 29-inch W-beam guardrail.

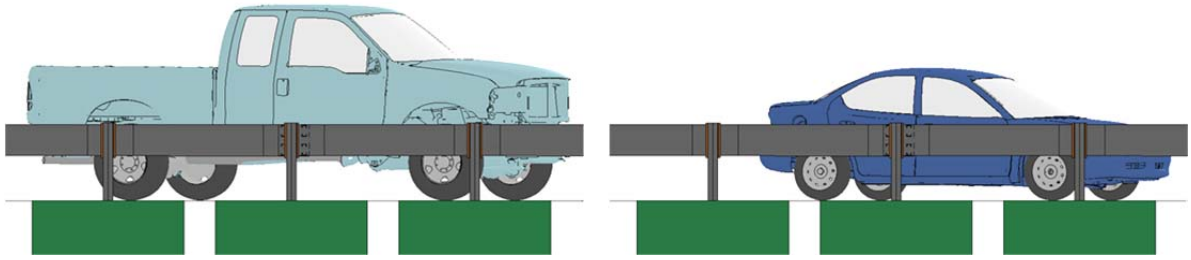

Fig. 1.8: Vehicle heights in relation to the 31-inch W-beam guardrail.

Simulations were conducted for all three guardrail placement heights under the standard MASH TL-2 conditions, i.e., at an impact speed of 44 mph (70 km/hour) and a 25º impact angle. For the 29- and 31-inch guardrail placement heights, simulations were also conducted under the standard MASH TL-3 conditions, i.e., at an impact speed of 62 mph (100 km/hour) and a 25º impact angle.

Task 3: Performance Evaluation of 27-inch G4(1S) W-beam Guardrail

The 27-inch G4(1S) W-beam guardrail was evaluated in this task under the impacts of a small passenger car and a large pickup truck as illustrated in Figure 1.3. The guardrail was installed on flat ground with no slope and no horizontal curvature. The impact speed was 44 mph (70 km/hour) and the impact angle was 25º for both vehicles, according to the MASH TL-2 conditions. In evaluating the guardrail's performance, the exit box criterion specified by MASH was adopted. In addition, the vehicle's responses in terms of redirection, rollover, lateral displacements and velocities, were extracted from simulation results and analyzed.

Fig. 1.9: Definition of vehicle responses.

For a guardrail to pass as a safe crash test, MASH also requires that the maximum roll and pitch angles of the impacting vehicle do not exceed 75 degrees. Figure 1.9 shows the definition of the three rotational responses (roll, pitch, and yaw) along with the corresponding translational responses (surge, sway, and heave). The time histories of the three rotational response parameters (the roll, pitch, and yaw angles) were recorded for the entire course of the simulations. The maximum roll and pitch angles were extracted and compared with the MASH threshold values. In addition to the aforementioned MASH evaluation criteria, the time histories of the vehicle's lateral displacements, velocities, and accelerations were also examined for performance evaluation. The effectiveness of the G4(1S) guardrail was then determined based on analysis of simulation results for both small and large vehicles.

Task 4: Performance Evaluation of 29-inch W-beam Guardrail

In this task, the 29-inch W-beam guardrail was evaluated using FE simulations of vehicle impacts under MASH TL-2 conditions. The simulation setup, evaluation parameters, and

evaluation criteria were the same as those for the 27-inch W-beam guardrail. Simulation results were analyzed and compared to those of the 27-inch and 31-inch guardrails for TL-2 conditions. The evaluation in this task was used to determine the performance gains over the 27-inch guardrail under TL-2 conditions. The 29-inch W-beam guardrail was also evaluated under MASH TL-3 conditions, i.e., at 62 mph (100 km/hour) and 25°, and compared to the 31-inch guardrail under the same conditions. This comparison, along with those under MASH TL-2 conditions, can be used in future consideration of new installations and retrofit options.

Task 5: Performance Evaluation of 31-inch W-beam Guardrail

In this task, the 31-inch W-beam guardrail was evaluated using FE simulations of vehicle impacts under MASH TL-2 and TL-3 conditions. The simulation setup, evaluation parameters, and evaluation criteria were the same as those for the 29-inch W-beam guardrail. Simulation results were analyzed and compared to those of the 27-inch and 29-inch guardrails. Some other designs of 31-inch W-beam guardrails from literature were shown to have similar cost to the G4(1S) guardrail but with significantly improved performance under TL-3 conditions. The evaluation in this task will determine the performance of NCDOT 31-inch guardrail compared to the 27- and 29-inch guardrails under TL-2 and TL-3 conditions. The results can be used in future consideration of new installations and retrofit options.

Task 6: Final Report

This final report provides a comprehensive summary of research activities, findings, and outcomes for this project. It synthesizes literature review, FE modeling efforts, simulation results, and the performance evaluation of W-beam guardrails with rail heights of 27, 29, and 31 inches under MASH TL-2 and TL-3 conditions.

2. Literature Review

Median barriers have been developed and used on U.S. highway for decades. Presently, W-beam guardrails and cable barriers are widely used across the U.S. In this section, we provide a comprehensive summary of studies related to W-beam guardrails, cable barriers, and other barrier systems. The topics cover performance evaluation (in-service and crash testing) and the application of FE modeling and simulations for highway safety research.

2.1 Performance Evaluation of W-beam Guardrails

In the early 1960s, New York State pioneered the development of weak-post barrier systems through analytical models and full-scale vehicle crash testing. In 1965, the state's guardrail and median barrier standards were changed to include only weak-post barriers. In the early 1970s, a study by Zweden and Bryden (1977) was conducted to evaluate the field performance of the older strong-post barriers and newly-developed weak-post barriers based on New York State accident data collected from 1967 to 1970. A statistical analysis was performed to compare the performance of the investigated barriers based on occupant injury, vehicular responses, and after impact maintenance. This study generated a number of significant conclusions on the performance of weak- and strong-post barriers. Although there was no significant difference in fatality rates between the two barriers, weak-post barriers exhibited a combined fatality/serious injury rate significantly lower than that for strong-post barriers. The resulting occupant injury appeared to be linked to barrier stiffness since the two barriers (both strong- and weak-post versions) had lower injury severity rates, while the stiffer median barriers had the highest injury rates. With respect to barrier penetrations, the weak-post barriers demonstrated a lower penetration rate than the strong-post barriers, which may be due to the lack of consistency between early strong-post barrier designs. The study also indicated that barrier penetrations on the weak-post systems were typically due to the low rail heights. Barrier end terminals (i.e., the first and the last 50 feet of the barrier) were observed to have higher rates of penetration and serious injury than the midsections. The study also related barrier damage to their stiffness: stiffer barriers (e.g., strong-post barriers) had less damage or shorter damaged sections than weaker barriers (e.g., weak-post barriers). Despite their longer damage lengths, weak-post barriers were on average less expensive to repair than strong-post barriers.

An analysis performed in the 1970s indicated that most guardrails did not perform well when placed on 1:6 or steeper slopes. Since that time, the vehicle fleet has changed dramatically with a significant increase in the popularity of light trucks and sport utility vehicles. In addition, there has been a significant change in the design of roadside barriers in recent decades. It is unclear how these changes affect the behavior of longitudinal barriers placed on slopes. Information from the Fatality Analysis Reporting System (FARS) database of the National Highway Traffic Safety Administration (NHTSA) indicated that some cross-median crashes occurred where median barriers were in place. A full-scale crash test also showed that a passenger vehicle could penetrate a cable barrier on the backside of a depressed median.

In the early 1980s, significant changes in vehicle designs led to a large increase in the number of smaller and lighter vehicles on highways. A study (Hiss and Bryden, 1992) was

initiated in 1983 by the New York State DOT to determine how impact severity on traffic barriers was affected by vehicle size and weight, barrier type and mounting height, and roadway features. Several conclusions were drawn regarding the performance of cable, W-beam, and box-beam guardrails. For cable and W-beam median barriers, however, the sample sizes were too small to assess their performance due to their limited use and exposure to possible accidents.

Ross et al. (1984) investigated the impact performance of longitudinal barriers when placed on sloped terrain using both crash tests and the Highway-Vehicle-Object Simulation Model (HVOSM) computer program. In the study, they determined typical conditions to place longitudinal barriers on sloped terrain and evaluated the impact behavior of widely used barrier systems. Guidelines were developed for the selection and placement of barriers on sloped terrain. It was found from the study that W-beam and Thrie-beam guardrails were more sensitive to the terrain slopes than cable barriers.

In the study conducted by Ross et al. (1993), uniform procedures were developed for evaluating the safety performance of candidate roadside hardware systems, including longitudinal barriers, crash cushions, breakaway supports, truck-mounted attenuators, and work zone traffic control devices. The report from this study, the NCHRP Report 350, was adopted as the standard guideline for evaluating the safety performance of roadside safety devices until 2009 when its successor, MASH, came into effect. The evaluation of devices in NCHRP 350 was facilitated through three main criteria: 1) structural adequacy; 2) occupant risk; and 3) post-impact trajectory. Structural adequacy referred to how well the device performed its intended task (i.e. a guardrail preventing a vehicle from striking a shielded object). The occupant risk criteria attempted to quantify the probability of severe occupant injury. The post-impact vehicle trajectory was adopted to ensure that the device would not cause subsequent harm (i.e. a vehicle being redirected back into traffic). The guideline recognized the infinite number of roadside hardware installations and crash configurations; therefore, standardized installation configurations and practical worst-case impact scenarios were used to provide a basis for comparing the performance of similar devices. A matter of particular note was, the multi-service level concept that provided six different test levels to allow for more or less stringent performance evaluation (ideally depending on the ultimate usage/placement of the hardware).

With respect to cross-median crashes, the NCHRP Report 350 was the standard by which median barriers were tested before the new standard, MASH, was developed. Although the report specified six different test levels, the warrants for devices satisfying an individual test level was outside the scope of the document and left to the judgment of the transportation agency implementing the hardware. Generally speaking, devices tested to the lower test levels (1 and 2) were mostly used on lower volume, lower speed roadways, and devices tested to higher levels (3 to 6) were typically used on larger volume, higher speed roadways. Note that the 2000P, 2000-kg (4,409-pound), test vehicle was used to evaluate the strength and redirecting capabilities of longitudinal barriers up to and including test level three. For the 2000P test vehicle, all impacts were performed at 25° and at 31, 44, and 62 mph (50, 70, and 100 km/hour) for test levels 1, 2, and 3, respectively.

In the NCHRP Project 22-14, "Improvement of the Procedures for the Safety Performance Evaluation of Roadside Features," updates were incorporated to the NCHRP Report 350 based on assessments at TL-3 conditions, which was the basic level used for devices on the National Highway System. In the report published by Mak and Bligh (2002), the effects of higher impact speeds and additional impact angles were considered for TL-3 conditions. These additional parameters were considered due to the fact that a number of states had changed maximum speed limits on some of their highways to 75 mph (121 km/hour) and most crashes occurring at an impact angle of 25°. These parameters often caused a concern on the stability of the test vehicle instead of containment capability. The report determined that increasing the impact speed to 68.4 mph (110 km/hour) would have significant effects on many of the existing roadside safety devices. Although some barriers could be modified to accommodate the higher impact speed with minor modifications, some other barriers would require major changes, and yet some barriers might never be able to accommodate the higher impact speed due to other design constraints. Increasing the impact speed could result in a whole new generation of roadside safety hardware. In return, the higher impact speed would only cover an additional 2.8% of the crashes and increase the percentage of covered crashes (i.e., crashes with impact speeds equal to or less than the design test speed) from approximately 90% to 92.7%. The reduction of the impact angle to 20° from 25° posed a number of arguments including the possibility for existing W-beam guardrail systems having difficulty containing vehicles at the higher impact speeds. It was emphasized that the selection of impact conditions was more of a policy decision than a technical issue to be resolved when updating the NCHRP Report 350 guidelines.

In the early 1990s, the Traffic Engineering Branch of NCDOT conducted a study (Lynch et al. 1993) of accidents on North Carolina's interstate highways in which vehicles crossed the median and entered the opposing travel lanes. The study analyzed accidents that occurred during the time period from April 1, 1988 through October 31, 1991. The objectives of this study were to identify interstate locations with unusually high cross-median accidents, to determine possible safety improvements, to develop a priority listing of these locations with recommended improvements, and to develop a model for identifying potentially dangerous locations on North Carolina interstate highways. Data collected in the study showed that 751 cross-median crashes took place in North Carolina, resulting in 105 fatalities. These crashes represented three percent of total crashes but 32% of total fatalities on interstate highways during the study period. One of the outcomes of this study was the recommendation to construct median barriers at 24 sections of interstate highways in North Carolina.

Ray and McGinnis (1997) provided a synthesis of information regarding the use of guardrails and median barriers in the U.S. and their performance with respect to the testing standards specified by the NCHRP Report 350. Comprehensive background information was provided for the evolution of testing procedures, selection and placement procedures, and in-service evaluation of longitudinal and median barriers. The notable advantages of steel-post cable guiderails, as indicated in the report, were their compliance to TL-3 conditions of the NCHRP Report 350, inexpensive installation, minimized sight distance problems, reduced occupant forces in collisions, and reduced snow drifting/accumulation. Disadvantages of this system were found to include periodic monitoring of cable tension, a large clear area for barrier deflection, and increased barrier damage in the event of a collision.

Using data collected from Connecticut, Iowa, and North Carolina from 1997 to 1999, Ray and Weir (2001) performed an in-service performance evaluation of four guardrail systems: the G1 cable guiderail, G2 weak-post W-beam guardrail, and the G4(1S) and G4(1W) strong-post W-beam guardrails. The study particularly focused on estimating the number of unreported collisions and the true distribution of occupant injuries. The collision performance was measured in terms of collision characteristics, occupant injury, and barrier damage. Within the sample size limitations of the data collected in the study, no statistically significant difference was found on the performance of the guardrails in the three states, and there was no difference between the performance of G1 and G2 guardrails and between G1 and G4(1W) guardrails. However, occupant injuries were found less common in collisions with a G1 cable guardrail than in collisions with G4(1S) or both G4 types combined.

Ray et al. (2003) reviewed literature on in-service evaluations and identified previously found effective methods. The in-service performance of common barriers and terminals was examined by collecting data in the following three areas: crash, maintenance, and inventory information. A procedure manual for planning and conducting in-service evaluations of roadside hardware was developed based on the methods used and the lessons learned in the evaluation study. The manual was subsequently used as a guide for an in-service evaluation project performed in Washington State by a different research team and modified based on their experiences and recommendations.

In the work of Bligh and Mak (1999), they evaluated the crashworthiness of roadside features across vehicle platforms. The impact performances of roadside safety features were typically evaluated through full-scale crash tests with two vehicles selected from the extremes of the passenger vehicle fleet in terms of weight and size. The implicit assumption was that if a roadside safety device successfully passed the test requirements for vehicles at the extremes of the fleet, it would perform satisfactorily for all other vehicles in between. Since many vehicle parameters could influence the performance during impacts, this assumption may or may not be valid. The safety performances of roadside features for various passenger car platforms and light-truck subclasses were evaluated in the study, which consisted of evaluations of the frequency and severity of roadside crashes for these generic platforms and subclasses by using recent crash data from the Fatal Accident Report System, the General Estimates System, and the Highway Safety Information System.

A new median barrier guideline was developed for Texas to assist highway engineers in the evaluation of median barrier needs with the intention of achieving the highest practical level of median safety (Miaou et al. 2005; Bligh et al. 2006). In this work, statistical crash models for various types of median-related crashes were developed based on an analysis of crash data in Texas. Using the estimates from the frequency and severity models and crash costs used by Texas Department of Transportation, an economic analysis of the median barrier need was performed. Guidelines for installing median barriers on divided, access-controlled freeways were developed as a function of average annual daily traffic and median width. Guidance to assist engineers evaluating median barriers needed on existing highway facilities was also developed based on the mean cross-median crash rate.

Under the guidelines of NCHRP Project 22-9, “Improved Methods for the Cost-Effectiveness Evaluation of Roadside Safety Features,” Mak and Sicking (2003) developed the Roadside

Safety Analysis Program (RSAP). The main objective of Project 22-9 was to develop an improved cost effective analysis procedure for assessing roadside safety improvements. The RSAP incorporated two integrated programs, the Main Analysis Program, which contained the cost-effectiveness procedure and algorithms, and the User Interface Program, which provided a user friendly environment for data input and review of program results. The cost-effectiveness procedure incorporated in RSAP was based on the concept of incremental benefit/cost analysis. In 2009, NCHRP Project 22-27, "Roadside Safety Analysis Program (RSAP) Update," was started to assist AASHTO Technical Committee on Roadside Safety to develop the next edition of the AASHTO Roadside Design Guide (RDG). The objectives of this project were to rewrite the software, update the manuals, improve the user interface, and update the embedded default data tables of the RSAP (NCHRP 22-27).

On observation of cross-median collisions (CMCs) that happened where median barriers were not warranted by the Pennsylvania DOT design policy, Donnell et al. (2002) reviewed the methods used to assess median safety on interstates and expressways in Pennsylvania. A critical literature review and assessment of median safety practices in various state DOTs were conducted, and qualitatively assessed median safety practices were used to provide input for quantitative data collection. Negative binomial regression models were used to model CMC frequencies on earth-divided highways. The qualitative results from the study suggested that three-strand cable barriers, strong-post W-beam guardrails, or concrete barriers were recommended as median barriers warranted by site conditions. The quantitative results showed that CMCs were rare events and that nearly 15% involved fatalities and 72% involved nonfatal injuries. Additional findings included that CMC rates at earth-divided highways decreased as the median width increased, that CMCs appeared more likely to occur downstream of interchange entrance ramps, and that CMCs were more likely to involve adverse pavement surface conditions (wet or icy) than other crashes.

In a project funded by the New Jersey DOT, Gabler et al. (2005) evaluated the post-impact performance of two median barrier systems in New Jersey: a three-strand cable median barrier system and a modified Thrie-beam median barrier system. FE modeling was adopted as a major means for the investigation. The project also included field investigation of crashes into the subject barriers and a survey of the median barrier experience of other state DOTs. This study concluded that three-strand cable barriers were capable of containing and redirecting passenger vehicles, that cable barriers were effective at reducing the incidence of cross-median collisions in wider medians, and that cable barriers reduced the overall collision severity despite typically increasing the total number of accidents.

In another study funded by the New Jersey DOT, Gabler and Gabauer (2006) investigated the fatalities and injuries in accidents involving W-beam guardrails on New Jersey highways. The study found that the guardrails generally performed well in vehicular crashes and only accounted for a small number (1.5%) of the total highway fatalities. This study also found that occupant injuries in guardrail crashes were not a major issue unless the vehicle had a rollover: three-fourths of all occupants in these crashes were found to have no injuries. Some of the issues related to the guardrail performance were also identified. For example, the study found that over half the fatal collisions on guardrails involved secondary events, i.e., either a second impact or a rollover. It was also found that 14% of all fatal crashes on guardrails

resulted in a rollover, and that light trucks had a significantly greater chance of "vaulting" and/or "rollover" than other vehicles when colliding with the guardrail.

The placement of median barriers on sloped medians imposed a significant challenge to retaining the desired performance as seen on flat terrains. The performance tests specified by the NCHRP Report 350 were all based on flat terrain conditions. Terrain conditions could have a significant effect on the barrier's impact performance (AASHTO 2011). Median slopes could affect the performance of the barrier, because the vehicle engages the barrier in a significantly different manner than on flat terrain. In NCHRP Project 17-14, "Improved Guidelines for Median Safety," researchers attempted to develop guidelines for using median barrier and selecting median widths and slopes (BMI-SG 2004). Unfortunately, collection of data needed for this project proved to be very expensive, and the data limitations hampered the strength of the recommendations. The project results have not been incorporated into practice, but should be very beneficial to future research.

To avoid some of the obstacles that NCHRP Project 17-14 faced, the NCHRP Project 22-21 focused on typical cross-section designs for a construction or reconstruction project rather than on the exact cross-section design at a particular point. The typical cross-section designs were determined early in the design process before adjustments were made to account for variations along the alignment (e.g., horizontal and vertical curves, interchanges and intersections, and special drainage requirements). The Project 22-21 was started on January 2006 and was completed in April 2011. However, the Midwest Research Institute has yet to release the final report, expected summer 2013, of the research findings. It is anticipated that the final report of Project 22-21 would contain guidance that practitioners can use to evaluate the safety implications of various median cross-section designs, including barrier type and placement guidelines (based on the NCHRP Project 22-22), so that a cost-effective design can be achieved. The NCHRP Project 22-22, "Placement of Traffic Barriers on Roadside and Median Slopes," has been extended to NCHRP Project 22-22(02) "Effectiveness of Traffic Barriers on Non-Level Terrain" to test the simulations in accordance with the approved plan developed in NCHRP Project 22-22. The results of NCHRP Project 22-22(02) are to be incorporated into the final product of NCHRP Project 22-21.

In 2009, the Manual for Assessing Safety Hardware (MASH) was published to supersede the old roadside safety standard, NCHRP Report 350. MASH presents uniform guidelines for crash testing permanent and temporary highway safety features and recommends evaluation criteria to assess test results. MASH does not supersede any guidelines for the design of roadside safety hardware, which are contained within the AASHTO *Roadside Design Guide*. A few of the significant changes from NCHRP Report 350 to MASH include:

- The weight of the small car test vehicle was increased from 1,800 lbs. (820C) to 2,420 lbs. (1100C)
- The impact angle of the small test vehicle was increased from 20° to 25°
- The weight of the pickup truck test vehicle was increased from 4,400 lbs. (2000P) to 5,000 lbs. (2270P)
- The mass of the single unit truck in TL-4 was increased from 18,000 lbs. (8,000 kg) to 22,000 lbs. (10,000 kg) and the impact speed was increased from 50 mph (80 km/hour) to 56 mph (90 km/hour).

As of January 1, 2011, the FHWA has required that all new product designs must be tested using MASH test criteria for use on the National Highway System.

Recently, a study was conducted to analyze the severity of median barrier crashes using five years of data from rural divided highways in North Carolina (Hu and Donnell 2010). The criteria used for the analysis included median barrier type, the barrier's offset distance from the edge of the travel lane, roadway segment characteristics, roadway surface conditions, driver and vehicle characteristics, median barrier placement, and median cross-slope data. The major conclusion of this study was that less severe crash outcomes pertained to those on cable median barriers when compared to concrete barriers and W-beam guardrail. It was also observed that the barrier's offset distance from the travel lane was associated with a lower probability of severe crash outcomes and that cable barriers placed on steep median slopes were associated with an increased probability of severe crashes.

In 2010, Hampton et al. (2010) conducted crash tests and finite element analysis (FEA) on already damaged sections of the G4(1S) W-beam guardrails. The FEA work will be discussed in depth in subsequent sections. The testing of already damaged barrier systems had not previously been conducted. Two crash tests were performed by the MGA Research Corporation for the NCHRP Project 22-23, "Criteria for Restoration of Longitudinal Barriers," to evaluate the performance of guardrails with pre-prescribed rail and post deflections. The first crash test was conducted at 30 mph (48.3 km/hour) with an impact angle of 25° and resulted in a 36-ft (10.97-m) damaged section of barrier with a maximum deflection of 1.21-ft (0.37-m). The second crash test was performed in the damaged location; however, the results were undesirable. The barrier provided little to no resistance to the impacting vehicle, which vaulted over the barrier. These results were due to a failed link present in the barrier that separated the post from the rail. The study concluded that a deflection of 0.92-ft (0.279-m) or more on the post and rail would result in the vehicle vaulting over the median barrier.

Ochoa and Ochoa (2011) completed a study to optimize guardrail barriers for rural roadways in the U.S., Europe, and some developing countries. In order to optimize the W-beam guardrail, the main methods for identifying failures had to be defined and considered. In the conventional strong post W-beam guardrails, the relatively high release load varied by approximately 360% and was further compounded by another 40% due to variations in the yield strength of guardrail panels. A physics-based guardrail analysis was performed to determine the solution of optimizing the release load in relation to post section properties. This optimization was accomplished by introducing an improved fastening system that incorporated a separate deformable release member to consistently provide a predefined release load of around 1,700 lbs. (7,565 N) with a maximum variation of 20%. The versatile W-beam guardrail incorporating these improvements was successfully crash tested and accepted by FHWA at NCHRP Report 350 test levels and at MASH TL-3 conditions.

In 2011, AASHTO published the new *Roadside Design Guide*, which presented a synthesis of current information and operating practices related to roadside safety. The guide was intended to be used as a resource document from which individual highway agencies could develop standards and policies. It was focused on safety treatments that could minimize the

likelihood of serious injuries when a motorist leaves the roadway. The 2011 edition was updated to include hardware systems that had been tested to meet the evaluation criteria contained in the NCHRP Report 350. It also included an outline of the most current evaluation criteria contained in MASH.

In 2012, Findley et al. (2012) at the Institute of Transportation Research and Education, North Carolina State University, conducted a statewide structural and safety investigation on the performance of weathered steel beam guardrails (WSBG) in North Carolina. This study was prompted when New Hampshire found that the WSBG deteriorates at a much faster rate compared to the galvanized steel guardrail (GSG) in the northeast due to the harsher weather conditions. The study concluded that in all test sites across North Carolina, there were no structural concerns about using WSBG in the state. Additionally, the research results suggested a lower percentage of injury collisions associated with WSBG installations than the GSG installations at comparison sites. However, this study used a small sample size and further investigation would need to be made for a more robust comparison.

Recently, researchers at the Midwest Roadside Safety Facility (MwRSF) performed a study on the safety performance of the Midwest Guardrail System (MGS) with no block-out. This revised design could possibly be used at locations where the required 12-inch block-out would not work and an alternative was required. They successfully crash tested the non-proprietary design of the MGS with 31 inch of rail height using a passenger car and a pickup truck under MASH TL-3 conditions (Schrum et al. 2013). The results of this report suggested that the MGS with no block-out could be used on roadways where the width of the block-out was a limiting factor and the standard MGS with block-outs was recommended for other locations.

2.2 Crash Modeling and Simulations

Mackerle (2003) provided a bibliography that included 271 references published between 1998 and 2002 on crash simulations using FEA and on impact-induced injuries. This bibliography categorized the references into four different topic areas: 1) Crash and impact simulations where occupants were not included; 2) Impact-induced injuries; 3) Human surrogates; and 4) Injury protection. Topics in the first area included crashworthiness of aircrafts and helicopters, automobiles, and vehicle rail structures. The second area of research utilized two major types of models for humans, the crash dummy and real human body models. Research topics in this area were mainly on biomechanics and impact analyses for various human injuries. Topics on human surrogates focused on the development FE models of hybrid and other types of human dummies. These dummy models were used to obtain dynamic responses of the whole human body during impacts, which were difficult to measure experimentally. In the area of injury protection, FEA were utilized to simulate and analyze injury protection systems such as seat belt, air bags, and collapsible structures to reduce serious or fatal injuries. The references included in Mackerle's bibliography were generally useful to the work on FE crash simulations; however, only a few references under injury protection were related to roadside safety.

Most publicly available FE models of vehicles and roadside safety structures were developed at the FHWA National Crash Analysis Center (NCAC) at George Washington University.

Since the 1990s, significant efforts have been put on the development of FE models for crash analysis; most of these models are available as LS-DYNA input files from NCAC's website (NCAC web1). A list of references on these modeling efforts and simulation work performed at NCAC is also available from NCAC's website (NCAC web2).

The modeling and simulation efforts at NCAC can be found in several representative works. Marzougui et al. (2000) developed the FE model of an F-shaped portable concrete barrier (PCB) and validated the model with full-scale crash test data. With the proven fidelity and accuracy of the modeling methodology, the models of two modified PCB designs were created and used in FE simulations to evaluate their safety performance. A third design was then developed based on the simulation results and its performance was analyzed. In the work by Zaouk et al. (2000a, 2000b), a detailed FE model of a 1996 Plymouth Neon was developed. The three dimensional geometric data of each component was obtained by using a passive digitizing arm and then imported into a preprocessor for mesh generation, part connections, and material properties. Tensile tests were conducted on specimen to obtain the material properties of the various sheet metal components. The body-in-white model was used in the simulation of a frontal impact and the results were compared with test data to evaluate the accuracy and validity of the model.

In the work of Kan et al. (2001), they developed an integrated FE model that included the vehicular structure, interior components, an occupant (Hybrid III dummy), and an airbag for crashworthiness evaluation. The integrated model was then used in a case study to demonstrate the potential benefit of the integrated simulation and analysis approach, which would further improve the engineering practice with cost savings and producing more accurate and consistent analysis results. Marzougui et al. (2004) developed a detailed suspension model and incorporated it into the previously developed FE model of a Chevrolet C2500 pickup truck (Zaouk et al. 1997). Pendulum tests were conducted at the Federal Outdoor Impact Laboratory (FOIL) of FHWA and compared with simulation results of deformations, displacements, and accelerations at various locations. Crash simulations were performed using the upgraded vehicle model and the results were compared with crash data from previously conducted full-scale tests.

To facilitate the use of FE simulations to evaluate roadside safety structures at higher test levels specified by the NCHRP Report 350, Mohan et al. (2007) improved and validated a previously developed model of a 1996 Ford F800 single unit truck. This 18,000-lb (8,172-kg) truck was used in the NCHRP Report 350 as the standard vehicle for test level 4. Simulations were performed using the improved model and the results were compared with those from a full-scale crash test. The global kinematics and the acceleration time histories of the truck from simulations were found to correlate well with the crash test data. Mohan et al. also suggested further improving the normal forces on non-impacted tires so as to correlate well on the vehicle's yaw by considering frictions between the tires and barrier and between the tires and ground.

In a study by Marzougui et al. (2007), the FE model of a W-beam guardrail was developed and validated using full-scale crash test data. The model was shown to give an accurate representation of the real system based on comparison of the vehicle's roll and yaw angles.

Using the validated model, they performed four simulations of a passenger truck impacting the W-beam guardrails with different rail heights. The simulation results showed that the effectiveness of the barrier to redirect a vehicle could be compromised when the rail height was lower than the recommended value.

Researchers from the roadside safety group at Worcester Polytechnic Institute utilized FE models in a number of roadside safety studies. Ray (1996a) analyzed data of full-scale crash tests and developed a criterion using statistical parameters to assess the repeatability of full-scale crash test and to evaluate simulation results compared to crash data. Ray (1996b) reviewed the history of using FEA in roadside safety research, and presented the vehicle, occupant, and roadside hardware models that had been developed to date. Ray and Patzner (1997) developed a nonlinear FE model of a modified eccentric loader breakaway cable terminal (MELT) and used it in simulating a full-scale crash test involving a small passenger car. Simulation results were analyzed and compared to crash data, and the FE model was recommended to be used in the evaluation of new design alternatives. Plaxico et al. (1997) developed a 3D FE model of a modified Thrie-beam and simulated the impact of a compact vehicle. The computational model was then calibrated with data from an actual field test that was previously conducted as part of a full-scale crash test program carried out under the auspices of FHWA. Plaxico et al. (1998) developed the FE model of a breakaway timber post and soil system used in the breakaway cable terminal (BCT) and the modified eccentric loader BCT. Simulation results were compared and found to correlate well to data from physical tests. In the work of Patzner et al. (1999), they examined the effects of post strength and soil strength on the overall performance of the MELT terminal system using a nonlinear FE model. A matrix of twelve simulations of particular full-scale crash test scenarios was used to establish the combinations of post and soil strengths from which favorable situation(s) could be identified. This parametric study showed that certain combinations of soil and post strengths increased the hazardous possibilities of wheel snagging, pocketing, or rail penetration, while other combinations produced more favorable results.

In the work of Plaxico et al. (2000), the impact performance of two strong-post W-beam guardrails, the G4(2W) and G4(1W), were compared. After validating the FE model of the G4(2W) guardrail with data of a full-scale crash test, the FE model of the G4(1W) guardrail was developed. The two guardrails were compared with respect to deflection, vehicle redirection, and occupant risk factors. The two systems were found to perform similarly in collisions and both to satisfy the requirements of the NCHRP Report 350 for the Test 3-11 conditions. Using LS-DYNA simulations and laboratory experiments, Plaxico et al. (2003) investigated the failure mechanism of the bolted connection of a W-beam rail to a guardrail post, which could have a significant effect on the performance of a guardrail system. A computationally efficient and accurate FE model of the rail-to-post connection was developed for use in performance evaluation of guardrail systems using LS-DYNA. Orengo et al. (2003) presented a method to model tire deflation in LS-DYNA simulations along with examples to use the model. The simulation results showed that deflated tires had significantly different behaviors from those of inflated tires, as observed in real world crashes and in full-scale crash tests. Vehicles' kinematics was found to be strongly coupled to the behaviors of deflated tires; therefore, modeling such behaviors was critical to roadside hardware simulations. Ray et al. (2004) used LS-DYNA simulations to determine if an extruded

aluminum bridge rail would pass the full-scale crash tests for test levels 3 and 4 conditions of the NCHRP Report 350. The simulation results, which were supported by a subsequent AASHTO load and resistance factor design (LRFD) analysis, indicated a high likelihood of passing the crash tests.

FE simulations have also been used by researchers at the Midwest Roadside Safety Facility (MwRSF). Reid (1996) utilized FEA to study the influence of material properties on automobile crash structures and attempted to develop crashworthiness guidelines for design engineers. In one of his later works, Reid (1998) demonstrated through two simple examples of the potential modeling issues that could be easily overlooked in FE impact simulations: contact definition and damping. He also suggested ways to check for modeling errors and to make improvements. In the work of Reid and Bielenberg (1999), FE simulations were performed for a bullnose median barrier crashed by a 4,405-lbs (2000-kg) pickup truck to determine the cause of failure and to obtain a potential solution to the problem. In a collaborative work to improve the FE model of a Chevrolet C2500 pickup truck (Reid and Marzougui 2002; Tiso et al. 2002), structural modeling methods were introduced for model improvement through refining meshes, using more sophisticated material models, adding details to simplified components, and improving connections between components. Suspension modeling, which was critical to the correct vehicle dynamic responses, was also investigated in this collaborative work and a new model was successfully developed with significant improvements.

To educate roadside safety engineers and promote the use of simulations, Reid (2004) summarized ten years of the simulation efforts at MwRSF on the development of new roadside safety appurtenances. In the work of Reid and Hiser (2004), they studied the friction effects, particularly between solid elements, on component connections and interactions in crash modeling and analysis. In their work on modeling bolted connections that allowed for slippage, Reid and Hiser (2005) investigated two modeling techniques that were based on discrete-spring clamping and stressed clamping model using deformable elements. The simulation results for both models compared well with test data, with the stressed clamping model using deformable elements having better accuracy accompanied by significantly increased computational cost. Hiser and Reid (2005) also investigated improved FE modeling methods for slip base structures, which could have a considerable potential for reducing the amount of crash resistance and thus occupant injury when struck by errant vehicles. They developed and evaluated two bolt preloading methods, with one using discrete spring elements and the other using pre-stressed solid elements. Similar to their findings in the work of modeling hook-bolts, they found that the method using solid elements was more accurate than that using discrete spring elements when the impact conditions became more severe. As a result, the model using pre-stressed solid elements was incorporated into the FE model of a cable guardrail system. The results showed that the slip base model was acceptable in both end-on impact and length of need impact simulations.

In 2009, Reid et al. (2009) investigated the potential of increasing the suggested flare rates for strong post W-beams to reduce guardrail installation lengths, which would result in decreased guardrail construction and maintenance costs, and reduce the impact frequency. Both computer simulations and full-scale crash tests were used in the evaluation of increased

flare rates up to, and including, 5H:1V. Simulation results indicated that the conventional G4(1S) guardrail modified to incorporate a routed wood block-out could not successfully meet NCHRP Report 350 crash test criteria when installed at any flare rates steeper than the recommended 15H:1V in the Roadside Design Guide. Their study also showed that the MGS could meet NCHRP Report 350 impact criteria when installed at a 5H:1V flare rate, yet with greater impact severities observed from the tests than anticipated. Reid et al. also indicated that whenever roadside or median slopes are relatively flat (10H:1V or flatter), increasing the flare rate on guardrail installations became practical and had some major advantages including significantly reducing the guardrail lengths and associated costs. The study, however, did not give any indications of W-beam performance on steeper slopes.

FE simulations were also found in the work of other researchers in roadside safety research. Whitworth et al. (2004) evaluated the crashworthiness of a modified W-beam guardrail using detailed FE models of a guardrail and a Chevrolet C2500 pickup truck. The simulation results were compared and found in agreement with crash test data in terms of roll and yaw angles. Simulations were also performed to evaluate the effects of certain guardrail design parameters, such as rail mounting height and routed/non-routed block-outs, on the crashworthiness and safety performance of the system. In the work of Bligh et al. (2004), FEA was utilized to develop new roadside features to address three roadside safety issues. An alternative design to the popular T6 tubular W-beam bridge rail was developed to address problems with vehicle instability observed in full-scale crash testing. A retrofit connection to TxDOT's grid-slot portable concrete barrier was developed to limit dynamic barrier deflections to levels that were more practical for work zone deployments. Finally, crashworthy mow strip configurations were developed for use when vegetation controls around guard fence systems were desired to reduce the cost and risk associated with hand mowing.

Computer simulations were also used by international researchers on roadside safety research. Using LS-DYNA simulations, Atahan (2002) analyzed a strong-post W-beam guardrail system that failed in a previously conducted full-scale crash test. After identifying the cause of failure and incorporating necessary improvements, a new W-beam guardrail was developed and showed improved performance based on simulation results. Atahan (2003) also studied the performance of G2 steel weak-post W-beam guardrail installed at the slope-break point on non-leveled terrains using LS-DYNA simulations. The simulation results showed that there was a risk of increased vehicle instability when the roadside slope adjacent to the W-beam guardrail became steeper than 6H:1V. Atahan and Cansiz (2005) investigated the failure of a bridge rail-to-guardrail transition design used in a full-scale crash test in which the vehicle rolled over the guardrail. They used full-scale models in their LS-DYNA simulations to replicate the crash tests and identified the root cause of the failure that was attributed to the low height of the W-beam rails. In the work by Atahan (2007), LS-DYNA simulations were used to study the crashworthiness behavior of a bridge rail-to-guardrail transition structure under 17,637 lbs (8,000 kg) of impact load. This work demonstrated the effectiveness of FE simulations for its reliability of replicating the actual dynamic interactions and mechanics of the crash. Atahan also pointed out that the use of a real soil model other than the simplified spring soil model could improve the accuracy of FE simulations but would significantly increase the computational costs.

Using LS-DYNA simulations, Fang et al. (2010) conducted a study to evaluate the performance of three types of barriers on sloped medians: a single-faced W-beam guardrail, two designs of double-faced W-beam guardrails, and a low-tension cable barrier. The three types of barriers were evaluated under vehicular impacts at multiple speeds and impact angles. The simulation results suggested that the effectiveness of the W-beam guardrails and cable barriers could be reduced on sloped medians compared to their performance on flat terrain as specified in the NCHRP Report 350. It was observed that the tendency and severity of vehicle rollover increased with the increase of impact angles while holding other conditions constant. This observation was shown to be true for the single-faced W-beam guardrail, both designs of the double-faced W-beam guardrails, and cable barriers. It was also observed that the performance of the barriers investigated in this project exceeded the TL-3 requirements of the NCHRP Report 350 considering the large median slopes (4H:1V and 2.5H:1V) and the higher impact speeds than the standard impact conditions.

The vehicular impact height is one of the important parameters in evaluating the performance of barrier systems. The vehicle's impact height can vary depending on the trajectory of the vehicle along the median and the lateral offset of the barrier. The performances of the modified G4(1S) W-beam guardrail, modified Thrie-beam guardrail, Midwest Guardrail System, and modified weak post W-beam guardrail were analyzed by Ferdous et al. (2011) using LS-DYNA. Each model was validated based on the results obtained from existing crash tests. Using vehicle models from NCHRP Report 350, the override and under-ride limits for each guardrail model were identified. The performance limit of each barrier was determined by parametrically varying the vehicle impact height to determine at what point the override or rollover for the pickup truck and under-ride for the small passenger car would occur.

In 2012, Marzougui et al. (2012) investigated some barrier systems that passed the NCHRP Report 350 requirements but failed to pass the MASH requirements to determine if the barrier systems could be retrofitted with various modifications to improve the performance. These modifications was conducted on six G9 Thrie-beam guardrails and three G4(1S) W-beam guardrails using FE simulations. The simulation results showed that with the proposed modifications, the guardrails that originally failed to pass the MASH requirements were able to retain the vehicle under MASH TL-3 conditions and to reduce the propensity to vault over the guardrails.

Hampton et al. (2013) performed a similar simulation to those in the work of Marzougui et al. (2012) in an effort of evaluating the performance of strong-post W-beam guardrails with missing posts under impact conditions specified by the NCHRP Report 350. The effects of missing posts on the guardrails performance were quantitatively evaluated using FE models of crash tests under impacts of a 4,409-lbs (2,000-kg) pickup truck. Simulations in which one, two, or three posts were removed from the guardrails were conducted with varying points of impact to evaluate the effects of missing posts. The FE simulation results demonstrated that guardrails missing even one post could have remarkably decreased performance under vehicular impacts due to wheel snagging. It was also observed that both the maximum deflection and maximum rail tension were greatly increased as more posts were removed from the guardrail. The overall conclusion of the study was that even if one

post was missing, the guardrail performance could be significantly reduced and post replacement should be a high-priority repair for guardrail maintenance.

FE simulations, particularly conducted with LS-DYNA, have been used increasingly more in roadside safety research. In addition to the abovementioned references, FHWA published several manuals on using LS-DYNA material models and evaluation of these models (Lewis 2004; Murray et al. 2005; Murray 2007; Reid et al. 2004). These references can also be useful in the crash modeling work using LS-DYNA.

3. Finite Element Modeling of Vehicles and W-beam Guardrails

The simulation work of this project included two vehicles models (i.e. 1996 Dodge Neon and 2006 Ford F250) and three guardrail models (i.e., the 27-, 29-, and 31-inch single-faced G4(1S) strong-post W-beam guardrails). Crash simulations were performed for all three guardrails under MASH TL-2 conditions. For the 29- and 31-inch guardrail, simulations were also performed to evaluate their performance under MASH TL-3 conditions. The FE models of the passenger car, pickup truck, and a single-faced G4(1S) W-beam guardrail were obtained from NCAC and modified to correct modeling issues and suit the needs of this project. The 29- and 31-inch guardrail models were developed from the 27-inch guardrail model according to NCDOT design specifications.

In all simulation cases, the vehicle left the shoulder at the prescribed speeds; therefore, vehicle trajectories were included in these simulations. The impact speeds were defined in the vehicle's travel direction, and the impact angle was defined as one between the vehicle's travel direction and the longitudinal direction of the barrier. The vehicle's initial impact point on the W-beam guardrail was in the middle of the effective barrier length and at the location of a rail splice.

3.1 FE Models of a Passenger Car and Pickup Truck

The vehicle models used in this project were a 1996 Dodge Neon passenger car and a 2006 Ford F250 pickup truck, as shown in Figure 3.1. The 1996 Dodge Neon had a curb weight of 2,403 lbs. (1,090 kg), overall length of 171.8 in (4.36 m), overall width of 67.5 in (1.71 m), overall height of 52.8 in (1.34 m), and ground clearance of 5.7 in (145 mm). The 2006 Ford F250 had a curb weight of 5,504 lbs. (2,499 kg), overall length of 226.4 in (5.75 m), overall width of 79.9 in (2.03 m), overall height of 76.5 in (1.94 m), and ground clearance of 8.3 in (211 mm).

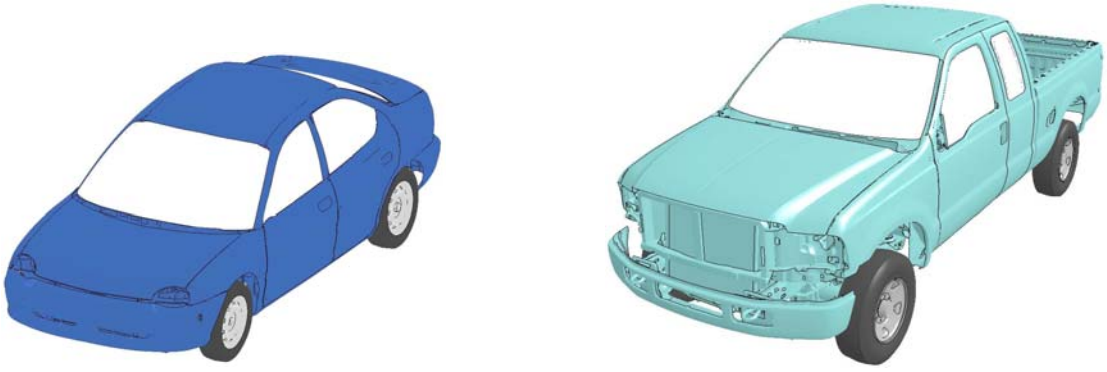

a. 1996 Dodge Neon b. 2006 Ford F250

Fig. 3.1: Finite element models of two vehicles used in crash simulations.

The FE model of the 2006 Ford F250 contained a total of 746 parts that were discretized into 737,990 nodes and 736,407 elements (25,905 solid, 2,305 beam, 707,656 shell, and 541 other elements). Eleven different constitutive models were used including the piecewise linear

plasticity model defined for most steel components, the linear and nonlinear elastic spring model for the suspension springs, the viscous damping model for the shock absorbers, the low-density foam model for the radiator core, the spot-weld model for sheet metal connections, the viscos-elastic model for rubber cushions, and the null material model defined for 48 parts for contact purposes. Hourglass control was used on various components that could potentially experience large deformations. The FE model of the F250 was originally developed at NCAC and validated using frontal-impact tests that were conducted on flat terrain according to the Federal Motor Vehicle Safety Standards and Regulations (FMVSS).

The FE model of the 1996 Dodge Neon contained a total of 339 parts that were discretized into 283,683 nodes and 270,727 elements (2,852 solid, 92 beam, 267,775 shell, and 8 other elements). Ten different constitutive models were used including the piecewise linear plasticity model defined for most steel components, the elastic model for the tires and a few other components, the viscous damping model for the shock absorbers, the low-density foam model for the radiator core, the spot-weld model for sheet metal connections, the Blatz-Ko rubber model for nearly incompressible rubber cushions, the rigid model for most mounting hardware, and the null material model defined for contact purposes. Hourglass control was used on various components that could potentially experience large deformations. The FE model of the Dodge Neon was originally developed at NCAC and validated with the NHTSA's Frontal New Car Assessment Program (NCAP) tests.

Simulations of the vehicles crashing into roadside barriers imposed significant challenges to the numerical models due to the large, nonlinear deformations and the large numbers of components being in contact. For example, in the simulations of the Ford F250 crashing into the W-beam guardrail, the W-beam rails and the vehicle's fender experienced severe deformations. The vehicle's wheel, fender, bumper cover, suspension, and a number of other parts were in contact with the guardrail post, rail, and bolts. These contacts needed to be handled by selecting the appropriate contact algorithms to eliminate the unrealistic penetrations of the elements. Otherwise, the simulations would encounter great numerical difficulties, resulting in premature termination of unrealistic behaviors of the vehicle and/or guardrail (e.g., the vehicle being entangled with the guardrail components). The Ford F250 initially experienced contact issues that was caused by the tow hook elements (on the front of the vehicle) impacting and penetrating the guardrail and becoming entangled. The contact definition between these two parts was investigated and modified to ensure a proper contact definition was used. The FE model of the Dodge Neon experienced a similar issue with the bumper elements penetrating the guardrail and becoming entangled due to contact definition that was used. The contact definition between the vehicle's bumper and the guardrail was investigated and changed to resolve this contact issue. Before running simulations for this project, simulations were conducted using the Ford F250 and the Dodge Neon to ensure appropriate contacts being defined for all parts in the guardrail and the vehicles.

3.2 FE Models of the W-beam Guardrails

The single-faced G4(1S) W-beam guardrail was originally developed at NCAC. It contained six different constitutive models including the piecewise linear plasticity model defined for most steel components, the elastic model for the wood block-outs and terminal posts, the soil

and foam model used for the soil blocks, the rigid model for the bolts and road surface, the nonlinear elastic spring model used for the bolt-tensioning spring (used on the long-bolts connecting the W-beam rails and wood block-outs to the posts), and the null material model used for contact purposes. In the original NCAC model, the soil around each post was a cylindrical block meshed into irregularly shaped solid elements. In this project, the guardrail model including the soil foundations was obtained from a previous NCDOT research project (Fang et al., 2010) in which an FE model of a square soil foundation was developed for use on both flat terrains and sloped medians (with minor modifications). The FE model of the square soil foundation was compared and found identical to the circular soil model using simulations of a vehicular crash test. The square soil model used the same material model and properties as the original NCAC soil model. Figure 3.2 illustrates the original, circular-shaped soil model and the square-shaped soil models developed for this project. This square-shaped soil model was used with the 400-ft (121.9-m) W-beam guardrail installed on a flat terrain, which is the site condition for this project.

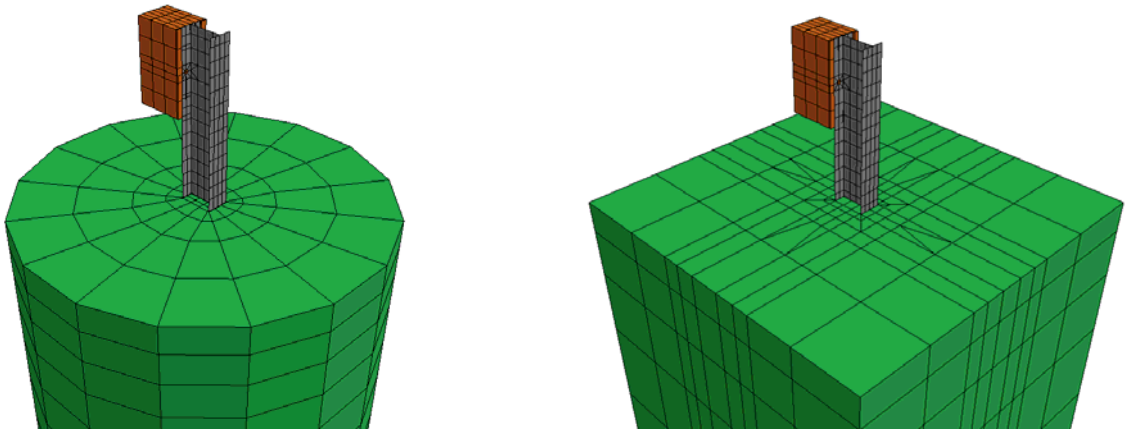

a. Circular soil foundation

b. Square soil foundation

Fig. 3.2: The FE soil models for guardrail posts.

In addition to modifications on the soil model, other modeling issues were found in the original guardrail model, e.g., penetrations among the components. By eliminating penetrations and changing contact algorithms in the modified guardrail models, these issues were resolved with improved numerical stability and accuracy of the simulations. To reduce the computational cost of the simulations and further improve the numerical stability, the guardrail models were simplified on the bolt connections of the rail splices. Figure 3.3 illustrates the location of a guardrail splice where the two W-beam rail sections (colored differently for ease of viewing) are

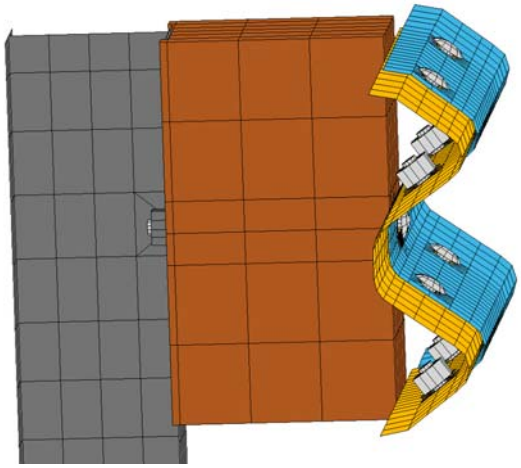

Fig. 3.3: Short-bolts on a guardrail splice.

joined and secured by eight short-bolts. In the original guardrail model, these short-bolts incorporated a failure mechanism that could separate the bolt and nut upon reaching the failure point (defined by a threshold value of the force). While realistic and capable of emulating the bolt's behavior, these bolt connections were modeled with their individual components and thus were computationally expensive. It was determined through simulation testing that these short-bolts would never reach their failure point under the impact conditions used in this research. Therefore, the failure mechanism was removed from these short-bolts and the component models were also simplified. In addition, there were 24 parts defining the short-bolts on a single splice (672 parts for the entire 400-ft section) in the original guardrail model. These parts were combined into one (1) part per splice (28 parts for the entire 400-ft section) in the updated model. The simplifications along with resolutions to other contact issues (e.g., initial penetrations due to mismatched geometries) were found to significantly improve the FE model's stability and efficiency.

Once the segment of the G4(1S) guardrail was effectively modified, it was duplicated to create the entire 400-ft (122-m) section of the guardrail required for this project. This duplication of the guardrail section was done with an in-house code developed to replicate not only the parts, nodes, elements, and material properties, but also the contact definitions defined between each pair of parts. The program was also capable of merging the ends of adjacent segments with proper numbering and contact definitions. With this program, the guardrail model was generated by duplicating the length of need section and connecting to two terminal sections obtained from the original guardrail model. For the 29- and 31-inch guardrail models, the FE models of the segments were first created according to NCDOT specifications and the entire guardrail models were created with this duplication program.

3.3 Simulation Setup

The three guardrail models were combined with the two vehicle models, respectively, to conduct the simulation work of this project. Figures 3.4 and 3.5 show the simulation models of the 27-inch guardrail, one with the Dodge Neon and the other with the Ford F250.

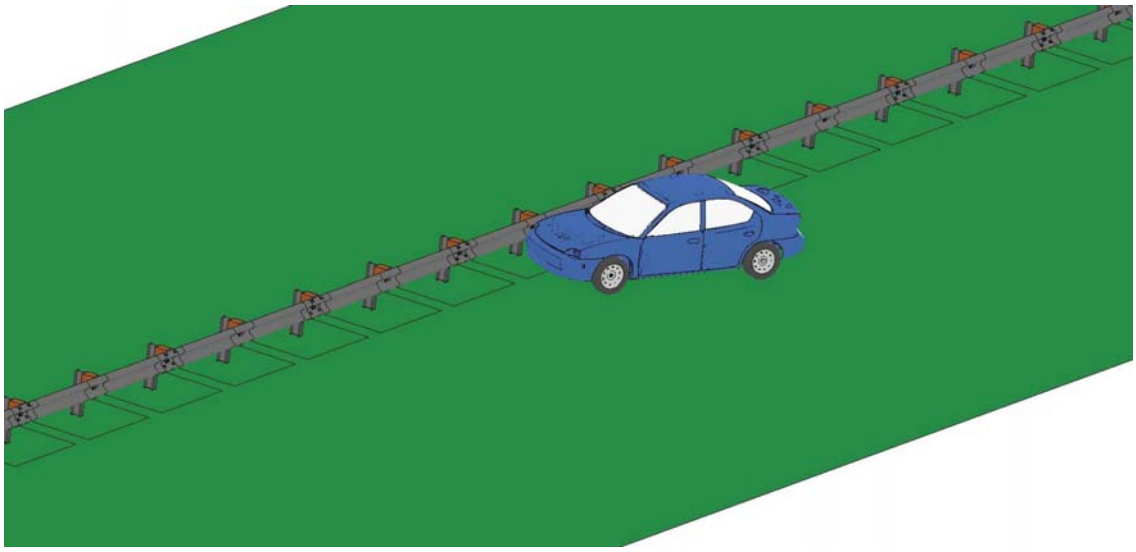

Fig. 3.4: Simulation model of the 27-inch guardrail impacted by a Dodge Neon.

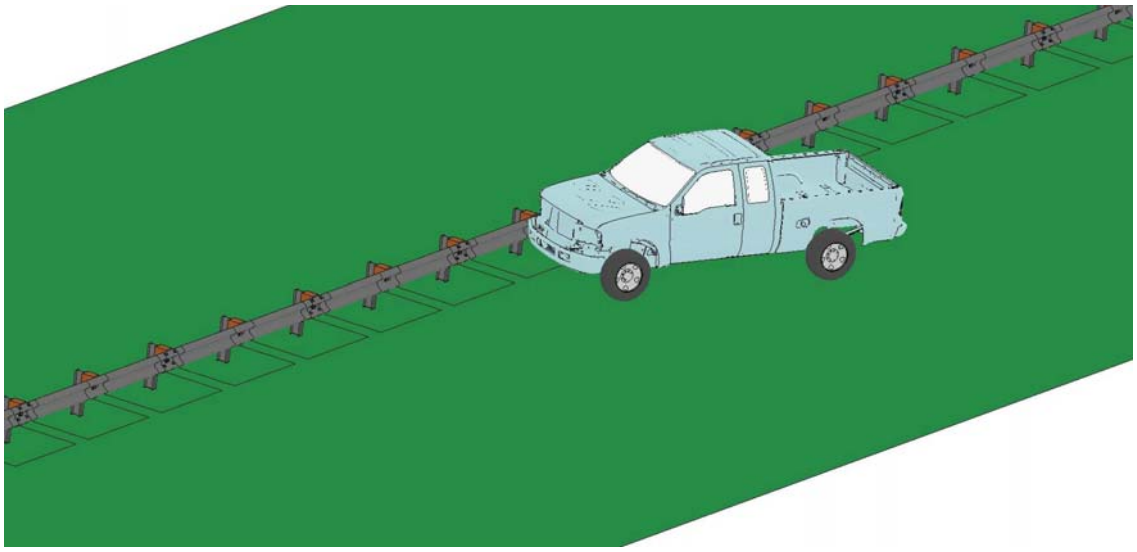

Fig. 3.5: Simulation model of the 27-inch guardrail impacted by a Ford F250.

The simulation work of this project was categorized into five major cases. Case 1 involved two simulations for the 27-inch guardrail conducted under MASH TL-2 conditions for both vehicles. Cases 2 and 3 involved four vehicular impact simulations for the 29-inch guardrail, two under MASH TL-2 and two under TL-3 conditions. Cases 4 and 5 involved four vehicular impact simulations for the 31-inch guardrail, two under MASH TL-2 and two under TL-3 conditions. Table 3.1 gives a summary of the five cases with their respective impact angles and speeds.

Table 3.1: Categories of simulation work

Case No.	Guardrail Height	Test Vehicle	MASH Impact Conditions	Impact Angle	Impact Speed
1	27 inches	Dodge Neon	TL-2	25°	44 mph (70 km/hour)
		Ford F250		25°	44 mph (70 km/hour)
2	29 inches	Dodge Neon	TL-2	25°	44 mph (70 km/hour)
		Ford F250		25°	44 mph (70 km/hour)
3	29 inches	Dodge Neon	TL-3	25°	62 mph (100 km/hour)
		Ford F250		25°	62 mph (100 km/hour)
4	31 inches	Dodge Neon	TL-2	25°	44 mph (70 km/hour)
		Ford F250		25°	44 mph (70 km/hour)
5	31 inches	Dodge Neon	TL-3	25°	62 mph (100 km/hour)
		Ford F250		25°	62 mph (100 km/hour)

Based on discussions with NCDOT engineers, the most critical impact scenario was considered as one in which the vehicle impacted directly at the guardrail spice where two W-beam rails were connected together and attached to the post. The vehicles in the simulations

were positioned in such a way that the impact location was at the location of a splice. The vehicles were positioned with an in-house code to ensure the correct location and the correct impact angle. Figure 3.6 shows the vehicles translated to a point in which they impacted a spliced guardrail section with the prescribed impact angle.

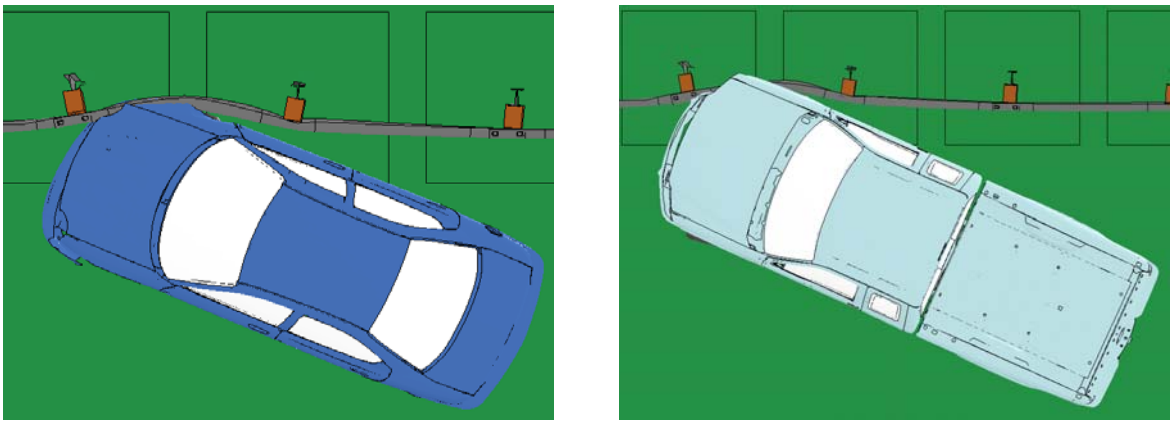

Fig. 3.6: A Dodge Neon (left) and Ford F250 (right) impacting a spliced guardrail section.

4. Simulation Results and Analysis

In this section, the FE simulation results for the five cases listed in Table 3.1 are presented. Simulations for Case 1 were for vehicles crashing into the 27-inch W-beam guardrail under MASH TL-2 conditions. Cases 2 and 3 were for vehicles crashing into the 29-inch W-beam guardrail under MASH TL-2 and TL-3 conditions, respectively. Cases 4 and 5 were for vehicles crashing into the 31-inch high W-beam guardrail under MASH TL-2 and TL-3 conditions, respectively. For each barrier height and impact condition, simulations were performed using both the 1996 Dodge Neon and 2006 Ford F250.

In order to assess the post-impact vehicular trajectory, the MASH exit box criterion was used to classify vehicular responses from the simulation results. This exit box criterion was designed to determine vehicle redirection based on the certain vehicular responses after impacting the barrier. Figure 4.1 illustrates the definition of the exit box, which begins at the point of vehicle's last contact with the barrier. If all four wheels remain inside the exit box for the distance *B*, the case is considered to be a safe redirect according to the exit box criterion. It should be noted that a large exit angle and/or spin-outs may still be present even for a case determined as a safe redirect. The large vehicular exit angles and spin-outs can be caused by pocketing and snagging of the vehicle on the guardrail posts. Although the exit box criterion is a useful tool for determining the post-impact vehicular trajectories, use of this criterion alone is not sufficient to determine if the vehicle has been safely redirected. The dimensions of the exit box can be determined using the equations and data in Table 4.1 in which the width of the exit box is determined by a constant plus the vehicle's width, V_W, and sixteen percent (16%) of the vehicle's length, V_L.

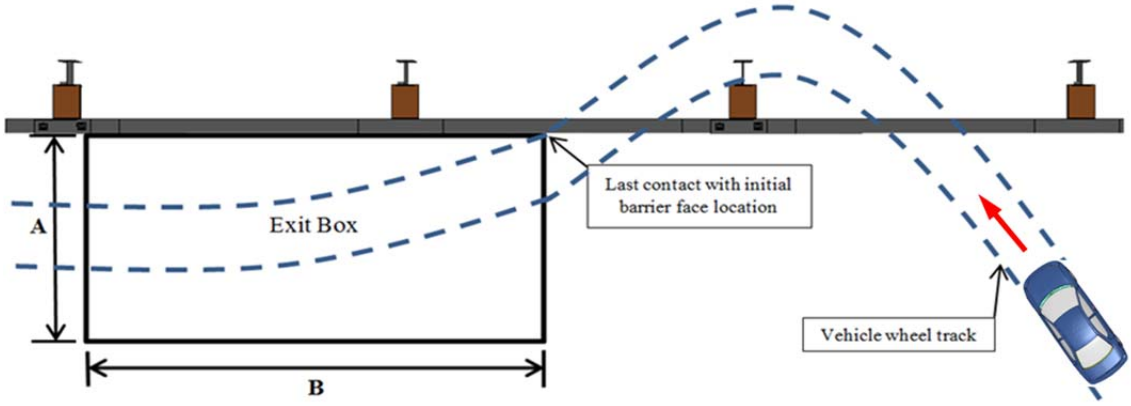

Fig. 4.1: Exit box criterion in MASH.

Table 4.1: The exit box criterion defined in MASH

Vehicle Type	Exit Box Dimension	
	A	**B**
Cars or Pickup Trucks	$7.2 + V_W + 0.16V_L$ (*ft*)	32.8 *ft* (10 *m*)
Other Vehicles	$14.4 + V_W + 0.16V_L$ (*ft*)	65.6 *ft* (20 *m*)

The exit box criterion for the Dodge Neon and Ford F250 were calculated and used to assess the post-impact vehicular responses from the simulation results. The exit box dimensions for both vehicles are given in Table 4.2. Throughout this section, the exit box for each simulation is shown in the vehicle's displacement path and denoted by the dotted yellow lines.

Table 4.2: Exit box dimensions for the test vehicles of this project

Vehicle	***A*** *ft* (*m*)	**B** *ft* (*m*)
1996 Dodge Neon	15.1 (4.6)	32.8 (10.0)
2006 Ford F250	16.9 (5.15)	32.8 (10.0)

4.1 The 27-inch W-beam Guardrail

The analysis of the 27-inch G4(1S) strong-post W-beam guardrail was performed through two simulations of Case 1, for vehicular impacts of both the 1996 Dodge Neon and the 2006 Ford F250 under MASH TL-2 conditions. Table 4.3 shows the simulation conditions and a summary of the guardrail performance in terms of vehicular responses.

Table 4.3: Simulation results of the 27-inch W-beam guardrail under MASH TL-2 conditions

Guardrail Height	**Impact Speed**	**Impact Angle**	**MASH Test Level**	**Test Vehicle**	**Test Results**
27 inches	44 mph (70 km/hour)	25°	TL-2	Dodge Neon	Vehicle redirected by guardrail
	44 mph (70 km/hour)	25°	TL-2	Ford F250	Vehicle redirected by guardrail (with a relatively large exit angle)

Figure 4.2 shows the displacement path of the Dodge Neon with the W-beam guardrail shown in its original shape and the exit box denoted by the yellow rectangle in dotted lines. The yaw, pitch, and roll angles of the Dodge Neon are shown in Figure 4.3. The exit angle of the Dodge Neon was determined to be 15°, which was calculated by subtracting the impact angle (25°) from the yaw angle at exit (40°). Figure 4.4 shows the permanent deformation of the guardrail after being impacted by the Dodge Neon. It can be seen that the damaged guardrail sections are small and localized; this serves as an indication of relatively low-severity impact from the small car. Figure 4.5 shows the detailed views of four instances of vehicle-barrier interactions. Figure 4.6 shows the time histories of transverse displacements and velocities measured at the center of gravity (CG) point of the vehicle. The transverse velocities, along with the exit angle, could be used to determine if a redirection was safe or temporary. For example, if the transverse velocity of a redirected vehicle remained large, the redirection could be followed by a secondary collision if the exit angle was also large. For the case of the Dodge Neon, the results in Figures 4.2 to 4.6 showed that it was safely redirected by the guardrail. The roll and pitch angles of this case were less than five degrees in either positive or negative direction; they passed the MASH evaluation criterion F, which specified a maximum 75° rotation.

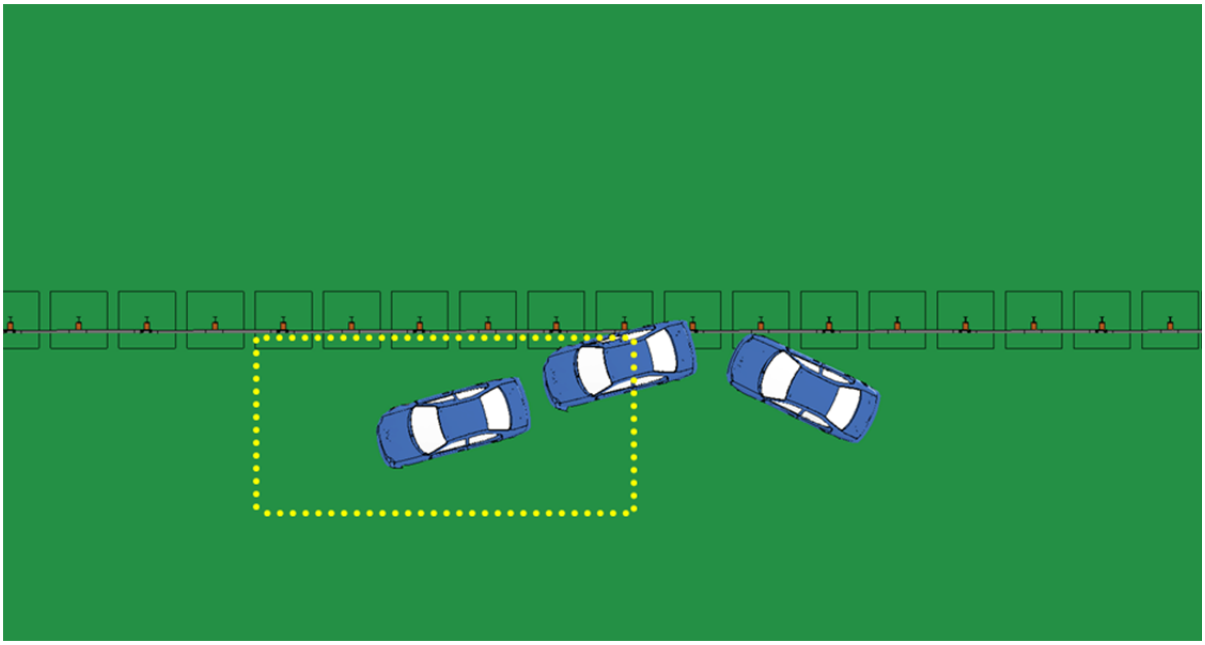

Fig. 4.2: A Dodge Neon impacting the 27-inch guardrail at 44 mph and 25°.

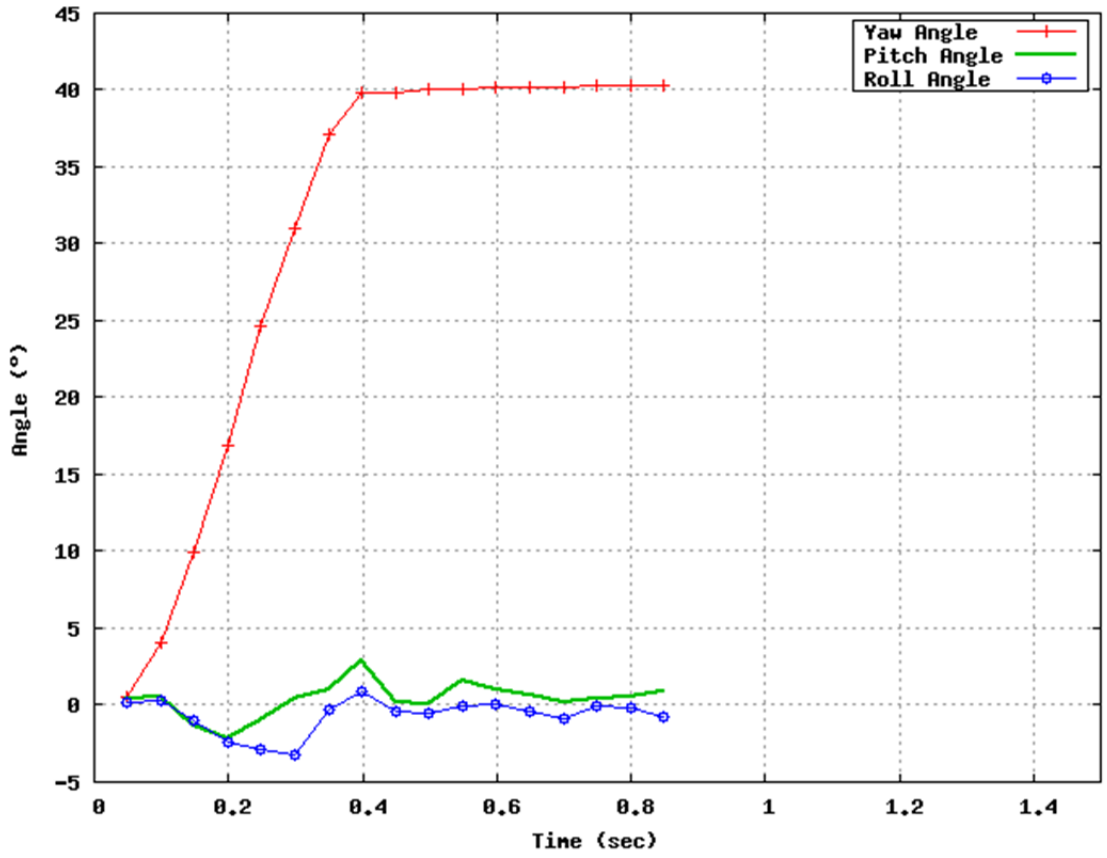

Fig. 4.3: Yaw, pitch, and roll angles of Dodge Neon impacting the 27-inch guardrail at 44 mph and 25°.

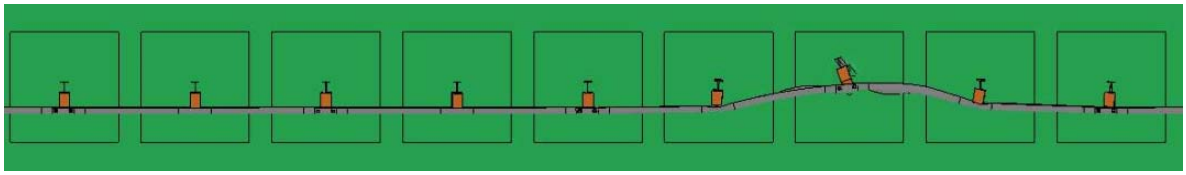

Fig. 4.4: Permanent deformation of the 27-inch guardrail impacted by a Dodge Neon at 44 mph and 25°.

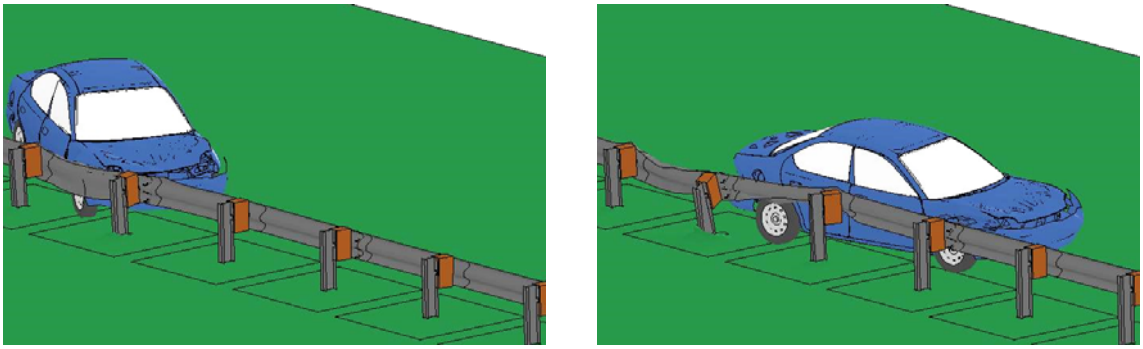

Trimetric view

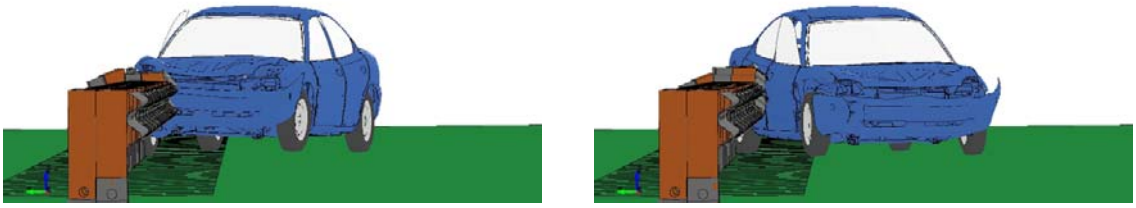

Front view

Fig. 4.5: Four instances of Dodge Neon impacting the 27-inch guardrail at 44 mph and 25°.

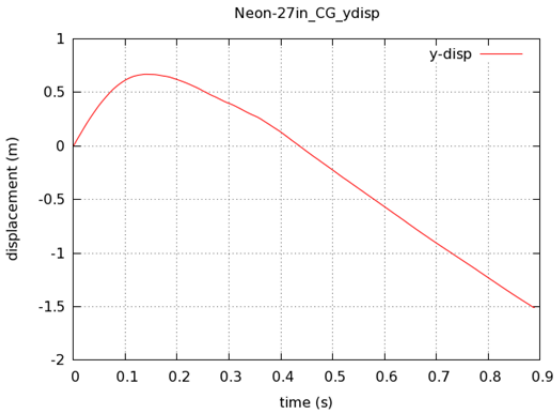

Transverse displacements

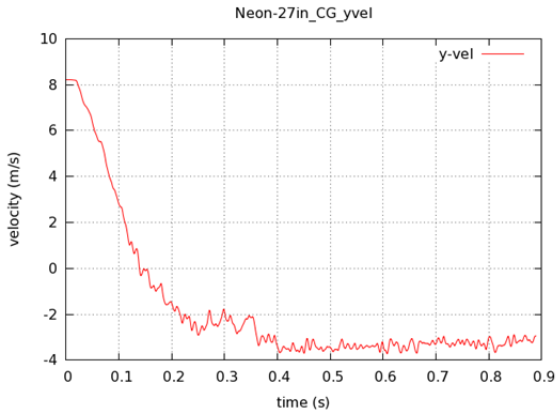

Transverse velocities

Fig. 4.6: Time histories of transverse displacements and velocities of the Dodge Neon impacting the 27-inch guardrail at 44 mph and 25°.

Under the impact of the Ford F250 at 44 mph (70 km/hour) and 25°, the 27-inch W-beam guardrail had a significantly larger deformed section than that under the impact of the Dodge Neon, as shown in Figure 4.7. This was caused by the significantly increased vehicle mass compared to the Dodge Neon. Despite the large increase of vehicle mass, the 27-inch guardrail was able to redirect the Ford F250 on the shoulder.

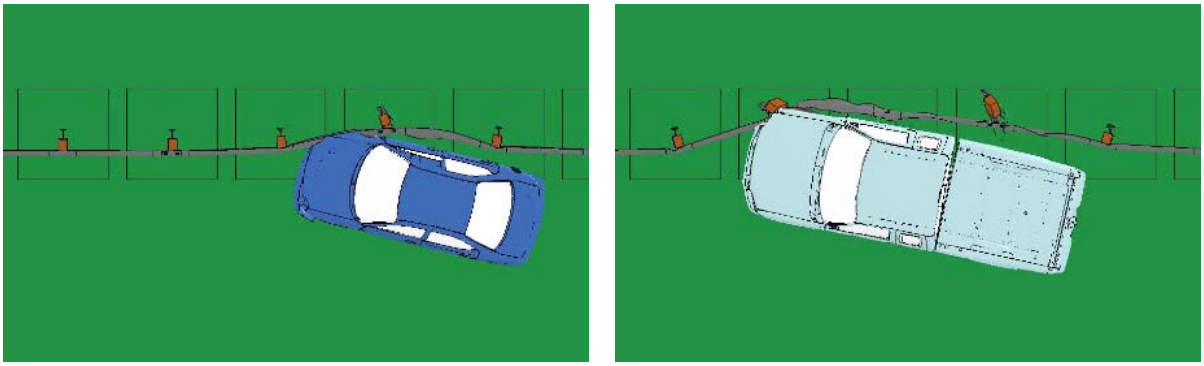

Guardrail impacted by Dodge Neon Guardrail impacted by Ford F250

Fig. 4.7: Comparison of dynamic deformation of the 27-inch guardrail under impacts at 44 mph and 25°.

Figure 4.8 shows the displacement path of the Ford F250 with the guardrail shown in its original shape and the exit box denoted by the yellow rectangle in dotted lines. It can be seen that the exit box criterion was satisfied. The yaw, pitch, and roll angles of the Ford F250 are shown in Figure 4.9. The exit angle of the Ford F250 was determined to be 38°, which was calculated by subtracting the impact angle (25°) from the yaw angle at exit (63°). Figure 4.10 shows the permanent deformation of the guardrail after being impacted by the Ford F250 and Figure 4.11 shows the detailed views of four instances of vehicle-barrier interactions. Figure 4.12 shows the time histories of transverse displacements and velocities measured at the CG point of the Ford F250. For the case of the Ford F250, the exit angle was relative large compared to the case of the Dodge Neon. As previously discussed, a high exit angle, along with a high transverse velocity, imposed an increased probability of reentering the traffic lane and causing a secondary collision. As for the roll and pitch angles, they were found to be well within five degree in either positive or negative direction, well below the 75 degree maximum rotation set by the MASH evaluation criterion F.

The results in Figures 4.8 to 4.12 showed that the 27-inch guardrail was able to redirect the Ford F250 at 44 mph (70 km/hour) and 25°. Along with results of the Dodge Neon, it was determined that the 27-inch W-beam guardrail met the MASH TL-2 requirements.

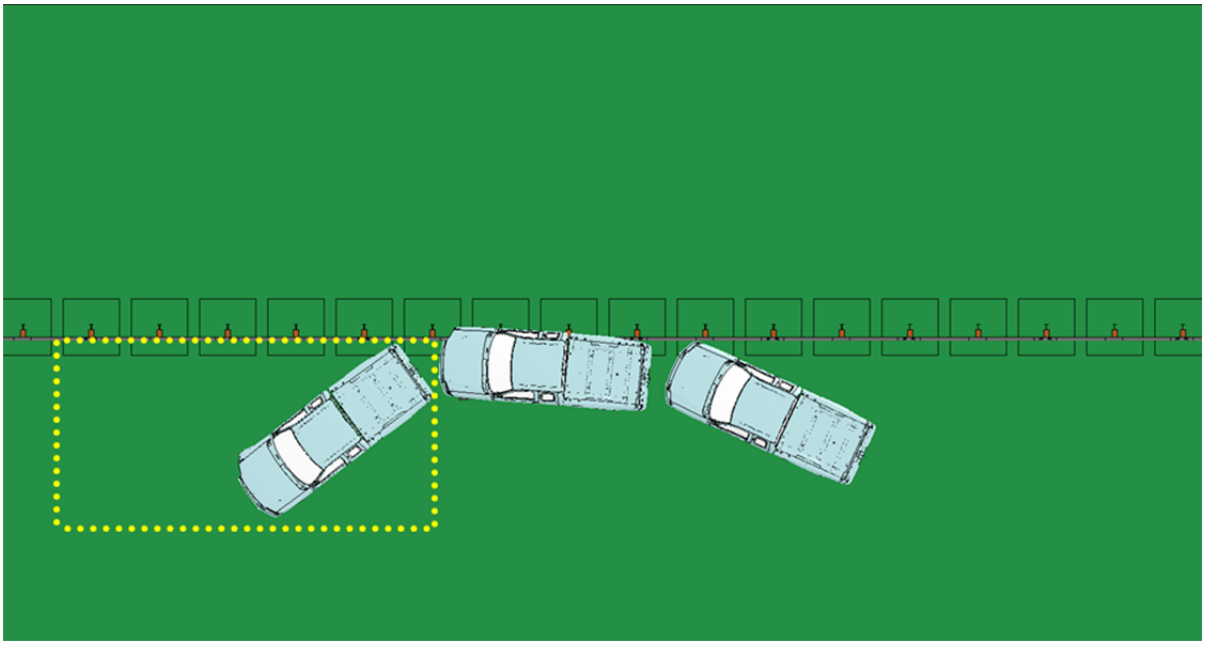

Fig. 4.8: A Ford F250 impacting the 27-inch guardrail at 44 mph and 25°.

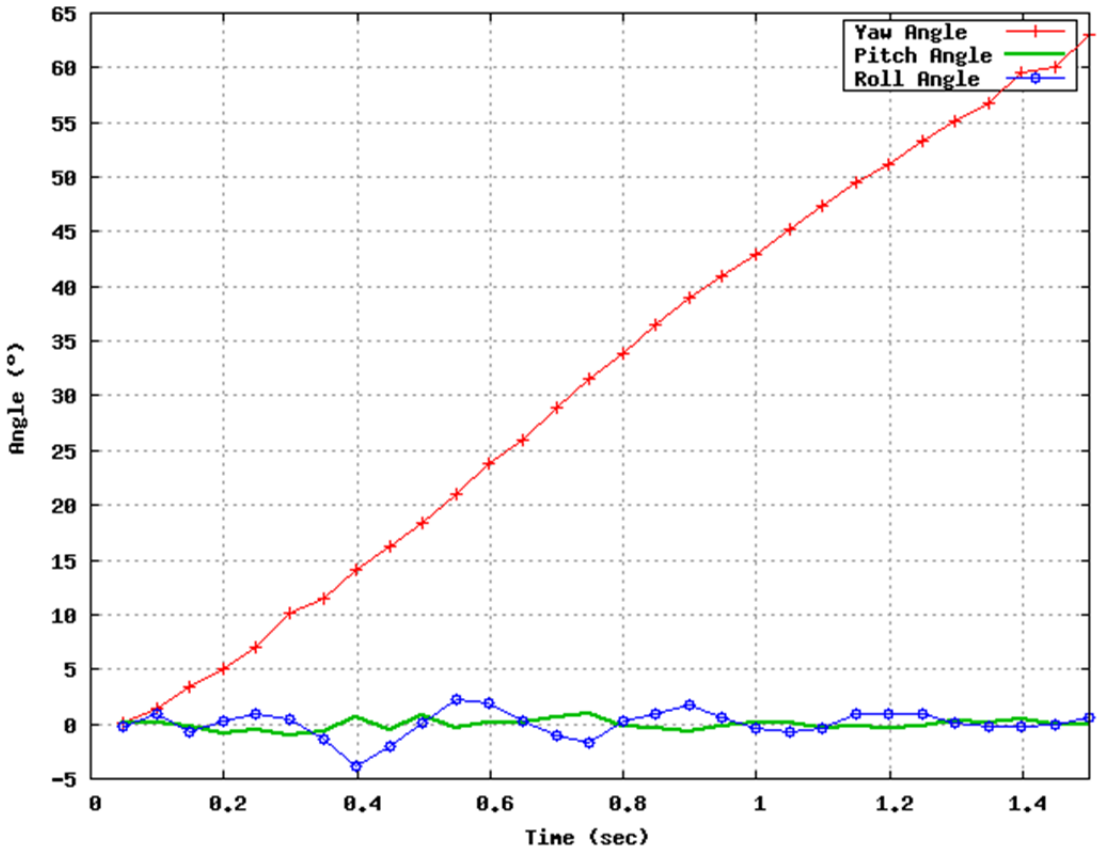

Fig. 4.9: Yaw, pitch, and roll angles of Ford F250 impacting the 27-inch guardrail at 44 mph and 25°.

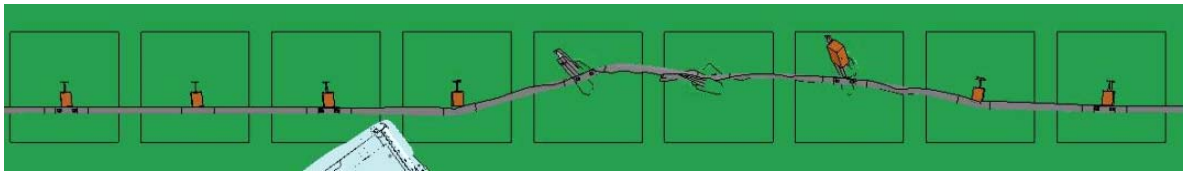

Fig. 4.10: Permanent deformation of the 27-inch guardrail impacted by a Ford F250 at 44 mph and 25°.

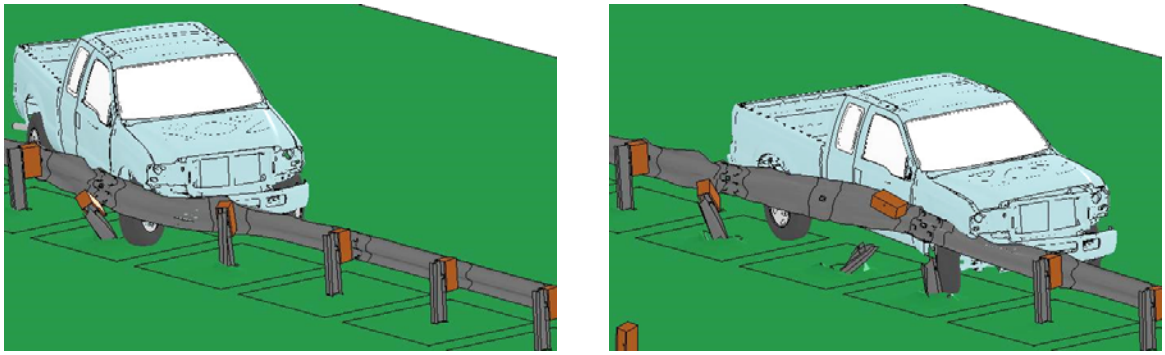

Trimetric view

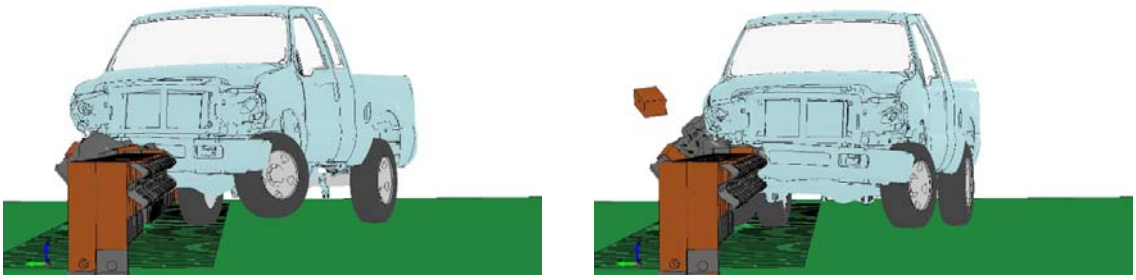

Front view

Fig. 4.11: Four instances of Ford F250 impacting the 27-inch guardrail at 44 mph and 25°.

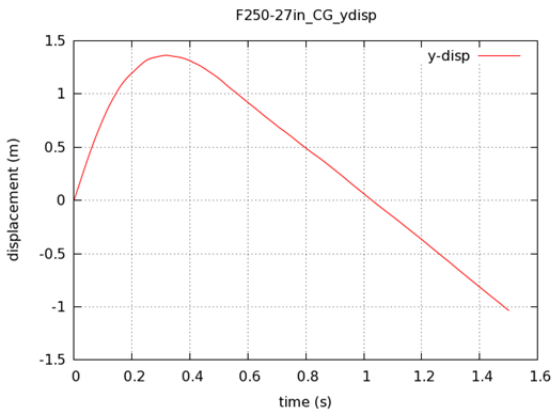

Transverse displacements

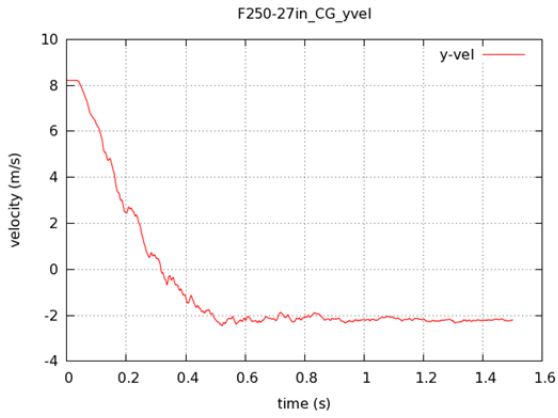

Transverse velocities

Fig. 4.12: Time histories of transverse displacements and velocities of the Ford F250 impacting the 27-inch guardrail at 44 mph and 25°.

4.2 The 29-inch W-beam Guardrail

In this project, the NCDOT 29-inch W-beam guardrail was evaluated under vehicular impacts of the Dodge Neon and Ford F250. The simulations were conducted in two cases, Case 2 and Case 3, for the MASH TL-2 and TL-3 conditions, respectively. The following sections summarized the simulation results for both cases.

4.2.1 The 29-inch Guardrail under MASH TL-2 Conditions

In this case (i.e., Case 2), the 29-inch guardrail was evaluated under MASH TL-2 conditions, i.e., under vehicular impacts of both a Dodge Neon and a Ford F250 at an impact speed of 44 mph (70 km/hour) and an impact angle of 25°. Table 4.4 gives a brief summary of the simulation conditions and results for Case 2.

Table 4.4: Simulation results of the 29-inch W-beam guardrail under MASH TL-2 conditions

Guardrail Height	Impact Speed	Impact Angle	MASH Test Level	Test Vehicle	Test Results
29 inches	44 mph (70 km/hour)	25°	TL-2	Dodge Neon	Vehicle redirected by guardrail
	44 mph (70 km/hour)	25°	TL-2	Ford F250	Vehicle redirected by guardrail

Figure 4.13 shows the displacement path of the Dodge Neon with the W-beam guardrail shown in its original shape and the exit box denoted by the yellow rectangle in dotted lines. The yaw, pitch, and roll angles of the Dodge Neon are shown in Figure 4.14. The exit angle of the Dodge Neon was determined to be 21°, which was calculated by subtracting the impact angle (25°) from the yaw angle at exit (46°). The roll and pitch angles of this case were less than five degrees in either positive or negative direction; these values were well below the maximum limit of 75° rotation as specified by the MASH evaluation criterion F.

Figure 4.15 shows the permanent deformation of the guardrail after being impacted by the Dodge Neon. It can be seen that the damaged guardrail sections are small and localized; this observation is the same as that on the 27-inch guardrail. Figure 4.16 shows the detailed views of four instances of vehicle-barrier interactions. Figure 4.17 shows the time histories of transverse displacements and velocities measured at CG point of the vehicle. The results in Figures 4.13 to 4.17 showed that the 29-inch guardrail had a satisfactory performance under the impact of a Dodge Neon at 44 mph (70 km/hour) and 25°.

Compared to the 27-inch guardrail, the 29-inch guardrail did not exhibit significant performance difference under the impact of the Dodge Neon at MASH TL-2 conditions. The two-inch increase on rail height resulted in a slightly increased exit angle with an indication of no performance gain for small-vehicle impacts.

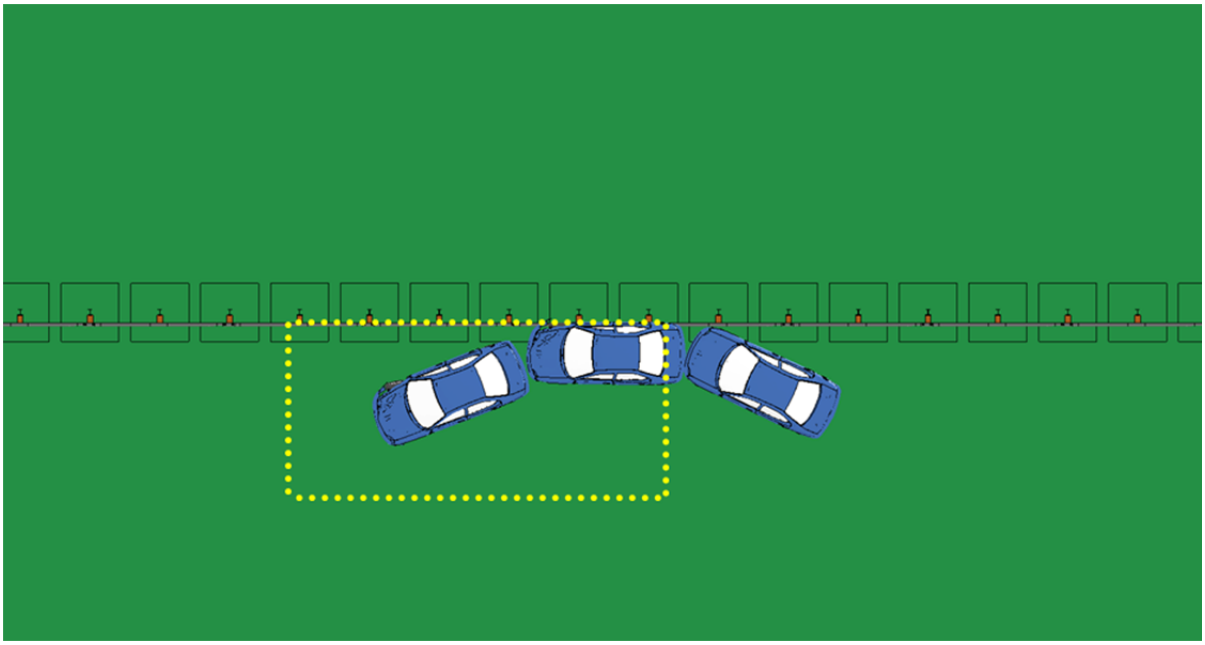

Fig. 4.13: A Dodge Neon impacting the 29-inch guardrail at 44 mph and 25°.

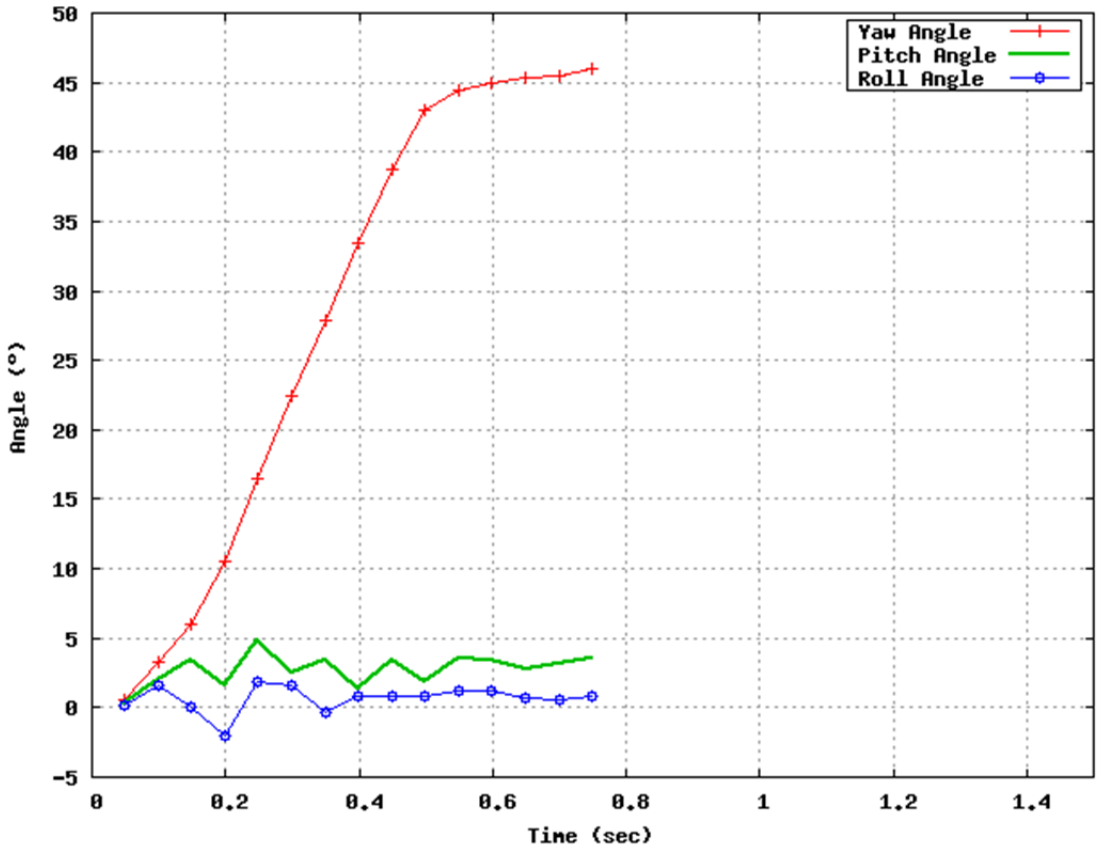

Fig. 4.14: Yaw, pitch, and roll angles of Dodge Neon impacting the 29-inch guardrail at 44 mph and 25°.

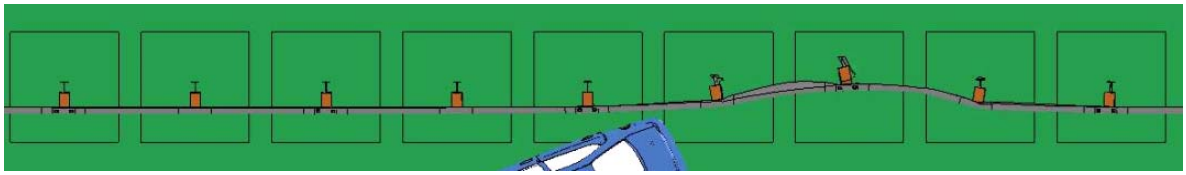

Fig. 4.15: Permanent deformation of the 29-inch guardrail impacted by a Dodge Neon at 44 mph and 25°.

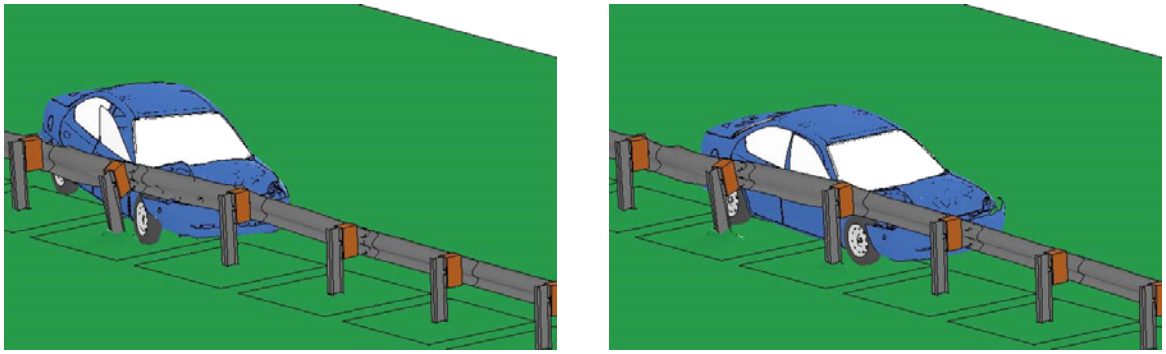

Trimetric view

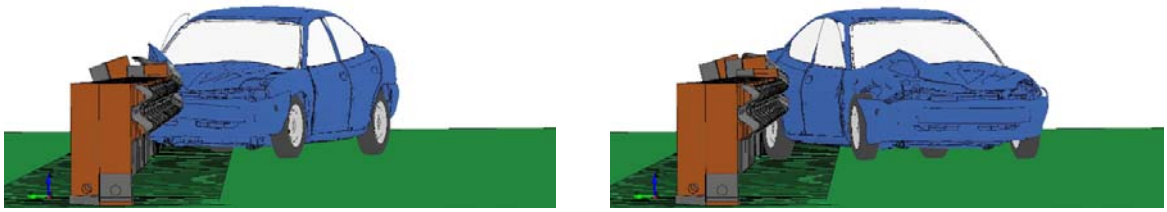

Front view

Fig. 4.16: Four instances of Dodge Neon impacting the 29-inch guardrail at 44 mph and 25°.

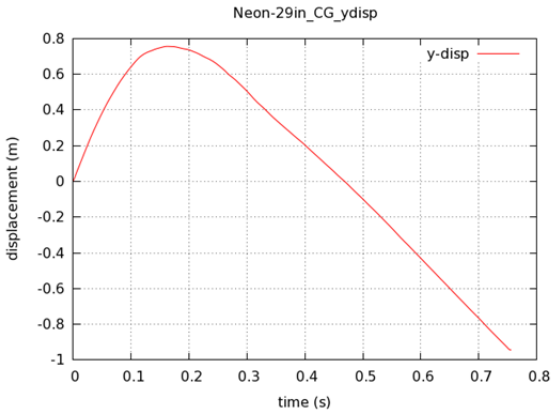

Transverse displacements

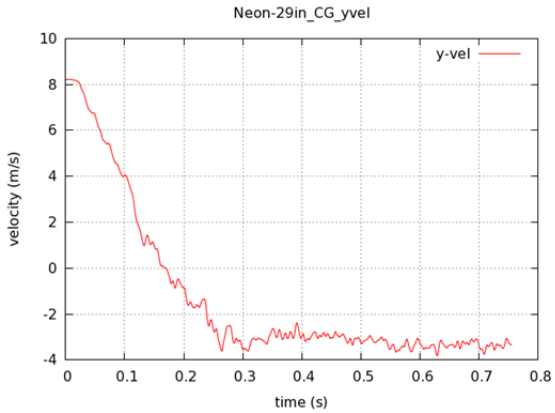

Transverse velocities

Fig. 4.17: Time histories of transverse displacements and velocities of the Dodge Neon impacting the 29-inch guardrail at 44 mph and 25°.

Under the impact of the Ford F250 at 44 mph (70 km/hour) and 25°, the 29-inch W-beam guardrail had a significantly larger deformed section than that under the impact of the Dodge Neon, as shown in Figure 4.18. Despite the large increase of vehicle mass, the 29-inch guardrail was able to safely redirect the Ford F250.

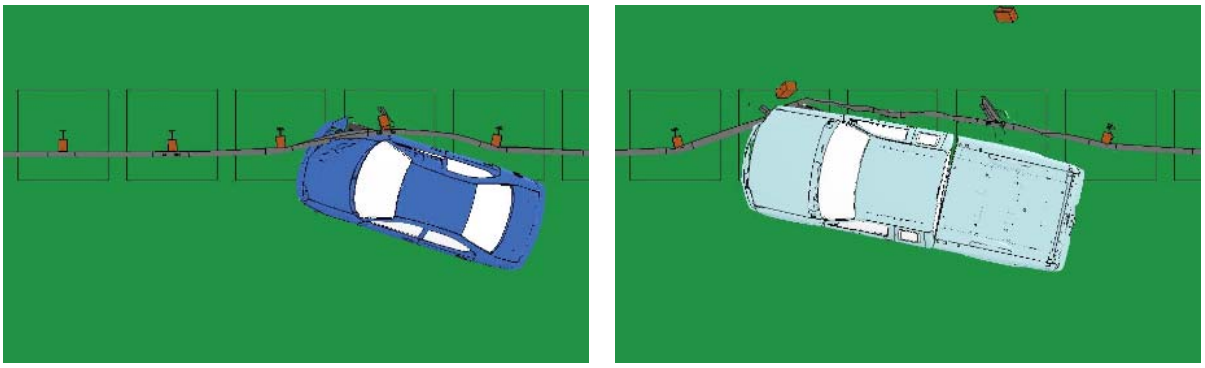

Guardrail impacted by Dodge Neon Guardrail impacted by Ford F250

Fig. 4.18: Comparison of dynamic deformation of the 29-inch guardrail under impacts at 44 mph and 25°.

Figure 4.19 shows the displacement path of the Ford F250 with the W-beam guardrail shown in its original shape and the exit box denoted by the yellow rectangle in dotted lines. The yaw, pitch, and roll angles of the Ford F250 are shown in Figure 4.20. The exit angle of the Ford F250 was determined to be 23°, which was calculated by subtracting the impact angle (25°) from the yaw angle at exit (48°). The roll and pitch angles of this case were both less than one degree in either direction, an indication of a smooth redirection of the vehicle. These values were also well below the maximum 75° rotation specified by the MASH evaluation criterion F. Figure 4.21 shows the permanent deformation of the guardrail after being impacted by the Ford F250. Figure 4.22 shows the detailed views of four instances of vehicle-barrier interactions. Figure 4.23 shows the time histories of transverse displacements and velocities measured at the CG point of the Ford F250. These results showed that the 29-inch guardrail had a satisfactory performance under the impact of the Ford F250 and met the MASH TL-2 requirements.

Compared to the 27-inch guardrail, the 29-inch guardrail showed an improvement on its performance under the impact of the Ford F250 at MASH TL-2 conditions. The two-inch increase on rail height resulted in a smoother vehicle redirection than that on the 27-inch guardrail. The exit angle of the Ford F250 was reduced from 38° on the 27-inch guardrail to 23° on the 29-inch guardrail. Although the damages on the guardrail sections appeared the same for the 27- and 29-inch guardrails, the latter clearly showed an improved performance for pickup-truck impacts.

Based on simulation results for both vehicles (i.e., the Dodge Neon and Ford F250) under MASH TL-2 conditions, the performance of the 29-inch guardrail was considered satisfactory. In addition, the 29-inch guardrail was found to have a smoother redirection and smaller exit angle than the 27-inch guardrail under the impact of the Ford F250.

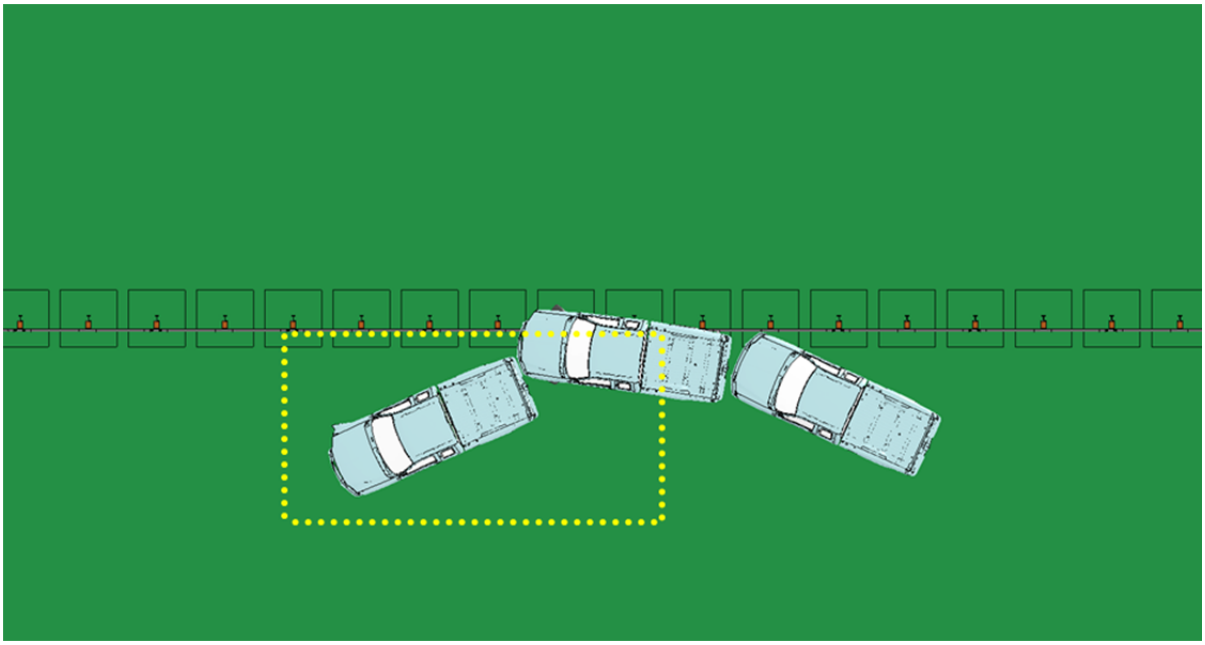

Fig. 4.19: A Ford F250 impacting the 29-inch guardrail at 44 mph and 25°.

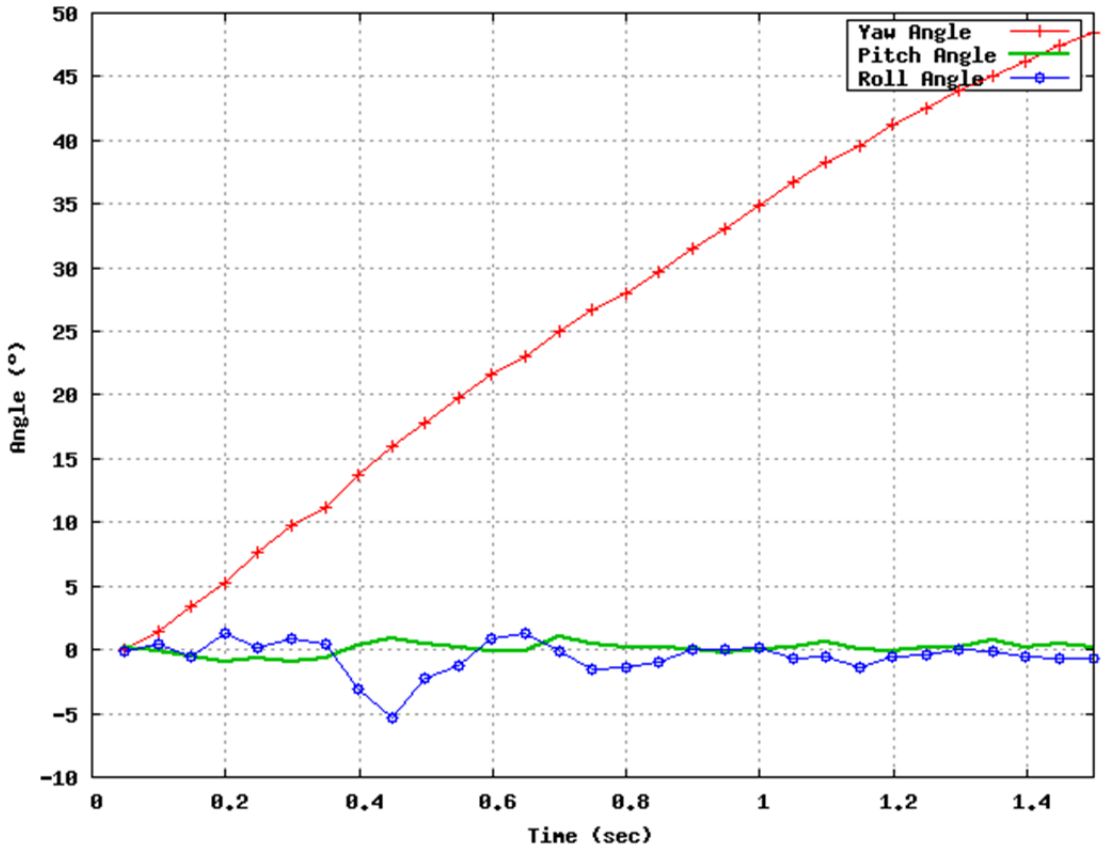

Fig. 4.20: Yaw, pitch, and roll angles of Ford F250 impacting the 29-inch guardrail at 44 mph and 25°.

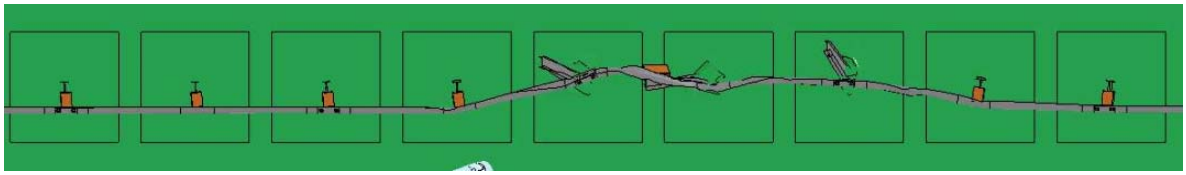

Fig. 4.21: Permanent deformation of the 29-inch guardrail impacted by a Ford F250 at 44 mph and 25°.

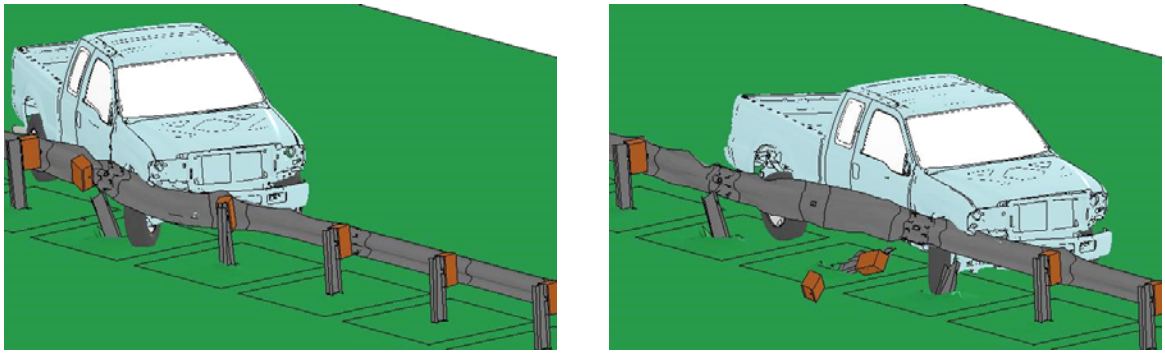

Trimetric view

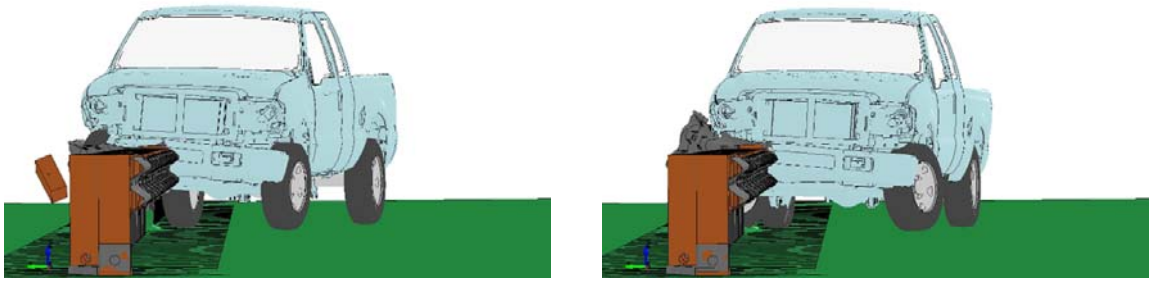

Front view

Fig. 4.22: Four instances of Ford F250 impacting the 29-inch guardrail at 44 mph and 25°.

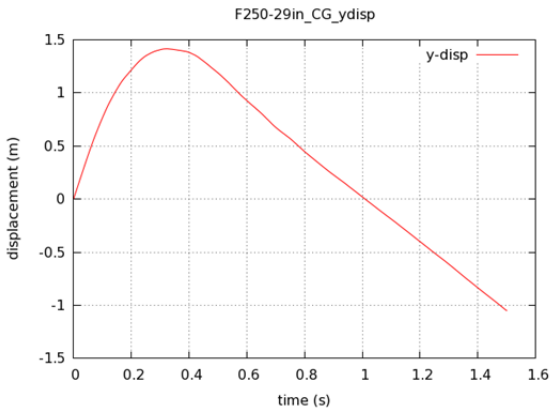

Transverse displacements

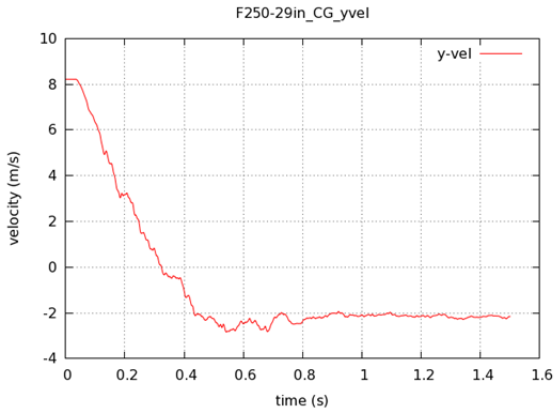

Transverse velocities

Fig. 4.23: Time histories of transverse displacements and velocities of the Ford F250 impacting the 29-inch guardrail at 44 mph and 25°.

4.2.2 The 29-inch Guardrail under MASH TL-3 Conditions

The simulations in this section pertain to Case 3, which are based on the evaluation of the 29-inch guardrail under MASH TL-3 conditions (i.e., at 62 mph (100 km/hour) and 25°). Table 4.5 summarizes the simulation conditions and results for this case.

Table 4.5: Simulation results of the 29-inch W-beam guardrail under MASH TL-3 conditions

Guardrail Height	Impact Speed	Impact Angle	MASH Test Level	Test Vehicle	Test Results
29 inches	62 mph (100 km/hour)	25°	TL-3	Dodge Neon	Vehicle retained in the exit box (with a relatively large exit angle)
	62 mph (100 km/hour)	25°	TL-3	Ford F250	Vehicle out of the exit box (with a relatively large exit angle)

Under the impact of the Dodge Neon at 62 mph (100 km/hour) and 25°, the 29-inch guardrail was able to retain the vehicle inside the exit box. Figure 4.24 shows the displacement path of the Dodge Neon with the W-beam guardrail shown in its original shape and the exit box denoted by the yellow rectangle with dotted lines. The yaw, pitch, and roll angles of the Dodge Neon are shown in Figure 4.25. The roll and pitch angles for this case were negligible (less than five degrees in either positive or negative direction); these values were well below the maximum limit of 75° rotation as specified by the MASH evaluation criterion F.

The exit angle of the Dodge Neon was determined to be -98°, which was calculated by subtracting the impact angle (25°) from the yaw angle at exit (-73°). This exit angle was significantly different from those observed in Case 1 and Case 2. The negative value indicated that the vehicle spun in the opposite way of a safe redirection. From the time history of the yaw angle in Figure 4.25, it can be seen that the Dodge Neon was first redirected (for approximately 7°) and then started to rotate in the opposite direction while remained in contact with the guardrail. This negative rotation went on even after the Dodge Neon lost contact with the guardrail, resulting in a large exit angle of the vehicle. It was observed from the simulation results that the Dodge Neon partially under-rode the guardrail and directly crashed on the posts, causing pocketing and snagging on the front part of the vehicle. Although this issue is related to the vehicle's low profile, it shows the impact conditions are a contributing factor because this problem did not occur to the 29-inch guardrail under MASH TL-2 conditions.

Figure 4.26 shows the permanent deformation of the guardrail after being impacted by the Dodge Neon. It can be seen that the damaged guardrail sections are much larger than that observed under MASH TL-2 conditions. This observation served as an indication of significantly increased impact severity. Figure 4.27 shows the detailed views of four instances of vehicle-barrier interactions. Figure 4.28 shows the time histories of transverse displacements and velocities measured at CG point of the vehicle. The results in Figures 4.24 to 4.28 show that the 29-inch guardrail has the capability of retaining the Dodge Neon (in the exit box) at 62 mph (100 km/hour) and 25°, and that pocketing/snagging can occur and result in a large exit angle.

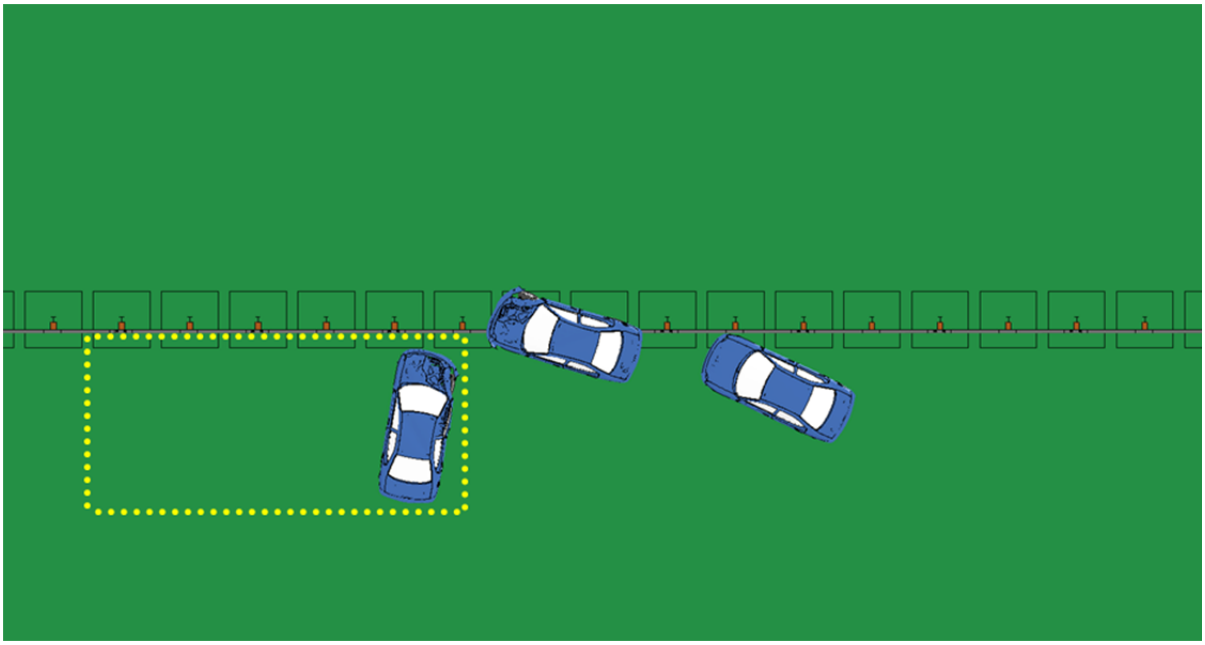

Fig. 4.24: A Dodge Neon impacting the 29-inch guardrail at 62 mph and 25°.

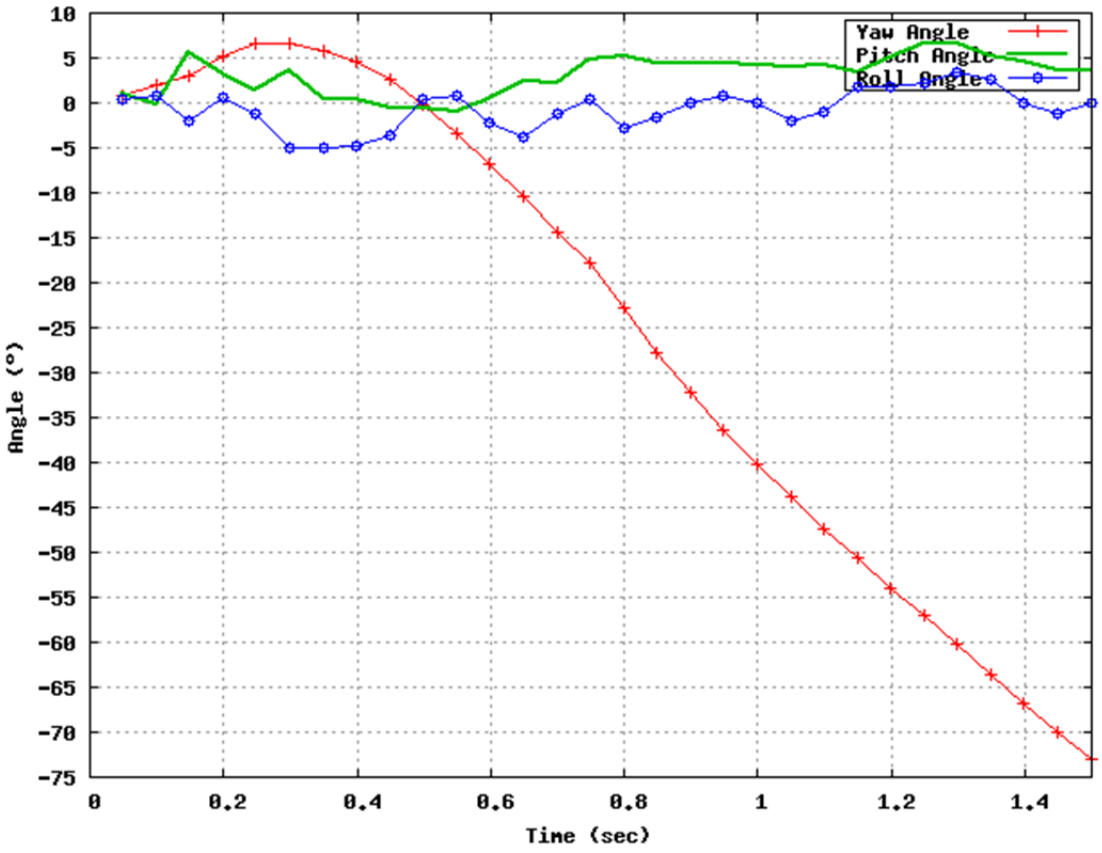

Fig. 4.25: Yaw, pitch, and roll angles of Dodge Neon impacting the 29-inch guardrail at 62 mph and 25°.

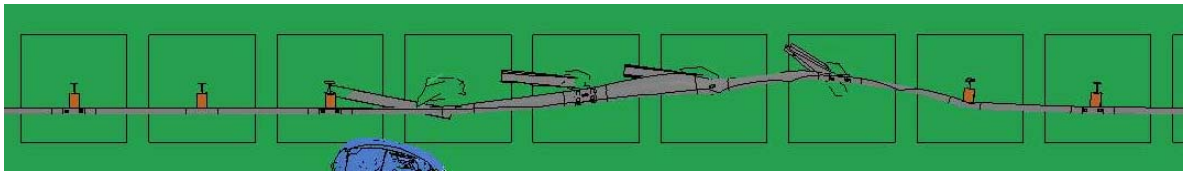

Fig. 4.26: Permanent deformation of the 29-inch guardrail impacted by a Dodge Neon at 62 mph and 25°.

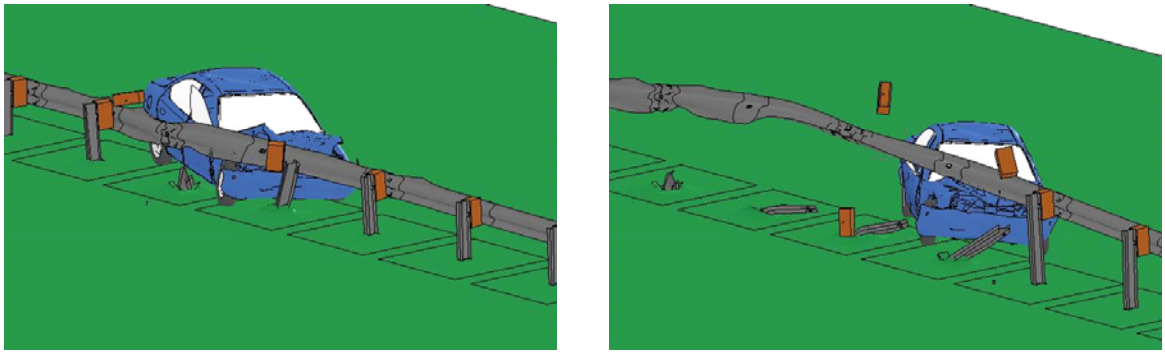

Trimetric view

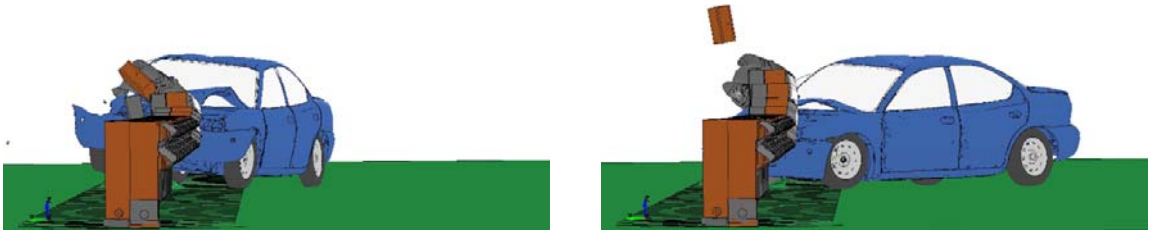

Front view

Fig. 4.27: Four instances of Dodge Neon impacting the 29-inch guardrail at 62 mph and 25°.

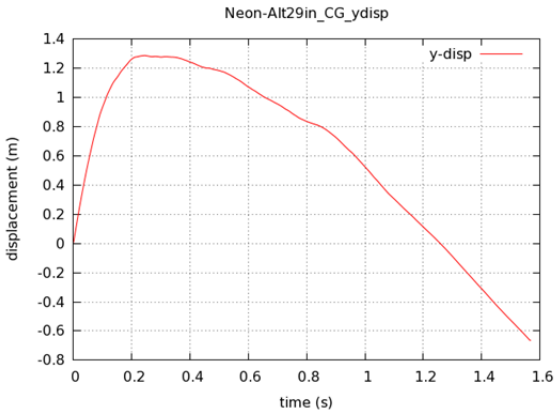

Transverse displacements

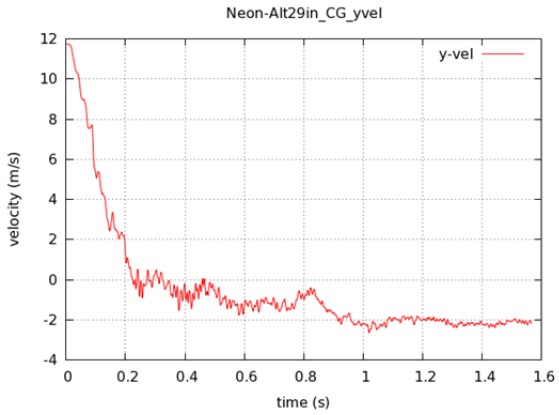

Transverse velocities

Fig. 4.28: Time histories of transverse displacements and velocities of the Dodge Neon impacting the 29-inch guardrail at 62 mph and 25°.

Under the impact of the Ford F250 at 62 mph (100 km/hour) and 25°, the 29-inch W-beam guardrail had a significantly larger deformed section than that under the impact of the Dodge Neon, as shown in Figure 4.29. Additionally, the damaged sections of the 29-inch guardrail in both cases shown in Figure 4.29 are much larger than the corresponding cases under MASH TL-2 conditions (Figure 4.18).

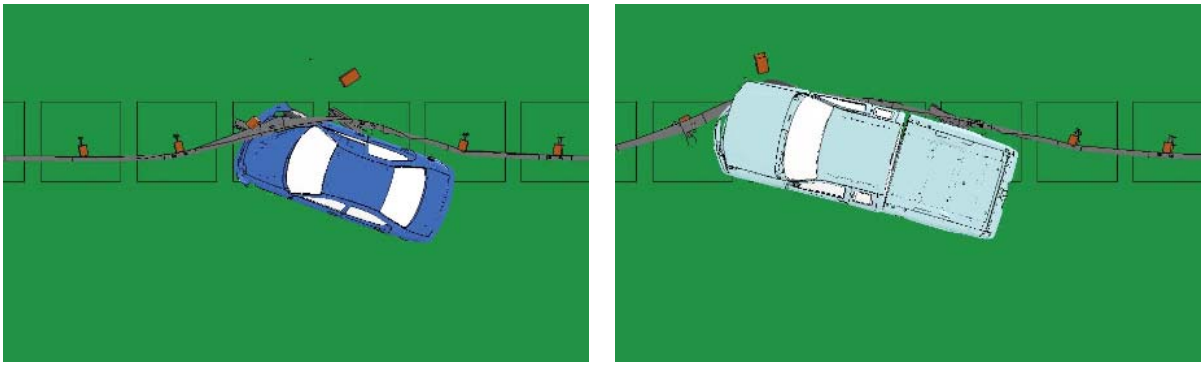

Guardrail impacted by Dodge Neon | Guardrail impacted by Ford F250

Fig. 4.29: Comparison of dynamic deformation of the 29-inch guardrail under impacts at 62 mph and 25°.

Figure 4.30 shows the displacement path of the Ford F250 with the W-beam guardrail shown in its original shape and the exit box denoted by the yellow rectangle in dotted lines. Under the impact of the Ford F250 at 62 mph (100 km/hour) and 25°, the 29-inch guardrail was unable to fully redirect the vehicle and retain it inside the exit box. The yaw, pitch, and roll angles of the Dodge Neon are shown in Figure 4.31. The roll angle of this case was still within the range of a 75° rotation as specified by the MASH evaluation criterion F. The pitch angle was small and negligible. The exit angle of the Ford F250 was determined to be -78°, which was calculated by subtracting the impact angle (25°) from the yaw angle at exit (-43°). Similar to the case of the Dodge Neon impacting the 29-inch guardrail under TL-3 conditions, this negative yaw angle indicated that the Ford F250 spun in the opposite way of a preferred redirection due to snagging on the guardrail posts. From the time history of the yaw angle in Figure 4.31, it can be seen that the Ford F250 was first redirected (for approximately 10°) in the safe direction and then started to rotate in the opposite direction. This negative rotation caused a large exit angle and, along with the large vehicle length, caused the vehicle's tail to shift outside the exit box.

Figure 4.32 shows the permanent deformation of the guardrail after being impacted by the Ford F250. It can be seen that the damaged guardrail sections are much larger than that observed under MASH TL-2 conditions, and that the damaged sections are also dragged towards the travel lane due to vehicle snagging. Figure 4.33 shows the detailed views of four instances of vehicle-barrier interactions. Figure 4.34 shows the time histories of transverse displacements and velocities measured at CG point of the vehicle. Given the small transverse velocity and the remaining spin of the vehicle at the end of the simulation, it could not be concluded that the Ford F250 would re-enter the travel lane.

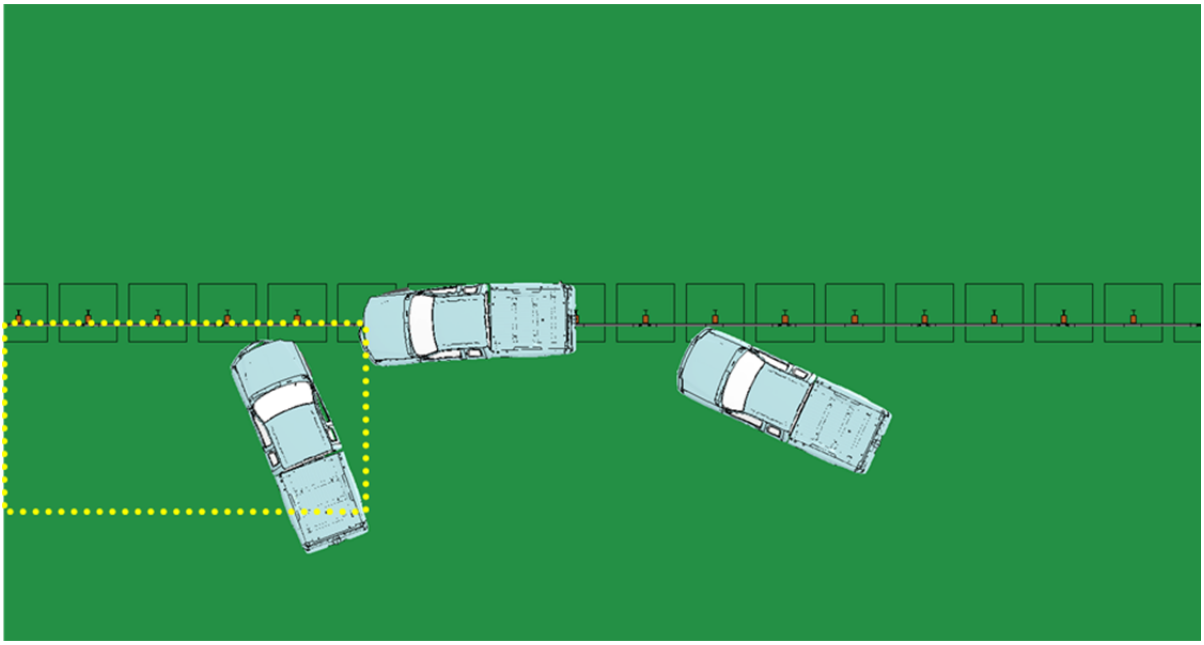

Fig. 4.30: A Ford F250 impacting the 29-inch guardrail at 62 mph and 25°.

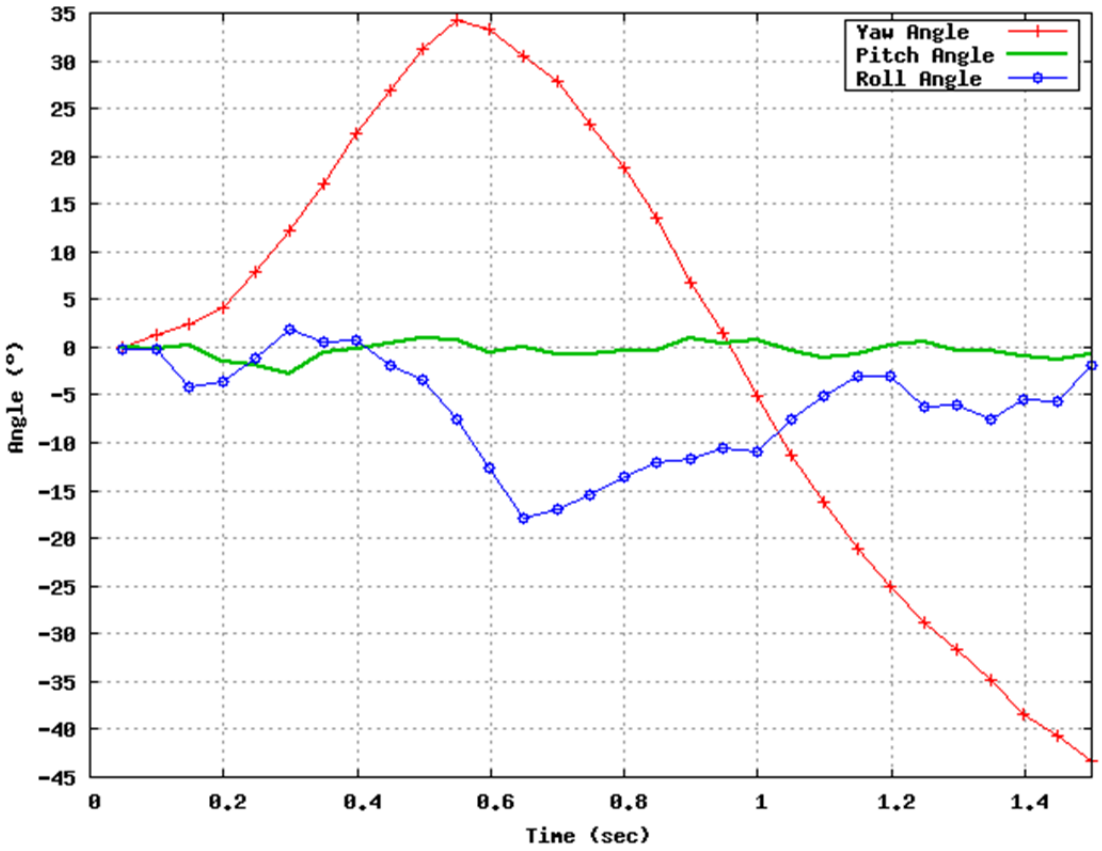

Fig. 4.31: Yaw, pitch, and roll angles of Ford F250 impacting the 29-inch guardrail at 62 mph and 25°.

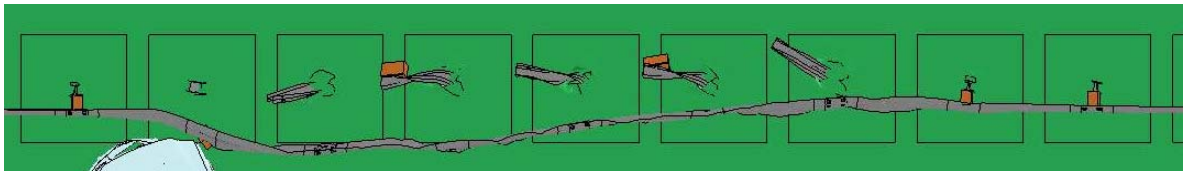

Fig. 4.32: Permanent deformation of the 29-inch guardrail impacted by a Ford F250 at 62 mph and 25°.

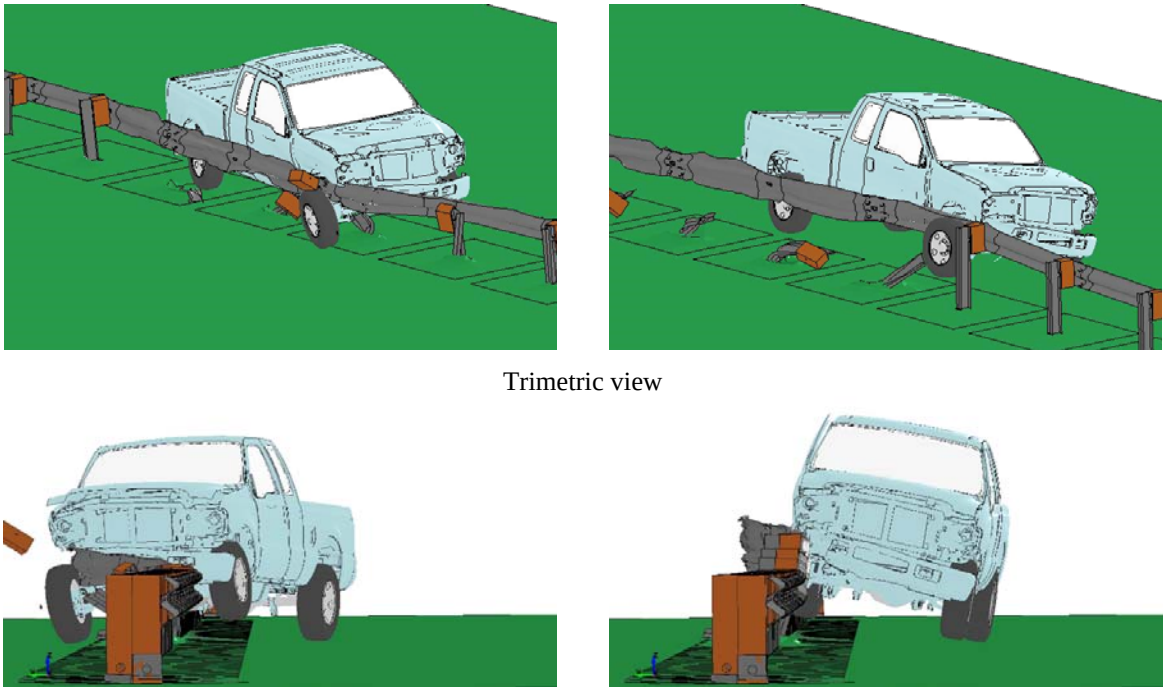

Trimetric view

Front view

Fig. 4.33: Four instances of Ford F250 impacting the 29-inch guardrail at 62 mph and 25°.

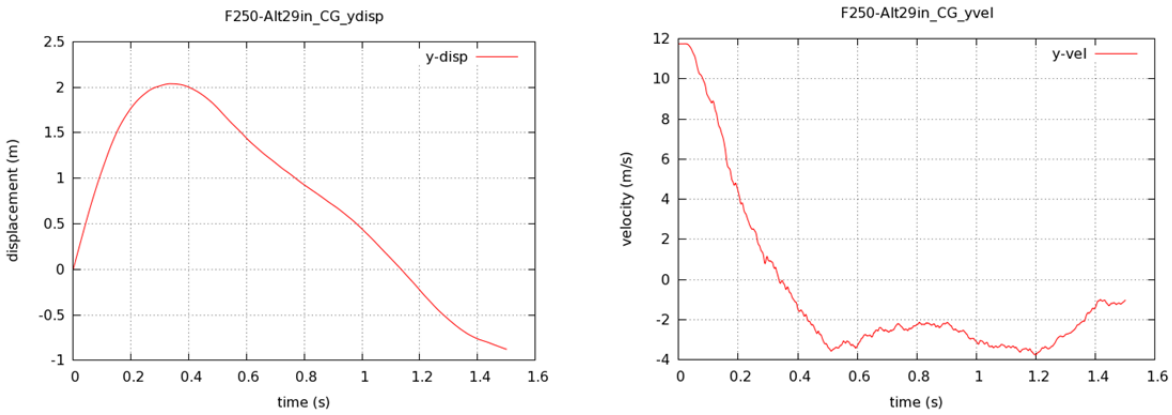

Transverse displacements

Transverse velocities

Fig. 4.34: Time histories of transverse displacements and velocities of the Ford F250 impacting the 29-inch guardrail at 62 mph and 25°.

The results in Figures 4.30 to 4.34 shows that the 29-inch guardrail cannot fully retain the Ford F250 within the exit box under MASH TL-3 conditions, and that vehicle snagging can occur and result in a large exit angle. Along with the simulation results for the Dodge Neon, it shows that the 29-inch guardrail can be used under MASH TL-3 conditions. However, the issue of vehicle snagging should be further investigated to address the concern on vehicle spin and large exit angles. Overall, both the 27- and 29-inch guardrails were found to meet the MASH TL-2 requirements, with the latter having improved performance.

4.3 The 31-inch W-beam Guardrail

In this project, the NCDOT 31-inch W-beam guardrail was also evaluated under vehicular impacts of the Dodge Neon and Ford F250. The simulations were conducted in two cases, Case 4 and Case 5, for the MASH T-2 and TL-3 conditions, respectively. The following sections summarized the simulation results for both cases.

4.3.1 The 31-inch Guardrail under MASH TL-2 Conditions

In this case (i.e., Case 4), the 31-inch guardrail was evaluated under MASH TL-2 conditions, i.e., under vehicular impacts of both a Dodge Neon and a Ford F250 at an impact speed of 44 mph (70 km/hour) and an impact angle of 25°. Table 4.6 gives a brief summary of the simulation conditions and results for Case 4.

Table 4.6: Simulation results of the 31-inch W-beam guardrail under MASH TL-2 conditions

Guardrail Height	Impact Speed	Impact Angle	MASH Test Level	Test Vehicle	Test Results
31 inches	44 mph (70 km/hour)	25°	TL-2	Dodge Neon	Vehicle retained in the exit box (with a relatively large exit angle)
	44 mph (70 km/hour)	25°	TL-2	Ford F250	Vehicle redirected by guardrail

Figure 4.35 shows the displacement path of the Dodge Neon with the W-beam guardrail shown in its original shape and the exit box denoted by the yellow rectangle in dotted lines. The yaw, pitch, and roll angles of the Dodge Neon are shown in Figure 4.36. Similar to the case of the 29-inch guardrail under MASH TL-2 conditions, the roll and pitch angles were negligible. Figure 4.37 shows the permanent deformation of the guardrail after being impacted by the Dodge Neon. It can be seen that the damaged guardrail sections are small and localized; this observation is consistent with those on the 27- and 29-inch guardrails. Figure 4.38 shows the detailed views of four instances of vehicle-barrier interactions. Figure 4.39 shows the time histories of transverse displacements and velocities measured at CG point of the vehicle.

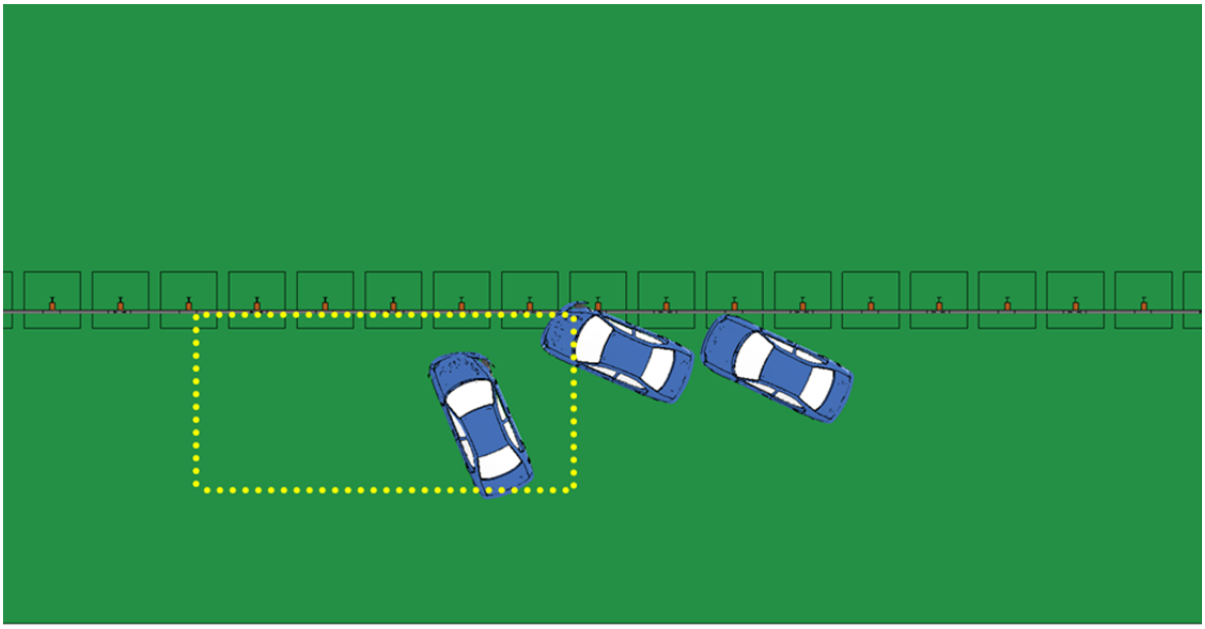

Fig. 4.35: A Dodge Neon impacting the 31-inch guardrail at 44 mph and 25°.

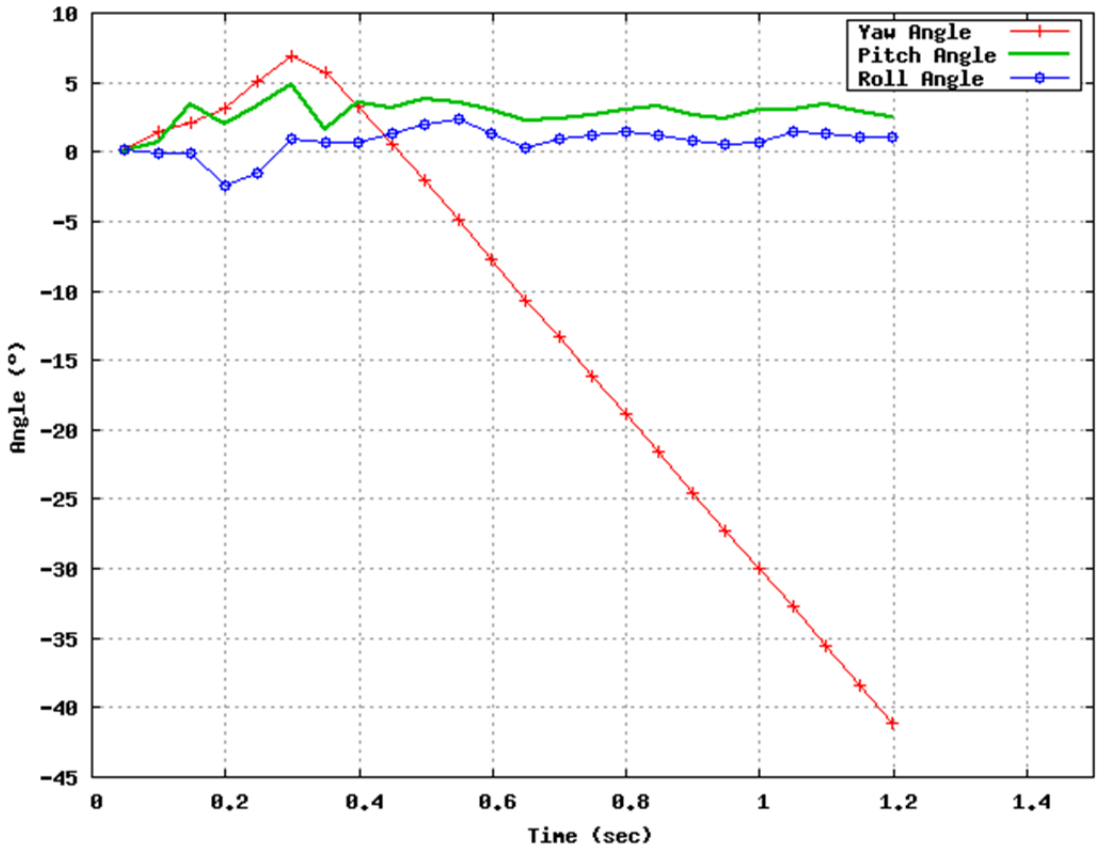

Fig. 4.36: Yaw, pitch, and roll angles of Dodge Neon impacting the 31-inch guardrail at 44 mph and 25°.

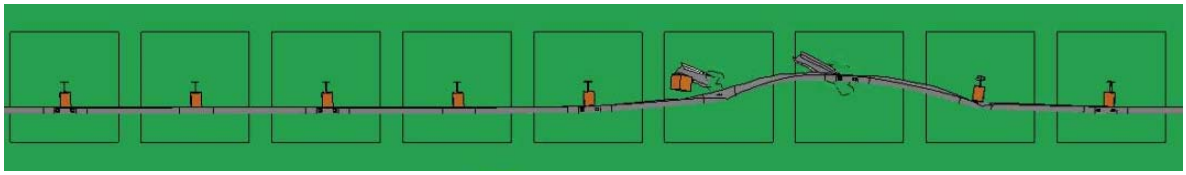

Fig. 4.37: Permanent deformation of the 31-inch guardrail impacted by a Dodge Neon at 44 mph and 25°.

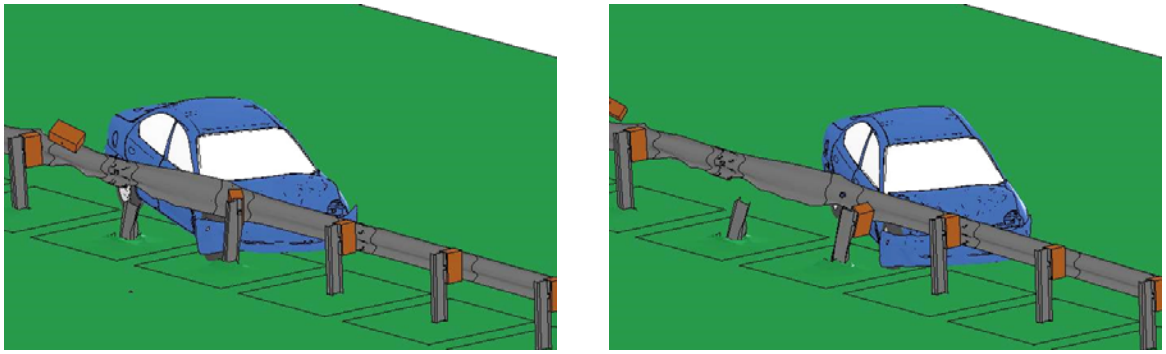

Trimetric view

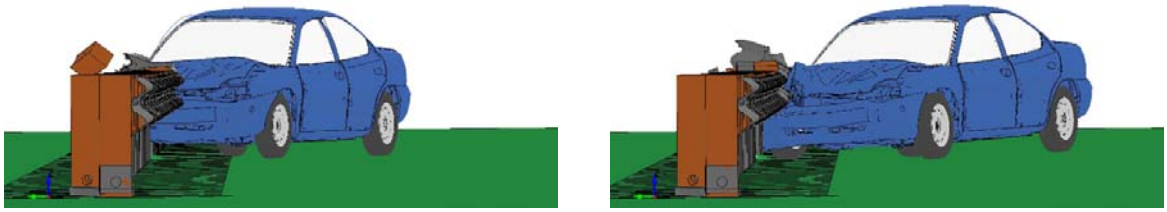

Front view

Fig. 4.38: Four instances of Dodge Neon impacting the 31-inch guardrail at 44 mph and 25°.

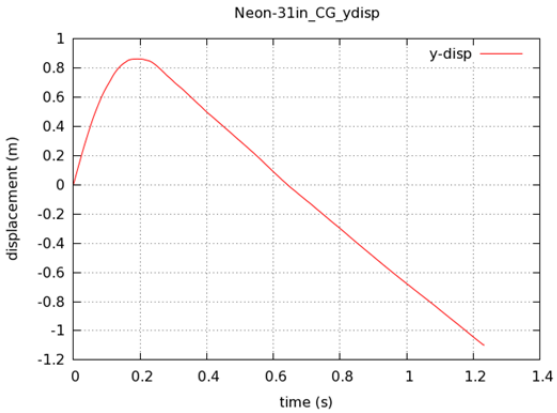

Transverse displacements

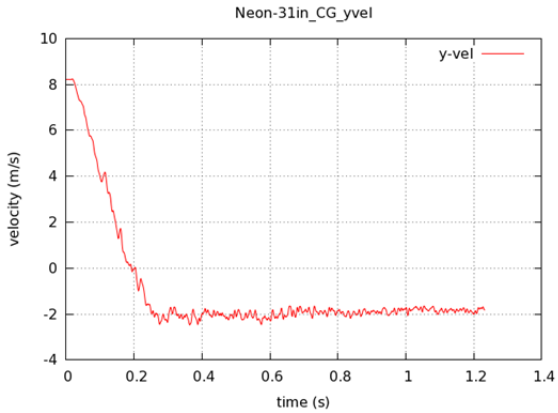

Transverse velocities

Fig. 4.39: Time histories of transverse displacements and velocities of the Dodge Neon impacting the 31-inch guardrail at 44 mph and 25°.

The exit angle of the Dodge Neon was determined to be -66°, which was calculated by subtracting the impact angle (25°) from the yaw angle at exit (-41°). This exit angle was similar to that from Case 3 but significantly different from those observed in Case 1 and Case 2. The negative value indicated that the vehicle spun in the opposite direction of a safe redirection. From the time history of the yaw angle in Figure 4.36, it can be seen that the Dodge Neon was first redirected (for approximately 7°) and then started to rotate in the opposite direction while it remained in contact with the guardrail. This negative rotation resulted in a large exit angle of the vehicle. It was observed from the simulation results that the Dodge Neon partially under-rode the guardrail and directly crashed into the posts, causing pocketing on the front part of the vehicle. A comparison among the 27- and 29-, and 31-inch guardrails shows that increasing the rail height did not improve the guardrails' performance for small-car impacts under MASH TL-2 conditions.

Under the impact of the Ford F250 at 44 mph (70 km/hour) and 25°, the 31-inch W-beam guardrail had a much larger deformed section than that under the impact of the Dodge Neon, as shown in Figure 4.40.

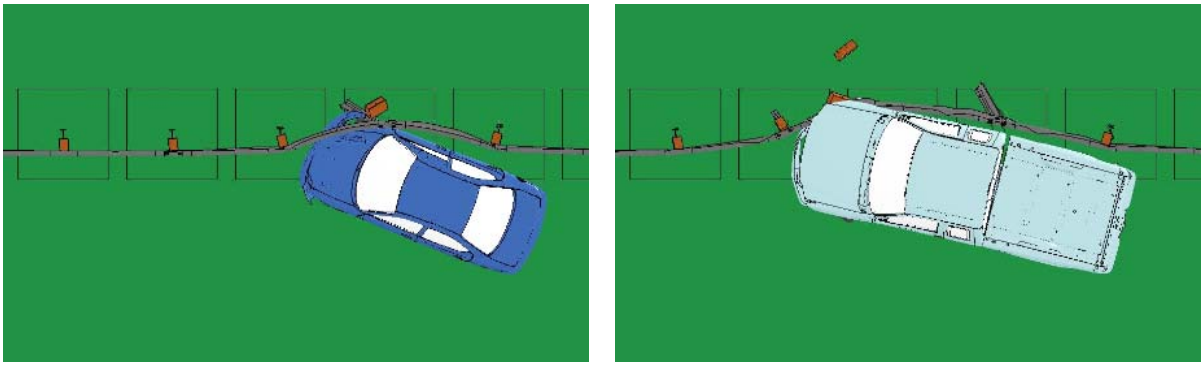

Guardrail impacted by Dodge Neon Guardrail impacted by Ford F250

Fig. 4.40: Comparison of dynamic deformation of the 31-inch guardrail under impacts at 44 mph and 25°.

Figure 4.41 shows the displacement path of the Ford F250 with the W-beam guardrail shown in its original shape and the exit box denoted by the yellow rectangle in dotted lines. Under MASH TL-2 conditions, the 31-inch guardrail successfully redirected the Ford F250 and retained it inside the exit box. Figure 4.42 shows the yaw, pitch, and roll angles of the Ford F250. The roll and pitch angles of this case were both negligible, well below the maximum limit of 75° rotation specified by the MASH evaluation criterion F. The exit angle of the Ford F250 was determined to be 8°, an indication of the satisfactory performance of the 31-inch guardrail. Figure 4.43 shows the permanent deformation of the guardrail after being impacted by the Ford F250. Figure 4.44 shows the detailed views of four instances of vehicle-barrier interactions and Figure 4.45 shows the time histories of transverse displacements and velocities measured at CG point of the vehicle. The simulation results of this case, shown in Figures 4.35 to 4.45, show that the 31-inch guardrail satisfies MASH TL-2 requirements.

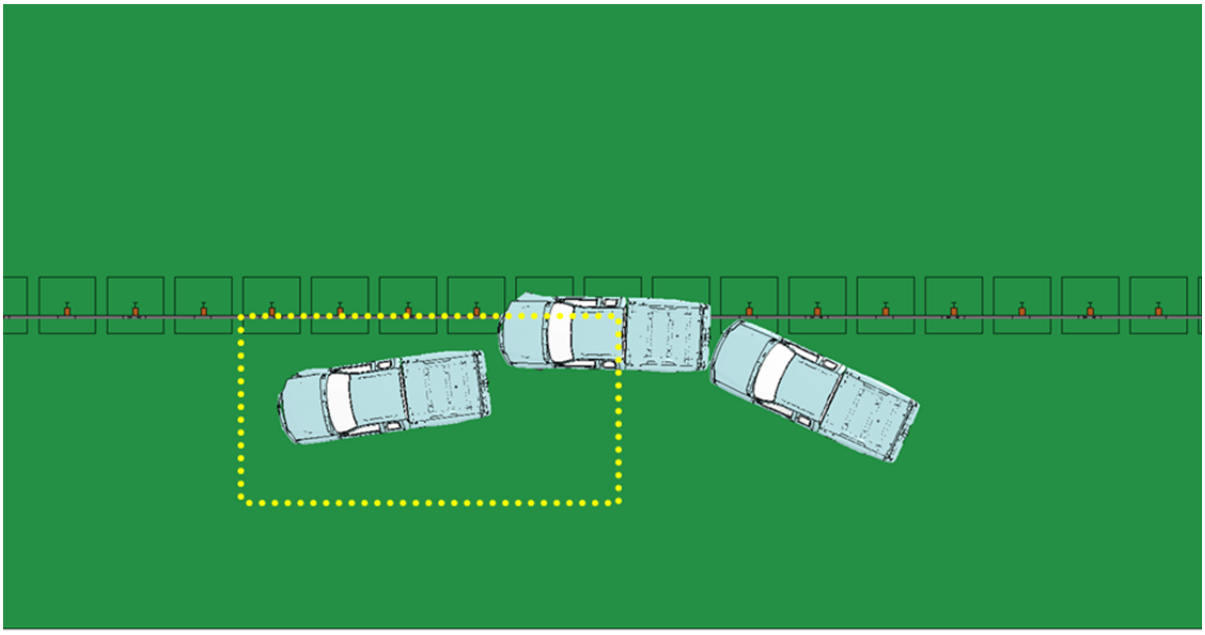

Fig. 4.41: A Ford F250 impacting the 31-inch guardrail at 44 mph and 25°.

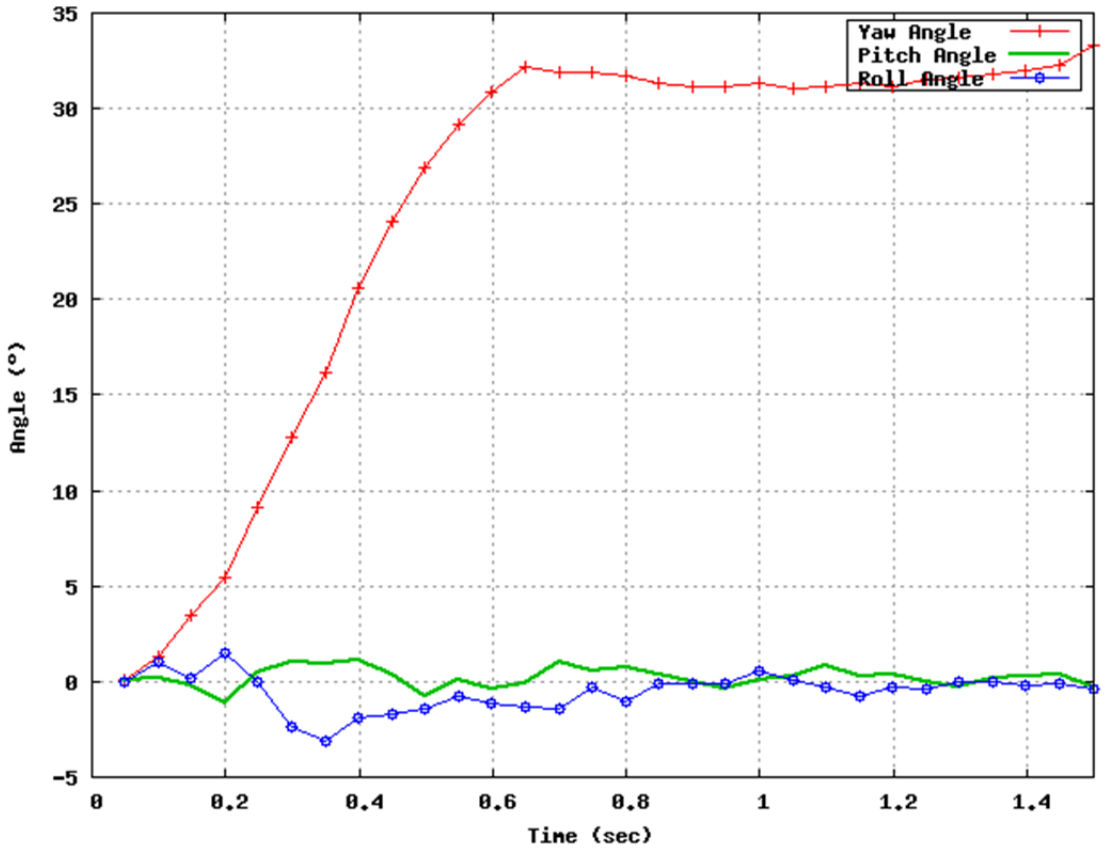

Fig. 4.42: Yaw, pitch, and roll angles of Ford F250 impacting the 31-inch guardrail at 44 mph and 25°.

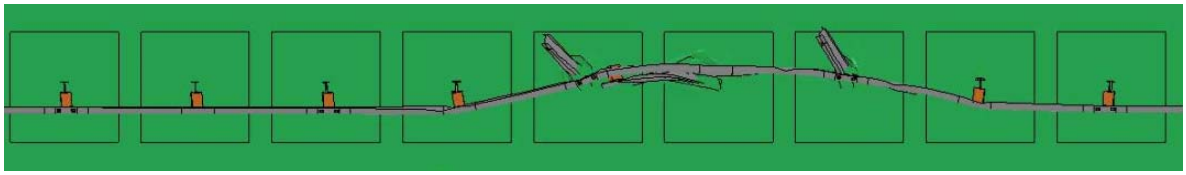

Fig. 4.43: Permanent deformation of the 31-inch guardrail impacted by a Ford F250 at 44 mph and 25°.

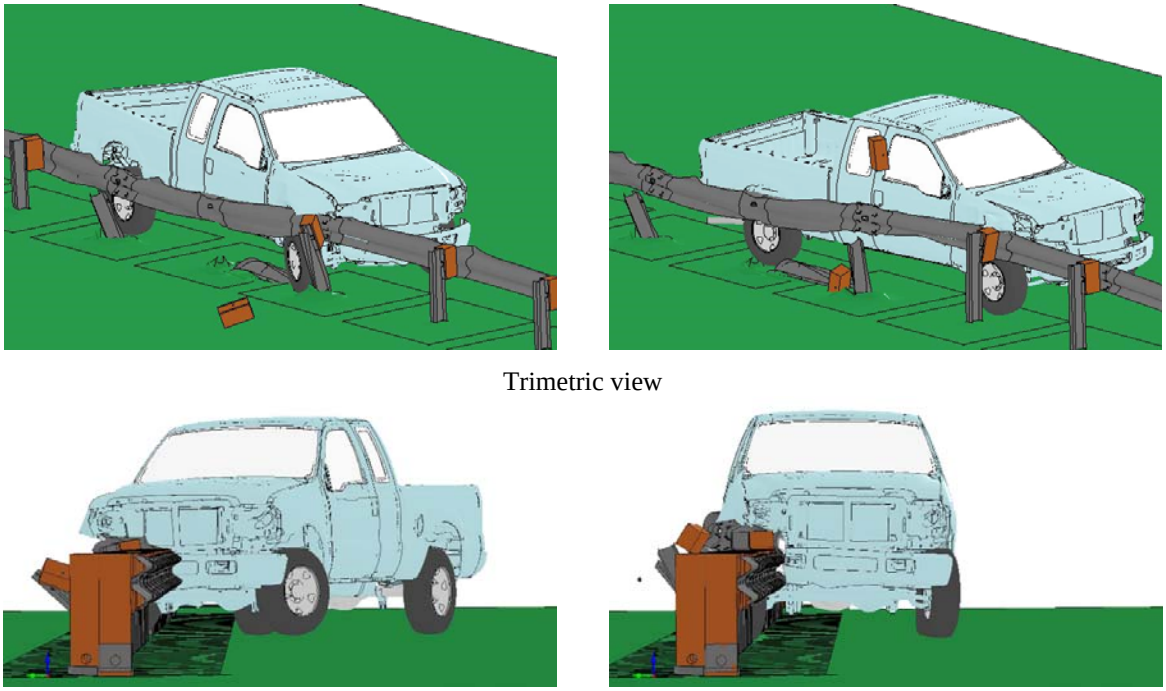

Trimetric view

Front view

Fig. 4.44: Four instances of Ford F250 impacting the 31-inch guardrail at 44 mph and 25°.

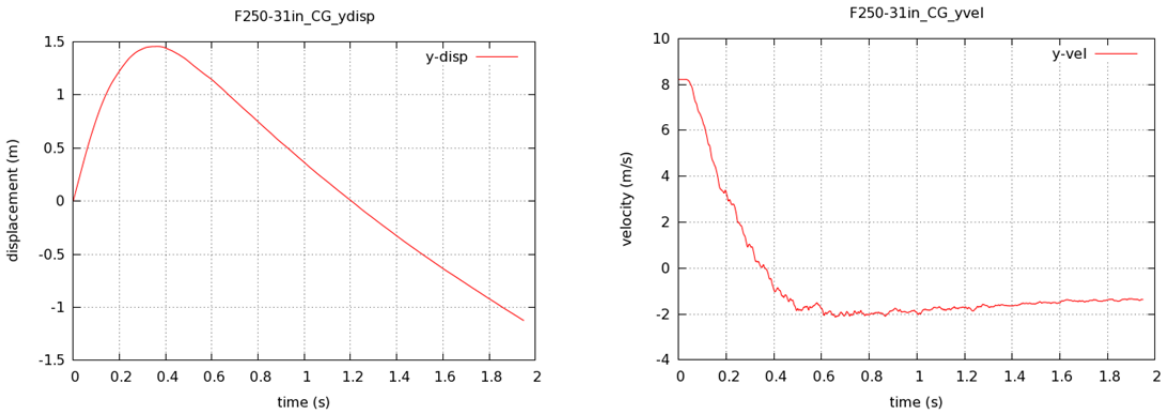

Transverse displacements

Transverse velocities

Fig. 4.45: Time histories of transverse displacements and velocities of the Ford F250 impacting the 31-inch guardrail at 44 mph and 25°.

4.3.2 The 31-inch Guardrail under MASH TL-3 Conditions

In this case (i.e., Case 5), the 31-inch guardrail was evaluated under MASH TL-3 conditions, i.e., under vehicular impacts of both a Dodge Neon and a Ford F250 at an impact speed of 62 mph (100 km/hour) and an impact angle of 25°. Table 4.7 gives a brief summary of the simulation conditions and results for Case 5.

Table 4.7: Simulation results of the 31-inch W-beam guardrail under MASH TL-3 conditions

Guardrail Height	Impact Speed	Impact Angle	MASH Test Level	Test Vehicle	Test Results
31 inches	62 mph (100 km/hour)	25°	TL-3	Dodge Neon	Vehicle retained in the exit box (with a relatively large exit angle)
	62 mph (100 km/hour)	25°	TL-3	Ford F250	Vehicle retained in the exit box

Under the impact of the Dodge Neon at 62 mph (100 km/hour) and 25°, the 31-inch guardrail was able to retain the vehicle inside the exit box. Figure 4.46 shows the displacement path of the Dodge Neon with the W-beam guardrail shown in its original shape and the exit box denoted by the yellow rectangle in dotted lines. The yaw, pitch, and roll angles of the Dodge Neon are shown in Figure 4.47. The roll and pitch angles of this case were larger than those in Case 4, but they were still far below the limit specified by the MASH evaluation criterion F. The exit angle of the Dodge Neon was determined to be -71°, which was calculated by subtracting the impact angle (25°) from the yaw angle at exit (-46°). This negative exit angle indicated that the vehicle spun in the opposite direction of a safe redirection. It was observed from the simulation results that the Dodge Neon partially under-rode the guardrail and directly crashed into the posts, causing pocketing and snagging on the front part of the vehicle as well as the large exit angle.

Figure 4.48 shows the permanent deformation of the guardrail after being impacted by the Dodge Neon. It can be seen that the damaged guardrail sections are much larger than that observed under MASH TL-2 conditions. Figure 4.49 shows the detailed views of four instances of vehicle-barrier interactions. Figure 4.50 shows the time histories of transverse displacements and velocities measured at CG point of the vehicle. The results in Figures 4.46 to 4.50 show that the 31-inch guardrail has the capability of retaining the Dodge Neon (in the exit box) at 62 mph (100 km/hour) and 25°, and that pocketing/snagging can occur and result in a large exit angle.

The dynamic deformation of the 31-inch guardrail under the impact of the Ford F250 at 62 mph (100 km/hour) and 25° is shown in Figure 4.51, along with that for the Dodge Neon under the same impact conditions. It can be seen that the deformed section by the Ford F250 is still larger than that by the Dodge Neon, but not as much as observed in previous cases. The reason for the large deformation incurred by the Dodge Neon was that the vehicle's front end under-rode the guardrail and raised the rail from the posts during the impact. Consequently, the rail did not have as much support from the posts as when the posts were attached to the ground.

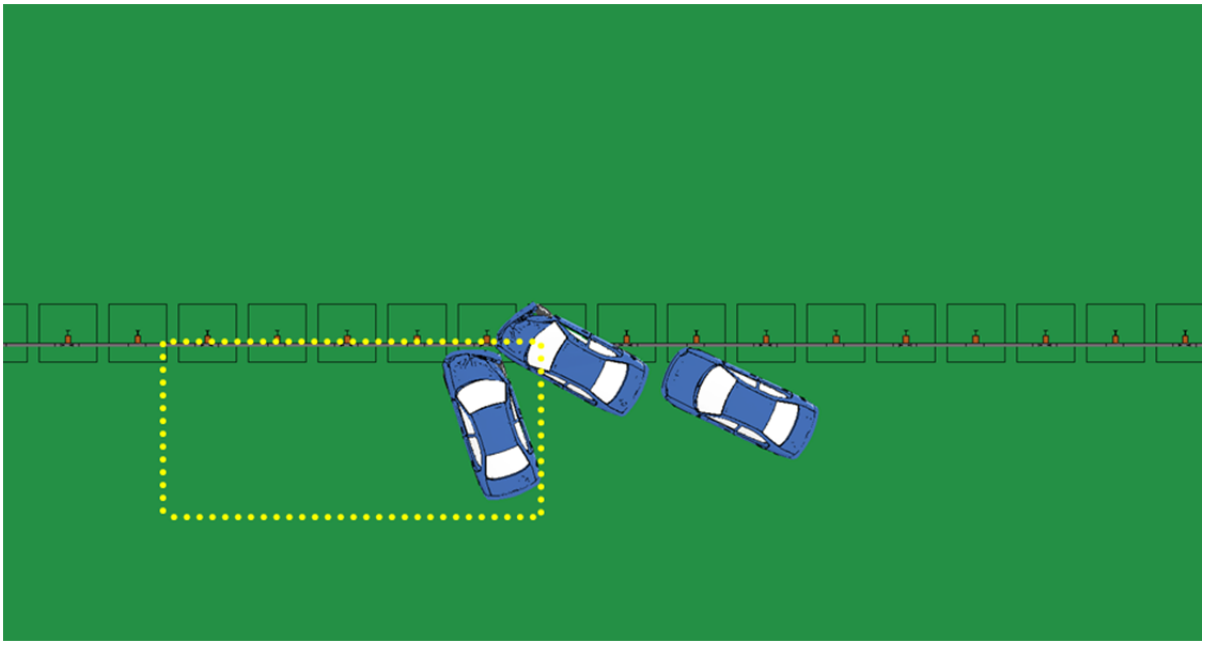

Fig. 4.46: A Dodge Neon impacting the 31-inch guardrail at 62 mph and 25°.

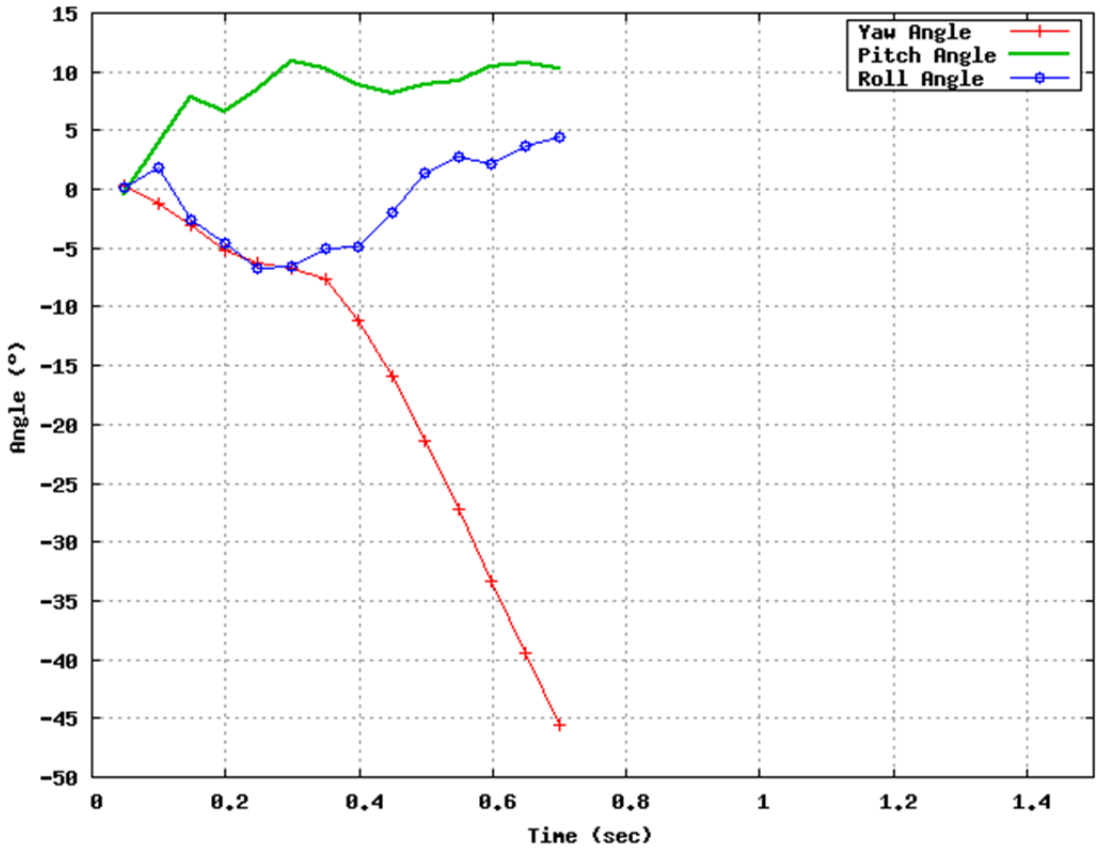

Fig. 4.47: Yaw, pitch, and roll angles of Dodge Neon impacting the 31-inch guardrail at 62 mph and 25°.

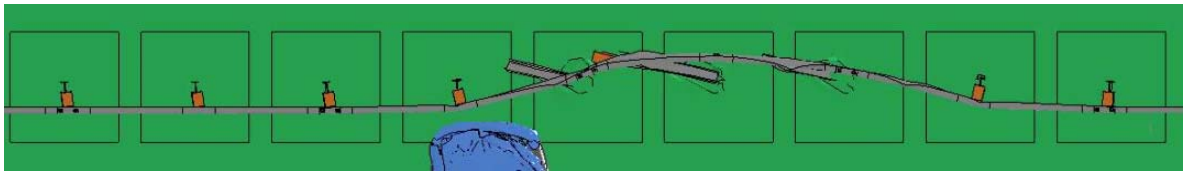

Fig. 4.48: Permanent deformation of the 31-inch guardrail impacted by a Dodge Neon at 62 mph and 25°.

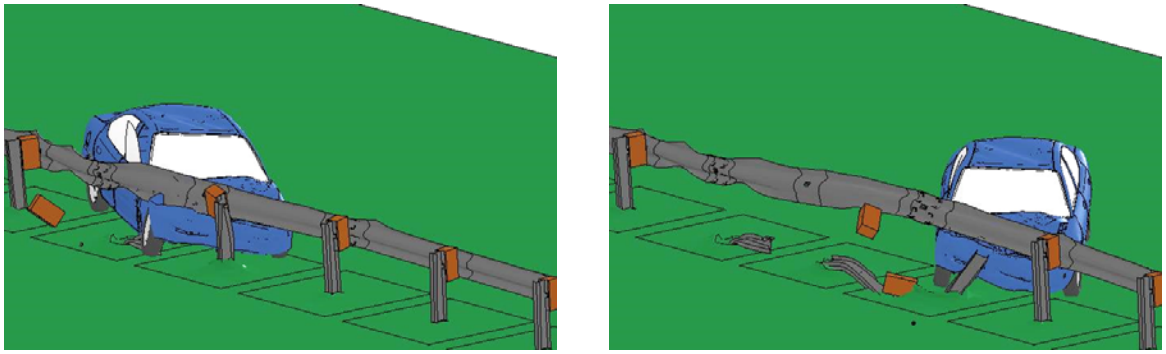

Trimetric view

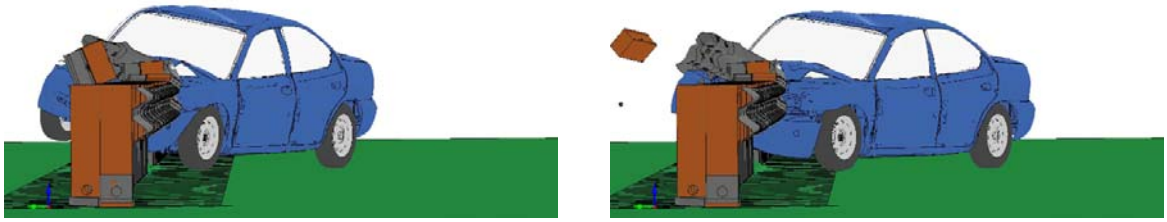

Front view

Fig. 4.49: Four instances of Dodge Neon impacting the 31-inch guardrail at 62 mph and 25°.

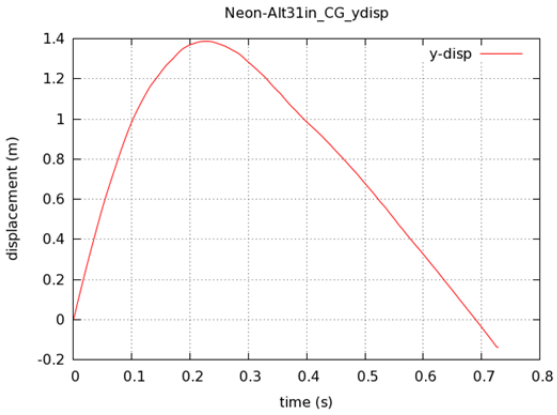

Transverse displacements

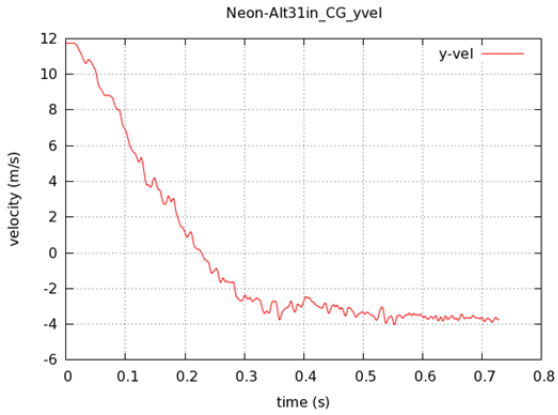

Transverse velocities

Fig. 4.50: Time histories of transverse displacements and velocities of the Dodge Neon impacting the 31-inch guardrail at 62 mph and 25°.

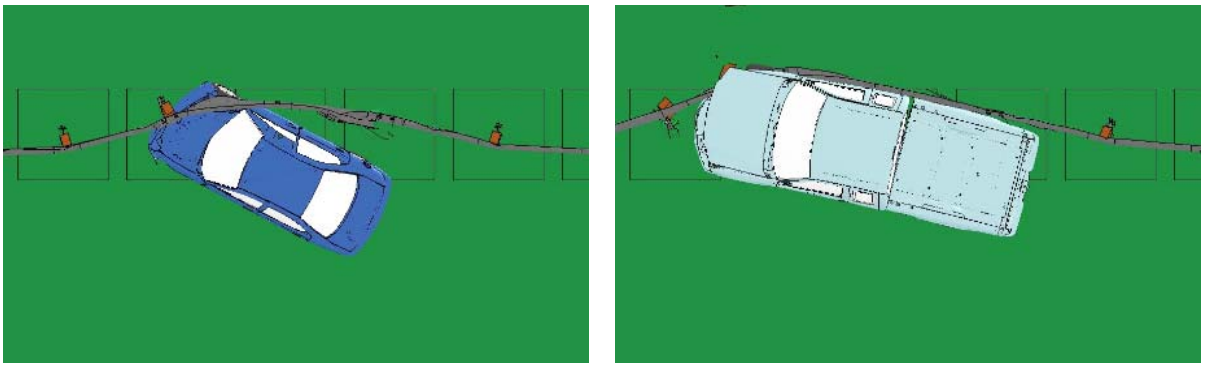

Guardrail impacted by Dodge Neon Guardrail impacted by Ford F250

Fig. 4.51: Comparison of dynamic deformation of the 31-inch guardrail under impacts at 62 mph and 25°.

Figure 4.52 shows the displacement path of the Ford F250 with the W-beam guardrail shown in its original shape and the exit box denoted by the yellow rectangle in dotted lines. Under MASH TL-3 conditions, the 31-inch guardrail successfully retained the Ford F250 inside the exit box. The yaw, pitch, and roll angles of the Ford F250 are shown in Figure 4.53 in which the pitch angle is found negligible. The roll angle of this case was approximately 17°, which was still within the allowed range of a 75° rotation specified by the MASH evaluation criterion F. The exit angle of the Ford F250 was determined to be -15°, which was calculated by subtracting the impact angle (25°) from the yaw angle at exit (10°). This negative exit angle indicated that the vehicle spun in the opposite direction of a safe redirection. It was observed from the simulation results that the Ford F250 was first redirected by the guardrail to an angle of 10° before it spun in the opposite direction caused by snagging.

Figure 4.54 shows the permanent deformation of the guardrail after being impacted by the Ford F250. Figure 4.55 shows the detailed views of four instances of vehicle-barrier interactions and Figure 4.56 shows the time histories of transverse displacements and velocities measured at CG point of the vehicle. The simulation results in Figures 4.52 to 4.56 shows that the 31-inch guardrail can successfully retain the Ford F250. Along with its performance under the impact of the Dodge Neon, the 31-inch guardrail was found to meet the MASH TL-3 requirements. Similar to the 29-inch guardrail, the 31-inch guardrail also experienced the issue of vehicle snagging under MASH TL-3 conditions.

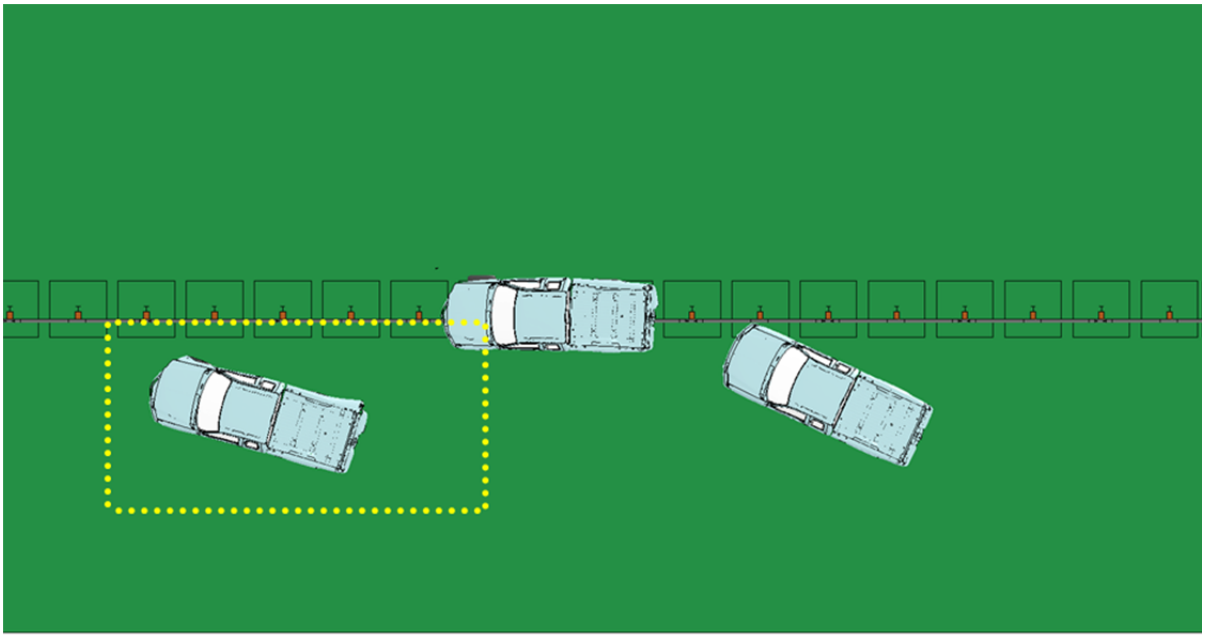

Fig. 4.52: A Ford F250 impacting the 31-inch guardrail at 62 mph and 25°.

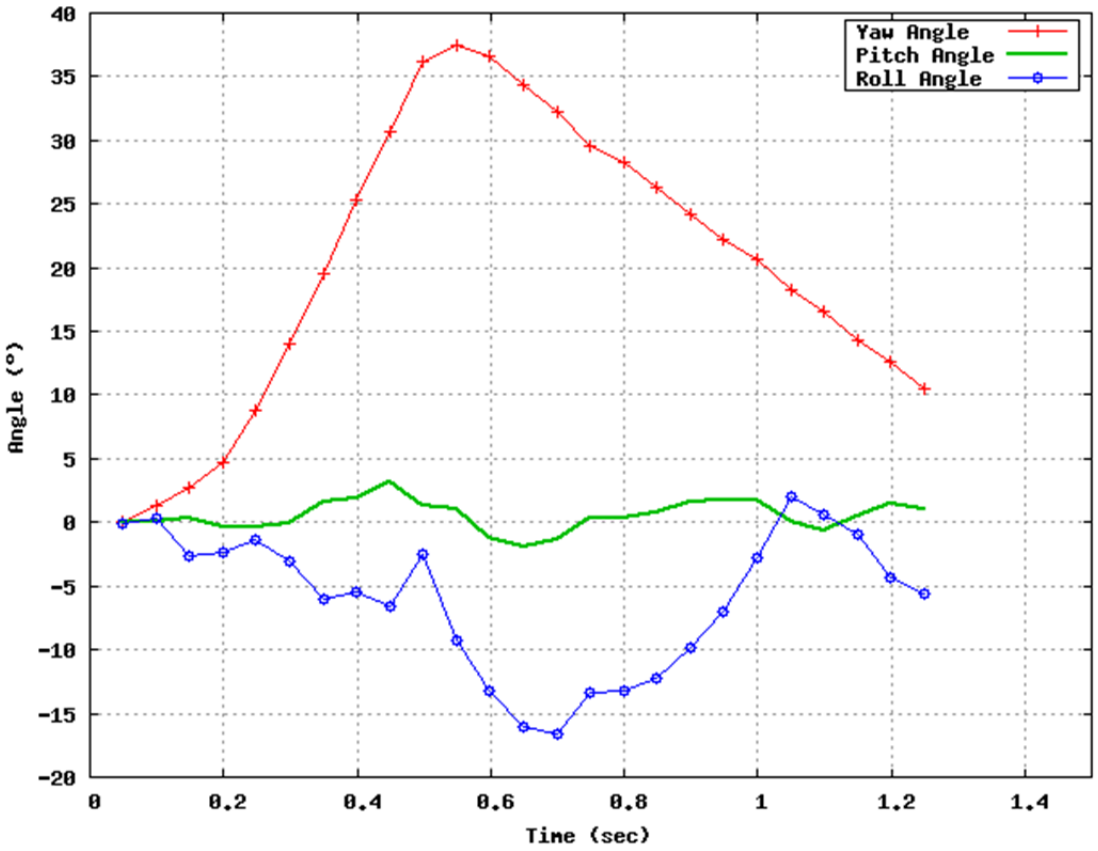

Fig. 4.53: Yaw, pitch, and roll angles of Ford F250 impacting the 31-inch guardrail at 62 mph and 25°.

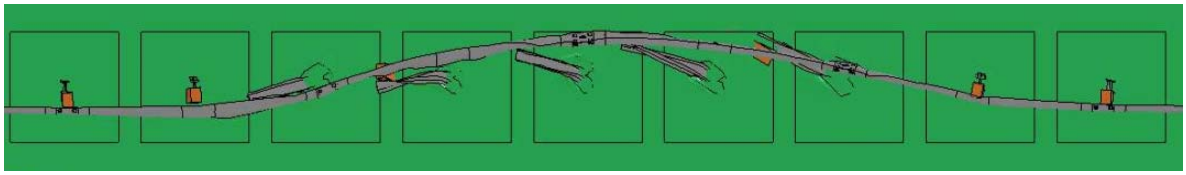

Fig. 4.54: Permanent deformation of the 31-inch guardrail impacted by a Ford F250 at 62 mph and 25°.

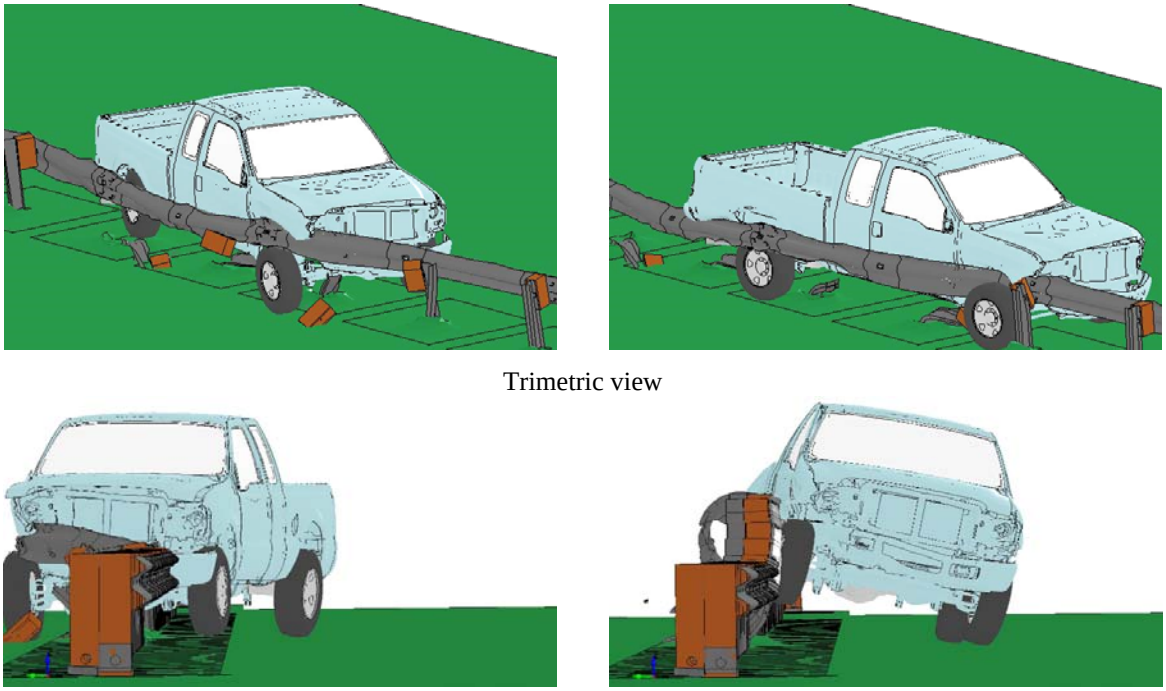

Trimetric view

Front view

Fig. 4.55: Four instances of Ford F250 impacting the 31-inch guardrail at 62 mph and 25°.

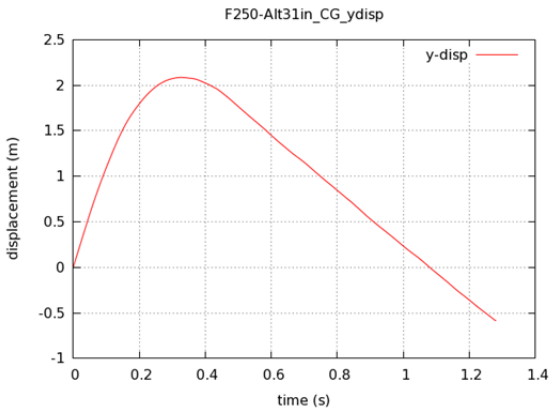

Transverse displacements

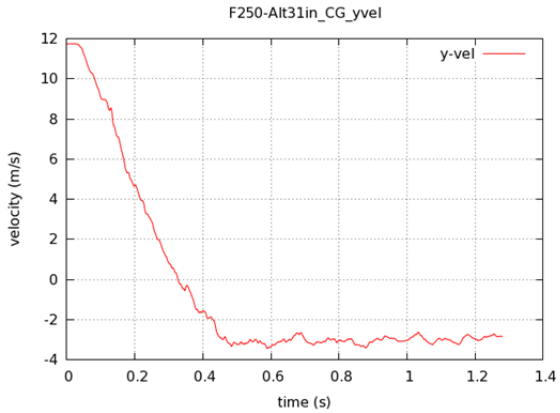

Transverse velocities

Fig. 4.56: Time histories of transverse displacements and velocities of the Ford F250 impacting the 31-inch guardrail at 62 mph and 25°.

Table 4.8 gives a summary of the maximum dynamic deflections of the 27-, 29-, and 31-inch guardrails in all the simulations for this project. The maximum dynamic deflection of the W-beam guardrail is defined as the largest lateral displacement of the rail during vehicular impact. It can be seen from the results in Table 4.8 that as the impact severity increases (i.e., from TL-2 to TL-3), the maximum deflection increases under impacts of the same vehicle (this is true for both the Dodge Neon and Ford F250). From 27 to 29 inches, the increase of guardrail heights does not appear to have a significant effect on the maximum deflections under MASH TL-2 conditions. From 29 to 31 inches, the maximum deflections under impacts of the Dodge Neon are noticeably affected and this is true for both MASH TL-2 and TL-3 conditions. Under impacts of the Ford F250, the change of guardrail height from 29 to 31 inches has no significant effect on the maximum deflection under MASH TL-2 conditions. Under the impacts of Ford F250 at MASH TL-3 conditions, however, the maximum dynamic deflection has a 10.8% increase when the guardrail height is changed from 29 to 31 inches.

Table 4.8: Maximum dynamic deflections of the 27-, 29-, and 31-inch guardrails

Guardrail Height	**Test Vehicle**	**Maximum Dynamic Deflection under MASH TL-2 conditions**	**Maximum Dynamic Deflection under MASH TL-3 conditions**
27 inches	Dodge Neon	1.67 *ft* (0.51 *m*)	–
	Ford F250	3.15 *ft* (0.96 *m*)	–
29 inches	Dodge Neon	1.50 *ft* (0.46 *m*)	2.87 *ft* (0.88 *m*)
	Ford F250	3.37 *ft* (1.03 *m*)	4.42 *ft* (1.35 *m*)
31 inches	Dodge Neon	2.26 *ft* (0.69 *m*)	3.49 *ft* (1.06 *m*)
	Ford F250	3.30 *ft* (1.01 *m*)	4.90 *ft* (1.50 *m*)

5. Findings and Conclusions

In this project, finite element simulations were performed to study the performance of the single-faced 27-, 29-, and 31-inch W-beam guardrails under the impacts of a 1996 Dodge Neon passenger car and a 2006 Ford F250 pickup truck. The simulations were performed under two MASH impact conditions, MASH TL-2 for all three guardrail heights and MASH TL-3 for the 29- and 31-inch guardrails. The simulation results provided insight into the mechanisms of vehicular impacts as well as guardrail performance in relation to guardrail heights and impact speeds. Some of the major research findings are summarized as follows.

- The 27-inch W-beam guardrail performed effectively under impacts of the passenger car and pickup truck at an impact speed of 44 mph (70 km/hr) and a 25° impact angle, which were the standard MASH TL-2 testing conditions. Based on the MASH exit-box criterion, both vehicles were successfully retained by the 27-inch guardrail, with the Dodge Neon exhibiting a smooth redirection and the Ford F250 having a large exit angle. In both of the simulations, the roll and pitch angles were small enough to be considered negligible and passed the MASH evaluation criterion F.
- The 29-inch W-beam guardrail performed effectively under MASH TL-2 testing conditions: both vehicles were redirected smoothly by the guardrail. In addition, the 29-inch guardrail successfully retained both vehicles inside the exit box defined by the MASH exit-box criterion. In both of the simulations, the roll and pitch angles were negligible and passed the MASH evaluation criterion F.
- The 31-inch W-beam guardrail met MASH TL-2 test requirements; it successfully retained both vehicles according to the MASH exit-box criterion. The 31-inch guardrail smoothly redirected the pickup truck but with the small passenger car partial under-riding and impacting directly on the posts followed by a snagging. In both of the simulations, the roll and pitch angles were negligible and passed the MASH evaluation criterion F.
- Under MASH TL-2 conditions, it was observed that with the increased rail heights, the guardrail performance improved under impacts of the pickup truck. For the three guardrail testing heights with the Ford F250, the simulation results showed a smooth redirection and reduced exit angel. However, the increased rail height increased the likelihood of vehicle pocketing and snagging for small passenger cars, which partially under-rode the guardrail and directly impacted the posts.
- Under MASH TL-3 conditions, the 29- and 31-inch guardrails performed similarly when impacted by the small passenger car; both guardrails were able to retain the vehicle inside the exit box but with large exit angles. The large exit angles were caused by vehicle spinning due to snagging on the guardrail post. Under TL-3 impacts of the pickup truck, the 29-inch guardrail caused vehicle snagging that resulted in the vehicle departing the exit box, while the 31-inch guardrail successfully retained the vehicle inside the exit box. In all of the TL-3 simulations, the roll and pitch angles passed the MASH evaluation criterion F.
- It was observed that under impacts of the small passenger car, the larger the guardrail height and the higher the impact speed, the higher the likelihood of excessive vehicle

pocketing and/or snagging as well as large exit angles. In addition, the maximum dynamic deflection of the guardrail was noticeably increased with the increase of guardrail height, for both MASH TL-2 and TL-3 conditions. Under the impacts of the pickup truck, the maximum guardrail deflection was not significantly increased with the increase of guardrail height.

- It was observed that all three W-beam guardrails did not cause vehicle rollovers under MASH TL-2 and TL-3 conditions.

The simulation results suggested that while all three guardrail heights were effective in retaining and redirecting the test vehicles, undesirable post-impact vehicular events such as snagging and high exit angles could be present, especially under MASH TL-3 test conditions. It was also observed that there was a potential for the guardrail to become engaged with the pickup truck behind the tire and to nest in the wheel-well of the impacting side of the vehicle. While this engagement was found desirable to retain the vehicle and reduce the vehicle's velocity, it increased the likelihood of a large post-impact exit angle.

It should be noted that the simulation results of this project can be used to interpret the performance trends of W-beam guardrails. They should not be used to draw definitive conclusions about their performance for a specific crash event, because some factors that could affect the performance were not considered in the simulations for this project. These factors included, but were not limited to, impact locations along the longitudinal axes of the barriers, soil conditions, and driver behaviors. Nevertheless, finite element analysis was demonstrated to be a useful tool in crash analysis and could be used in future investigations of other research issues.

6. Recommendations

Based on the simulation results of this project, it was determined that the W-beam guardrails with 27-, 29-, and 31-inch mounting heights all met the MASH TL-2 requirements. The 27-inch guardrails are effective on low-volume and low speed highways where site conditions along with other considerations warrant their use. The 29- and 31-inch guardrails are appropriate for new installations and/or resurfacing projects in which the 27-inch guardrails will no longer meet the initial construction tolerance. Higher steel beam guardrail placement will allow for future resurfacing without having to make adjustments to the guardrail. As noted in the FHWA memo (Nicol 2010) from the Office of Safety Design, "research on standard 27-inch guardrail shows it does not meet NCHRP Report 350 Test Level 3 (TL-3) criteria."

7. Implementation and Technology Transfer Plan

The simulation results of this project will be submitted to NCDOT for consideration in future projects to install or retrofit W-beam guardrails when allowed by site conditions and deemed necessary by NCDOT personnel. Detailed simulation results will be provided to NCDOT engineers for a comprehensive understanding in evaluating proposed roadside features and/or improving the safety performance of the current system. The modeling and simulation work, along with research findings, will be presented at technical conferences and submitted for publication in technical journals to help researchers and DOT engineers nationwide with similar needs. The research results of this project will be distributed to the public through this report, which will be made available by NCDOT.

References

1. AASHTO (2011). *Roadside Design Guide*, 4th edition, American Association of State Highway and Transportation Officials, Washington, D.C.
2. Atahan, A. O. (2002). "Finite element simulation of a strong-post W-beam guardrail system." *Simulation*, 78(10), 587-599.
3. Atahan, A. O. (2003). "Impact behaviour of G2 steel weak-post W-beam guardrail on nonlevel terrain." *International Journal of Heavy Vehicle Systems*, 10(3), 209-223.
4. Atahan, A. O. (2007). "Crashworthiness analysis of a bridge rail-to-guardrail transition." *Accident Analysis and Prevention*, in press.
5. Atahan, A. O., and Cansiz, O. F. (2005). "Crashworthiness analysis of a bridge rail-to-guardrail transition." *Finite Elements in Analysis and Design*, 41, 371-396.
6. Bligh, R. P., and Mak, K. K. (1999). "Crashworthiness of roadside features across vehicle platforms." *Transportation Research Record*, 1690, 68-77.
7. Bligh, R. P., Abu-Odeh, A. Y., Hamilton, M. E., and Seckinger, N. R. (2004). "Evaluation of roadside safety devices using finite element analysis." *Report 0-1816-1*, Texas Transportation Institute, College Station, TX.
8. Bligh, R., Miaou, S.-P., Lord, D., and Cooner, S. (2006). "Median barrier guidelines for Texas." *Report 0-4254-1*, Texas Transportation Institute, College Station, TX.
9. BMI-SG. (2004). "Improved guidelines for median safety." *NCHRP 17-14(2) Draft Report of Analysis Findings*, Transportation Research Board, National Research Council, Vienne, VA..
10. Donnell, E. T., Harwood, D. W., Bauer, K. M., Mason, J. M., and Pietrucha, M. T. (2002). "Cross-median collisions on Pennsylvania interstates and expressways." *Transportation Research Record*, 1784, 91-99.
11. Fang, H., Li, N., Tian, N., (2010). "Median barrier placement on six-lane, 46-foot median divided freeways." *Final Report NCDOT 2009-04*, North Carolina Department of Transportation, Raleigh, NC.
12. Ferdous, M. R., Abu-Odeh, A., Bligh, R. P., Jones, H. L., Sheikh, N. M., (2011). "Performance limit analysis for common roadside and median barriers using LS-DYNA." *International Journal of Crashworthiness*, 16(6), 691-706.
13. Findley, D. J., Cunningham, C. M., Schroeder, B. J., Vaughan, C. L., Fowler, T. J., (2012). "Structural and safety investigation of statewide performance of weathered steel beam guardrail in North Carolina" *Transportation Research Record: Journal of the Transportation Research Board*, 2309, 63-72.
14. Gabler, H. C., Gabauer, D. J., and Bowen, D. (2005). "Evaluation of cross median crashes." *Final Report FHWA-NJ-2005-004*, Rowan University, Glassboro, NJ.
15. Gabler, H. C. and Gabauer, D. J. (2006). "Safety audit of fatalities and injuries involving guide rail." *Final Report FHWA-NJ-2007-001*, Virginia Tech, Blacksburg, VA.
16. Hampton, C. E., Gabauer, D. J., Gabler, H. C., (2010) "Limits of acceptable rail-and-post deflection in crash-damaged strong-post W-beam guardrail*" Transportation Research Record: Journal of the Transportation Research Board*, 2195, 95-105.

17. Hampton, C. and Gabler, H. (2013). ”Development of a missing post repair guideline for longitudinal barrier crash safety.” *Journal of Transportation Engineering*, 139(6), 549–555.

18. Hiser, N. R., and Reid, J. D. (2005). “Modeling slip base mechanisms.” *International Journal of Crashworthiness*, 10(5), 463-472.

19. Hiss, J. G. F., Jr., and Bryden, J. E. (1992). “Traffic barrier performance.” *Report 155*, New York State Department of Transportation, Albany, NY.

20. Hu, W., Donnell, E. T., (2010) “Median barrier crash severity: some new insights” *Accident Analysis & Prevention*, 42(6), 1697-1704.

21. Kan, C.-D., Marzougui, D., Bahouth, G. T., and Bedewi, N. E. (2001). “Crashworthiness evaluation using integrated vehicle and occupant finite element models.” *International Journal of Crashworthiness*, 6, 387-398.

22. Lewis, B. A. (2004). “Manual for LS-DYNA soil material model 147.” *FHWA-HRT-04-095*, U.S. Department of Transportation, Federal Highway Administration, McLean, VA.

23. LSTC (2007). “LS-DYNA keyword user’s manual - version 971.” Livermore Software Technology Corporation (LSTC), Livermore, CA.

24. Lynch, J. M., Crowe, N. C., and Rosendahl, J. F. (1993). “Interstate across median accident study: a comprehensive study of traffic accidents involving errant vehicles which cross the median divider strips on North Carolina interstate highways.” *1993 AASHTO Annual Meeting Proceedings*, Publisher American Association of State Highway and Transportation Officials, 125-133.

25. Mackerle, J. (2003). “Finite element crash simulations and impact-induced injuries: an addendum. A bibliography (1998–2002).” *The Shock and Vibration Digest*, 35(4), 273-280.

26. Mak, K.K., and Bligh, R.P. (2002). “Assessment of NCHRP Report 350 test conditions.” *Transportation Research Record 1797*, 38-43.

27. Mak, K. K., and Sicking, D. L. (2003). “NCHRP Report 492 roadside safety analysis program (RSAP) – engineer’s manual.” *Transportation Research Board*, 7-28.

28. Marzougui, D., Bahouth, G., Eskandarian, A., Meczkowski, L., and Taylor, H. (2000). “Evaluation of portable concrete barriers using finite element simulation.” *Transportation Research Record*, 1720, 1-6.

29. Marzougui, D., Zink, M., Zaouk, A. K., Kan, C.-D., and Bedewi, N. E. (2004). “Development and validation of a vehicle suspension finite element model for use in crash simulations.” *International Journal of Crashworthiness*, 9(6), 565-576.

30. Marzougui, D., Mohan, P., Kan, C.-D., and Opiela, K. S. (2007). “Evaluation of rail height effects on the safety performance of W-beam barriers.” *2007 TRB Annual Meeting*, Washington, D.C.

31. Marzougui, D., Mohan, P., Kan, C.-D., and Opiela, K. S. (2012). “Assessing options for improving barrier crashworthiness using finite element models and crash simulations.” *Final Report NCAC-2012-W-008*, National Crash Analysis Center, George Washington University, Washington, D.C.

32. MASH (2009). “Manual for assessing safety hardware (MASH).” American Association of State Highway and Transportation Officials (AASHTO), Washington D.C.

33. Miaou, S.-P., Bligh, R. P., and Lord, D. (2005). “Developing guidelines for median barrier installation: benefit-cost analysis with Texas data.” *Transportation Research Record*, 1904, 3-19.

34. Mohan, P., Marzougui, D., and Kan, C.-D. (2007). “Validation of a single unit truck model for roadside hardware impact.” *International Journal of Vehicle Systems Modelling and Testing*, 2(1), 1-15.

35. Murray, Y. D., Reid, J. D., Faller, R. K., Bielenberg, B. W., and Paulsen, T. J. (2005). “Evaluation of LS-DYNA wood material model 143.” *FHWA-HRT-04-096*, U.S. Department of Transportation, Federal Highway Administration, McLean, VA.

36. Murray, Y. D. (2007). “User manual for LS-DYNA concrete material model 159.” *FHWA-HRT-05-062*, U.S. Department of Transportation, Federal Highway Administration, McLean, VA.

37. NCAC (web1). “NCAC finite element models.” <*http://www.ncac.gwu.edu/vml/models.html*>.

38. NCAC (web2). “NCAC publications.” <*http://www.ncac.gwu.edu/filmlibrary/publications.html*>.

39. NCHRP 22-21 (2011). “Project 22-21: median cross-section design for rural divided highways.” <*http://apps.trb.org/cmsfeed/TRBNetProjectDisplay.asp?ProjectID=694*>.

40. NCHRP 22-22 (2010). “Project 22-22: placement of traffic barriers on roadside and median slopes.” <*http://apps.trb.org/cmsfeed/TRBNetProjectDisplay.asp?ProjectID=695*>.

41. NCHRP 22-27 (2012). “Project 22-27: roadside safety analysis program (RSAP) update.” <*http://apps.trb.org/cmsfeed/TRBNetProjectDisplay.asp?ProjectID=2517*>.

42. Nicol, D. A., (2010) “Roadside design: steel strong post W-beam guardrail.” *Memorandum 051710*, U.S. Department of Transportation, Federal Highway Administration, McLean, VA.

43. Ochoa, C. M., Ochoa, T. A., (2011) “Guardrail optimization for rural roads.” *Transportation Research Board of the National Academies*, 2203, 71-78.

44. Orengo, F., Ray, M. H., and Plaxico, C. A. (2003). “Modeling tire blow-out in roadside hardware simulations using LS-DYNA.” *IMECE2003-55057*, 2003 ASME International Mechanical Engineering Congress & Exposition, Washington, D.C.

45. Patzner, G. S., Plaxico, C. A., and Ray, M. H. (1999). “Effects of post and soil strength on performance of modified eccentric loader breakaway cable terminal.” *Transportation Research Record*, 1690, 78-83.

46. Plaxico, C. A., Hackett, R. M., and Uddin, W. (1997). “Simulation of a vehicle impacting a modified thrie-beam guardrail.” *Transportation Research Record*, 1599, 1-10.

47. Plaxico, C. A., Patzner, G. S., and Ray, M. H. (1998). “Finite element modeling of guardrail timber posts and the post-soil interaction.” *Transportation Research Record*, 1647, 139-146.

48. Plaxico, C. A., Ray, M. H., and Hiranmayee, K. (2000). “Impact performance of the G4(1W) and G4(2W) guardrail systems: comparison under NCHRP Report 350 test 3-11 conditions.” *Transportation Research Record*, 1720, 7-18.

49. Plaxico, C. A., Mozzarelli, F., and Ray, M. H. (2003). “Tests and simulation of a w-beam rail-to-post connection.” *International Journal of Crashworthiness*, 8(6), 543-551.

50. Ray, M. H. (1996a). “Repeatability of full-scale crash tests and criteria for validating simulation results.” *Transportation Research Record*, 1528, 155-160.

51. Ray, M. H. (1996b). “Use of finite element analysis in roadside hardware design.” *Transportation Research Circular*, 453, 61-71.

52. Ray, M. H., and McGinnis, R. G. (1997). “Guardrail and median barrier crashworthiness: synthesis of highway practice.” Transportation Research Board, Washington, D.C.

53. Ray, M. H., and Patzner, G. S. (1997). “Finite element model of modified eccentric loader terminal (MELT).” *Transportation Research Record*, 1599, 11-21.

54. Ray, M. H., and Weir, J. A. (2001). “Unreported collisions with post-and-beam guardrails in Connecticut, Iowa, and North Carolina.” *Transportation Research Record*, 1743, 111-119.

55. Ray, M. H., Weir, J., and Hopp, J. (2003). “In-service performance of traffic barriers.” *NCHRP Report 490*, Transportation Research Board, National Research Council, Washington, D.C.

56. Ray, M. H., Oldani, E., and Plaxico, C. A. (2004). “Design and analysis of an aluminum F-shape bridge railing.” *International Journal of Crashworthiness*, 9(4), 349-363.

57. Reid, J. D. (1996). “Towards the understanding of material property influence on automotive crash structures.” *Thin-Walled Structures*, 24, 285-313.

58. Reid, J. D. (1998). “Admissible modeling errors or modeling simplifications?” *Finite Elements in Analysis and Design*, 29, 49-63.

59. Reid, J. D. (2004). “LS-DYNA simulation influence on roadside hardware.” *Transportation Research Record*, 1890, 34-41.

60. Reid, J. D., and Bielenberg, B. W. (1999). “Using LS-DYNA simulation to solve a design problem: bullnose guardrail example “ *Transportation Research Record*, 1690, 95-102.

61. Reid, J. D., and Marzougui, D. (2002). “Improved truck model for roadside safety simulations: Part I - structural modeling.” *Transportation Research Record*, 1797, 53-62.

62. Reid, J. D., Coon, B. A., Lewis, B. A., Sutherland, S. H., and Murray, Y. D. (2004). “Evaluation of LS-DYNA soil material model 147.” *FHWA-HRT-04-094*, U.S. Department of Transportation, Federal Highway Administration, McLean, VA.

63. Reid, J. D., and Hiser, N. R. (2004). “Friction modelling between solid elements.” *International Journal of Crashworthiness*, 9(1), 65-72.

64. Reid, J. D., and Hiser, N. R. (2005). “Detailed modeling of bolted joints with slippage.” *Finite Elements in Analysis and Design*, 41, 547-562.

65. Reid, J. D., Kuipers, B. D., Sicking, D. L., and Faller, R. K. (2009). “Impact performance of W-beam guardrail installed at various flare rates.” *International Journal of Impact Engineering*, 36, 476-485.

66. Ross Jr, H. E., and Sicking, D. L. (1984). “Guidelines for placement of longitudinal barriers on slopes.” *Transportation Research Record*, 970, 3-9.

67. Ross, H. E., Jr., Sicking, D. L., Zimmer, R. A., and Michie, J. D. (1993). “Recommended procedures for the safety performance evaluation of highway features.” *NCHRP Report 350*, Transportation Research Board, National Research Council, Washington, D.C.

68. Schrum, K.D., Lechtenberg, K.A., Bielenberg, R.W., Rosenbaugh, S.K., Faller, R.K., Reid, J.D., and Sicking, D.L., (2013). “Safety performance evaluation of the non-blocked midwest guardrail system (MGS).” Midwest Roadside Safety Facility. TRP-03-262-12.

69. Tiso, P., Plaxico, C., and Ray, M. (2002). “Improved truck model for roadside safety simulations: Part II - suspension modeling.” *Transportation Research Record*, 1797, 63-71.

70. Whitworth, H. A., Bendidi, R., Marzougui, D., and Reiss, R. (2004). “Finite element modeling of the crash performance of roadside barriers.” *International Journal of Crashworthiness*, 9(1), 35-43.

71. Zaouk, A. K., Bedewi, N. E., Kan, C.-D., and Marzouigui, D. (1997). “Development and evaluation of a C-1500 pickup truck model for roadside hardware impact simulation.” *FHWA-RD-96-212*, Federal Highway Administration, Washington, D.C.

72. Zaouk, A. K., Marzougui, D., and Bedewi, N. E. (2000a). “Development of a detailed vehicle finite element model, Part I: methodology.” *International Journal of Crashworthiness*, 5(1), 25-36.

73. Zaouk, A. K., Marzougui, D., and Kan, C.-D. (2000b). “Development of a detailed vehicle finite element model, Part II: material characterization and component testing.” *International Journal of Crashworthiness*, 5(1), 37-50.

74. Zweden, J. V., and Bryden, J. E. (1977). “In-service performance of highway barriers.” *Report NYSDOT-ERD-77-RR51*, New York State Department of Transportation, Albany, NY.